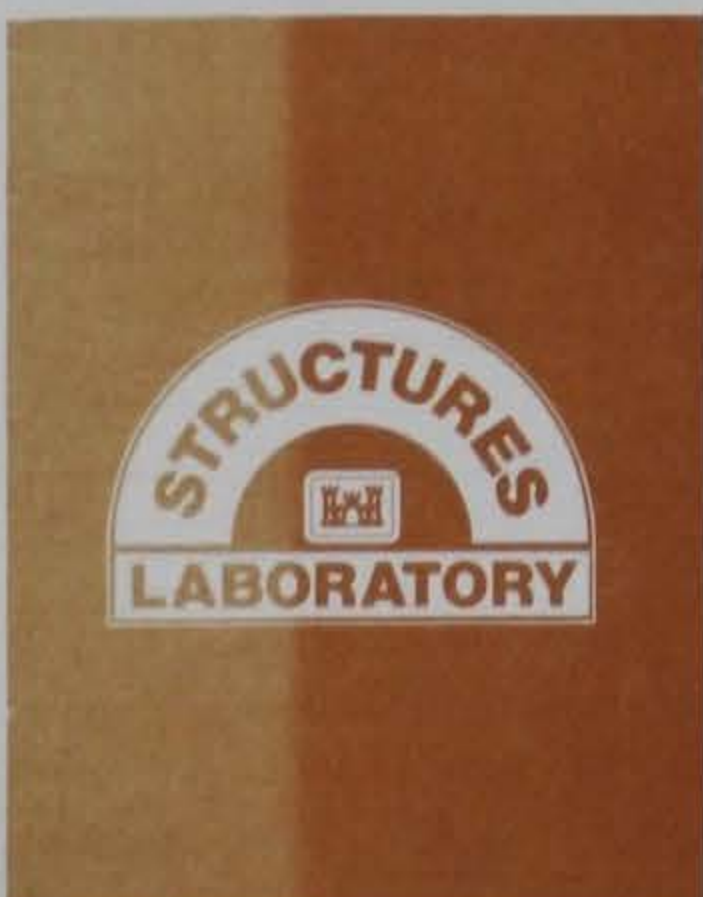


TA7
W34
no.
SL-86-8
cop. 2

Corps
of Engineers



TECHNICAL REPORT SL-86-8

TESTS AND ANALYSES OF THE PANAMA CANAL LOCKS TOW TRACK SYSTEM

by

V. T. Cost

Structures Laboratory

DEPARTMENT OF THE ARMY
Waterways Experiment Station, Corps of Engineers
PO Box 631, Vicksburg, Mississippi 39180-0631

US-CE-C Property of the
United States Government



May 1986

Final Report

Approved For Public Release; Distribution Unlimited

Library Branch
Technical Information Center
U.S. Army Engineer Waterways Experiment Station
Vicksburg, Mississippi

Prepared for

Panama Canal Commission
Engineering Division
APO Miami, Florida 34011

Unclassified

SECURITY CLASSIFICATION OF THIS PAGE (When Data Entered)

TA 7
W34
no. SL-86-8
c. 2

REPORT DOCUMENTATION PAGE		READ INSTRUCTIONS BEFORE COMPLETING FORM
1. REPORT NUMBER Technical Report SL-86-8	2. GOVT ACCESSION NO.	3. RECIPIENT'S CATALOG NUMBER
4. TITLE (and Subtitle) TESTS AND ANALYSES OF THE PANAMA CANAL LOCKS TOW TRACK SYSTEM		5. TYPE OF REPORT & PERIOD COVERED Final report
7. AUTHOR(s) V. T. Cost		6. PERFORMING ORG. REPORT NUMBER
9. PERFORMING ORGANIZATION NAME AND ADDRESS US Army Engineer Waterways Experiment Station Structures Laboratory PO Box 631, Vicksburg, Mississippi 39180-0631		8. CONTRACT OR GRANT NUMBER(s)
11. CONTROLLING OFFICE NAME AND ADDRESS Panama Canal Commission Engineering Division APO Miami, Florida 34011		10. PROGRAM ELEMENT, PROJECT, TASK AREA & WORK UNIT NUMBERS
14. MONITORING AGENCY NAME & ADDRESS (if different from Controlling Office)		12. REPORT DATE May 1986
		13. NUMBER OF PAGES 81
		15. SECURITY CLASS. (of this report) Unclassified
		15a. DECLASSIFICATION/DOWNGRADING SCHEDULE
16. DISTRIBUTION STATEMENT (of this Report) Approved for public release; distribution unlimited.		
17. DISTRIBUTION STATEMENT (of the abstract entered in Block 20, if different from Report)		
18. SUPPLEMENTARY NOTES Available from National Technical Information Service, 5285 Port Royal Road, Springfield, Virginia 22161.		
19. KEY WORDS (Continue on reverse side if necessary and identify by block number) Locks (Hydraulic engineering)--Panama--Panama Canal--Maintenance and repair (LC) Panama Canal--Maintenance and repair (LC)		
20. ABSTRACT (Continue on reverse side if necessary and identify by block number) The Panama Canal has in recent decades experienced increasingly heavier traffic volume and gross tonnage. These increased demands have contributed to serious structural deterioration of the tow track system used in the locks. A procedure for repairing the structural damage without disrupting locks traffic was devised by Panama Canal Commission (PCC) engineers, and implementation was begun in 1981. Concern arose that the repaired tow track might not be resistant to continued deterioration. An evaluation of the structural integrity of the (Continued)		

Unclassified

SECURITY CLASSIFICATION OF THIS PAGE (When Data Entered)

Unclassified

SECURITY CLASSIFICATION OF THIS PAGE(When Data Entered)

20. ABSTRACT (Continued).

repaired track system was needed to assist in determining whether more comprehensive alternatives to the expensive repair procedure should be considered.

In November 1981, the US Army Engineer Waterways Experiment Station was funded by the PCC to conduct structural tests and analyses on the repaired tow track structure. The tests were conducted during March and April 1982 at the Miraflores Locks. Finite element analyses and supporting calculations were made and compared with test results.

Although track system component stress levels documented in the tests were not critical, analyses suggest the development of progressive cycles of localized overstressing and subsequent redistribution of loads, the cumulative effects of which may eventually threaten areas of supporting concrete and certain track system components, especially tie sections.

Unclassified

SECURITY CLASSIFICATION OF THIS PAGE(When Data Entered)

PREFACE

This report contains results of research conducted by personnel of the US Army Engineer Waterways Experiment Station (WES) under sponsorship of the Panama Canal Commission (PCC). The PCC Project Monitor was Mr. Felipe Len Rios.

The study was conducted during March and April 1982 by personnel of the Structures Laboratory (SL), WES, under the general supervision of Messrs. Bryant Mather, Chief, SL; Mr. William Flathau, former Assistant Chief, SL; Mr. James T. Ballard, Assistant Chief, SL, and former Chief, Structural Mechanics Division (SMD); and Dr. Jimmy P. Balsara, Chief, SMD. Direct supervision was also provided by Mr. C. D. Norman as Project Manager, SMD. The WES Project Engineer was Mr. Van T. Cost. This report was prepared by Mr. Cost and was edited by Ms. Janean Shirley, Publications and Graphic Arts Division, WES.

The following PCC personnel are acknowledged for technical guidance which they provided during testing: Messrs. Felipe Len Rios and Tommy Miro, Engineering Division; CAPT Rick Ferrin and Mr. Terry Deakins, Maintenance Division, and Mr. Hector Escoffery, Locks Division. Also acknowledged for their participation in testing are the following personnel of the WES Instrumentation Services Division: Mr. George P. Bonner, Chief, and Messrs. George Williams and Bryant Peterson, technicians.

Director of WES was COL Allen F. Grum, USA. Technical Director was Dr. Robert W. Whalin.

CONTENTS

	<u>Page</u>
PREFACE.....	1
CONVERSION FACTORS, NON-SI TO SI (METRIC) UNITS OF MEASUREMENT.....	3
PART I: INTRODUCTION.....	4
Background.....	4
Objectives.....	6
Scope.....	6
PART II: THE TOW TRACK STRUCTURAL SYSTEM.....	7
Structure Description.....	7
Locomotive Operation.....	7
Tow Track Structural Damage.....	12
Repair Procedures--The "Alternate Tie" Method.....	12
PART III: TESTING PROCEDURES.....	26
Preparation of Test Sections.....	27
Test Methods.....	36
Instrumentation and Data Reduction.....	44
PART IV: RESULTS OF TESTING.....	47
Tests of the Crosstie-Supported Tow Track.....	48
Tests at the Gate Recess.....	53
PART V: ANALYSES.....	55
Preliminary Calculations.....	56
FE Analyses.....	61
Supporting Conventional Analyses.....	75
PART VI: CONCLUSIONS.....	78
REFERENCES.....	80

TABLE 1

CONVERSION FACTORS, NON-SI TO SI (METRIC) UNITS OF MEASUREMENT

Non-SI units of measurement used in this report can be converted to SI (metric) units as follows:

<u>Multiply</u>	<u>By</u>	<u>To Obtain</u>
degrees (angle)	0.01745329	radians
feet	0.3048	metres
inches	2.54	centimetres
inches to the fourth power	41.62314	centimetres to the fourth power
inch-kips (force)	11.29848	centimetre-kilonewtons
kips (force)	4.448222	kilonewtons
kips (force) per square inch	6.894757	megapascals
miles	1.609347	kilometres
pounds (force)	4.448222	newtons
pounds (force) per square inch	6.894757	kilopascals
pounds (force) per yard square inches	4.86463	newtons per metre square centimetres
	6.4516	

TESTS AND ANALYSES OF THE PANAMA CANAL LOCKS

TOW TRACK SYSTEM

PART I: INTRODUCTION

Background

1. Since its completion in 1914, the Panama Canal has played an essential role in world commerce. Approximately 14,000 transits are now made each year through the 50-mile* waterway. Any moment of the day typically finds dozens of vessels anchored near each canal entrance, awaiting the passage which requires an average of 9 hr, deep water to deep water. A ship entering the canal is raised in three steps to Gatun Lake, one of the largest man-made lakes in the world. After a 23-1/2-mile trip across the lake (about 85 ft above sea level), the ship is lowered in three steps back to sea level. The steps consist of side-by-side pairs of locks, each operated independently, accommodating two lanes of traffic. Ships are towed in and out of the locks by electric locomotives equipped with powerful hydraulic winches, or windlasses. The locomotives run on tracks on both sides of the locks and are driven through pinion wheels which engage a toothed rack between the tracks. For many years, the facility has operated at full capacity, around the clock, 365 days per year. Maintenance on locks hardware is scheduled for low-traffic periods, and only very rarely requires a shutdown of operations. Even then, repair efforts are confined to only one of the two lanes at a time, while traffic continues to move in the other. The marine traffic control experts of the Panama Canal Commission (PCC) use a computerized control system and are constantly studying new ways to streamline operations and increase traffic flow capacity.

2. Seventy years of developments in maritime technology as well as world trade and shipping have had many effects on the operation of the canal. In addition to traffic volume, the size and load capacity of ships have increased over the years. In 1914, it was difficult to conceive of a ship large

* A table of factors for converting non-SI units of measurement to SI (metric) units is presented on page 3.

enough to fill one of the 1,000-ft-long by 110-ft-wide lock chambers. Today, the design and construction of many of the world's tankers, dry bulk carriers, and containerized cargo ships are influenced by the length, beam, and draft limitations of the chambers. In response to the evolution of the shipping industry, many improvements have been made in the excavated channels which comprise much of the canal length; channels have been widened, curves have been straightened out, etc. But the locks remain basically unchanged. Heavier, stronger locomotives were put into service in the early 1960's to cope with the increased loads of the larger ships. Of course, all of the loads involved in towing and braking of ships are ultimately borne by the tow track and its supporting structure. In recent years, the tow track system and some of its components have shown progressive structural damage. By the late 1970's, this problem had become so severe that an extensive tow track rehabilitation effort was urgently needed to prevent ultimate disruption of canal traffic. In response to this need, PCC engineers devised a method of repairing the tow track system and upgrading certain severely damaged components which could be accomplished without interrupting canal traffic. This procedure was begun in 1981, yet there was still concern among the PCC technical staff that the largely field-engineered repair method might not completely eliminate component overstressing and prevent long-term recurring deterioration of the structure. When the scope and expense (\$2 to \$3 million annually) of the project were realized, it was questioned whether a more complete redesign and upgrading of the tow track system might ultimately be a better investment.

3. In November 1981, the US Army Engineer Waterways Experiment Station (WES) was funded by the PCC to evaluate the structural integrity of the repaired tow track system by conducting a series of structural tests and analyses. The tests were conducted during March and April 1982 at the Miraflores Locks. The test data were presented in a draft data report.* The final results of finite element and conventional analyses of the tow track system, data analyses, and conclusions are presented herein.

* US Army Engineer Waterways Experiment Station. 1982. "Panama Canal Locks Tow Track System Tests" (draft report), Vols 1 and 2, Vicksburg, Miss.

Objectives

4. The objectives of the tow track tests and analyses were to determine the adequacy of the tow track's structure, as repaired by PCC, under its present loadings and to identify critical regions or structure components where overstressing and associated premature failures might be expected.

Scope

5. Tests were conducted at three sites along the east wall of the Miraflores Locks. These sites were selected by PCC as representative repair areas. Responses of the rails and supporting components were monitored using up to 48 channels of active electronic instrumentation (mostly strain measurements), recorded on magnetic tape through the duration of each test. A total of 74 individual tests, each consisting of one locomotive pass, were conducted. Those tests included actual towing situations and special load cases which simulated certain tow conditions.

6. Analyses of test results were conducted to determine tow track component response tendencies and critical regions of stress. A three-dimensional beam finite element model of a tow track section was developed and used for analyses of component responses and boundary condition sensitivity studies. Additional conventional analyses and supporting calculations were made to investigate potential development of structural damage.

PART II: THE TOW TRACK STRUCTURAL SYSTEM

Structure Description

7. The tow track consists of a pair of rails spaced at slightly over 5 ft and the rack, a heavy casting centered between the rails. The rack serves two purposes. First, transverse slots in the top surface of the casting accept the teeth of the massive locomotive drive gears in rack and pinion fashion. This arrangement provides all of the traction for towing and braking. Additionally, the upper sides of the rack form flanges against which special locomotive safety wheels bear, preventing overturning when extreme cable loads are applied. Except for certain track areas in the proximity of the lock miter gates and their associated machinery, the rails and rack are supported by steel crossties which resemble I-beams. These are spaced at 3 ft and are referred to as "long ties." Short lengths of the crosstie beams, or "short ties," support only the rails and are located halfway between long ties. Through most of the crosstie-supported tow track, the complete steel structure rests on a solid concrete foundation, with additional concrete cast around and above the ties so that only the rail heads and upper portion of the rack assembly are exposed. Figure 1 is a cutaway sketch of this tow track construction, and Figure 2 shows more detailed section and elevation views. In certain special areas where the tow track must span a below-deck machinery or access room, the ties are supported by reinforced concrete walls and/or heavy girders, with concrete encasing all members. This construction is illustrated in Figure 3.

8. The massive lock miter gates are about 5 ft thick and recess into the lock walls when swung open to give passing ships benefit of the entire lock width. Tow track sections directly over these gate recesses are supported by specially designed members which span cantilever girders. Figure 4 shows details of this construction.

Locomotive Operation

9. Each electric locomotive is about 35 ft long and 8 ft wide, overall, with a wheelbase of 15 ft. Pinion drive gears at each axle provide all towing and braking traction. Two hydraulically controlled windlasses, each capable

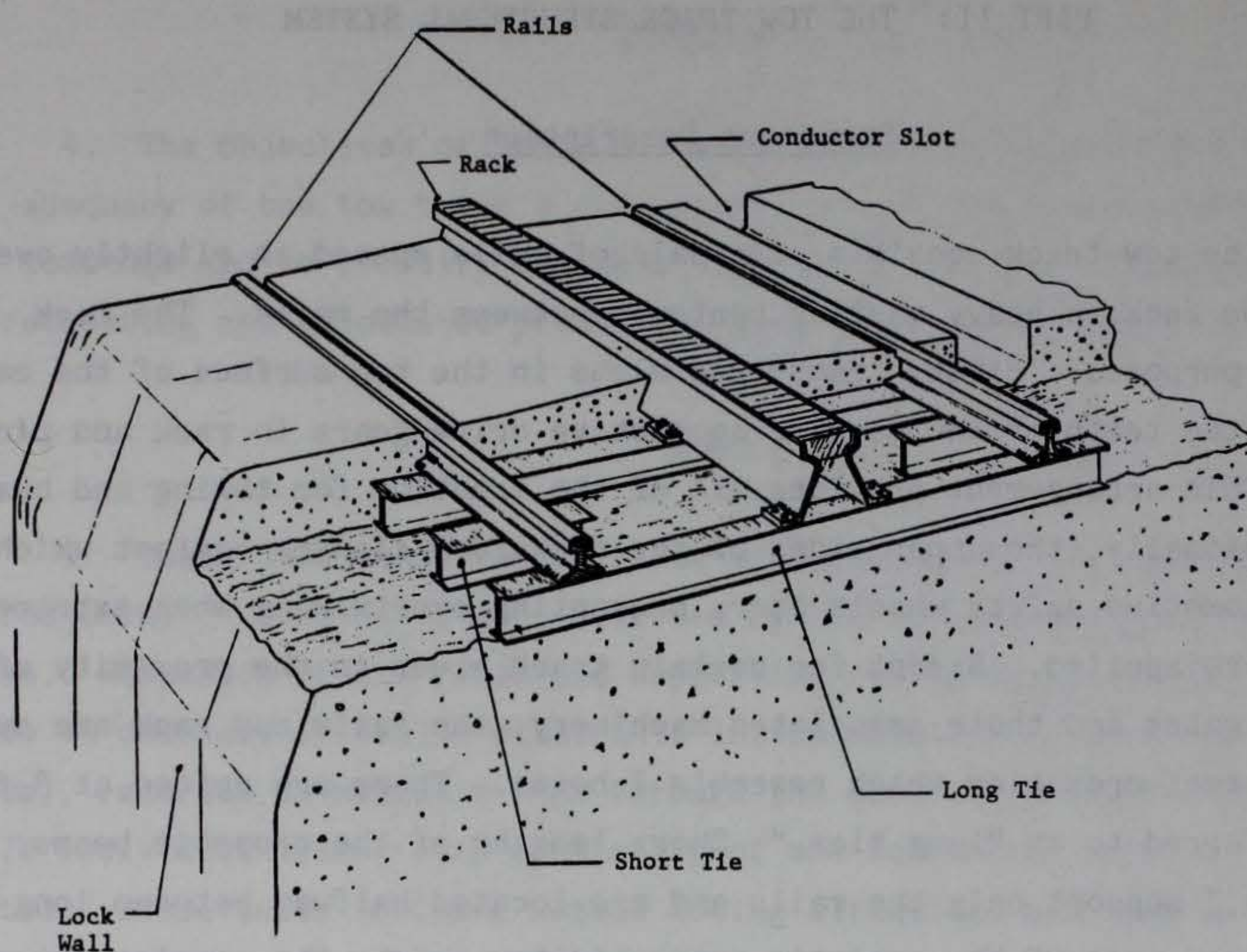
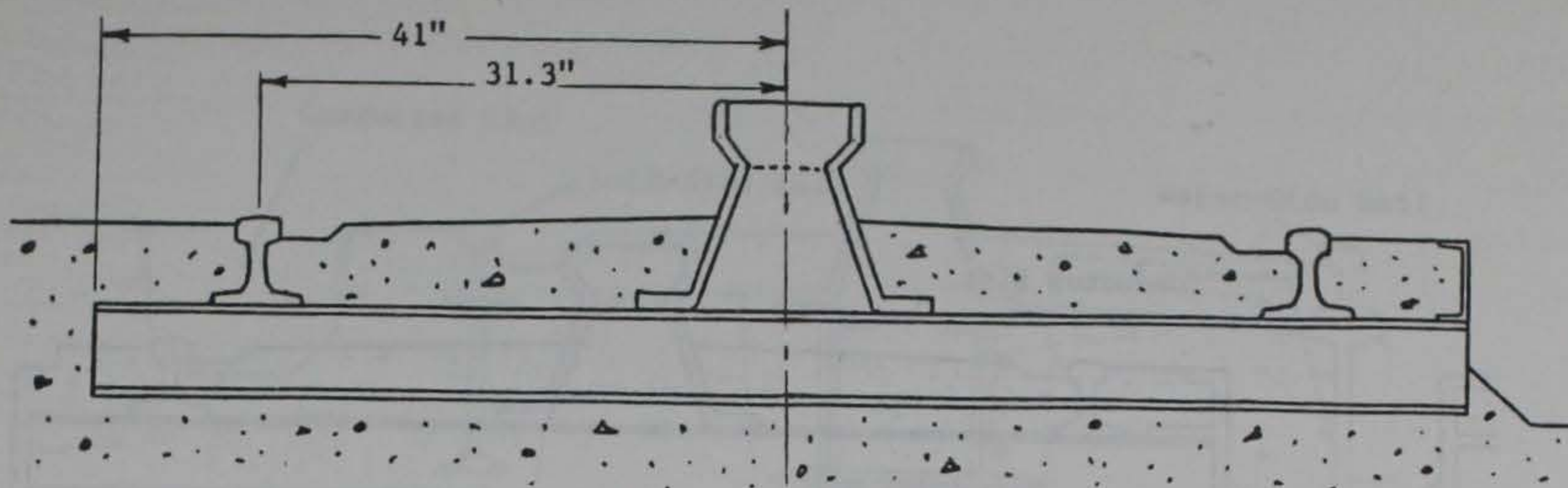


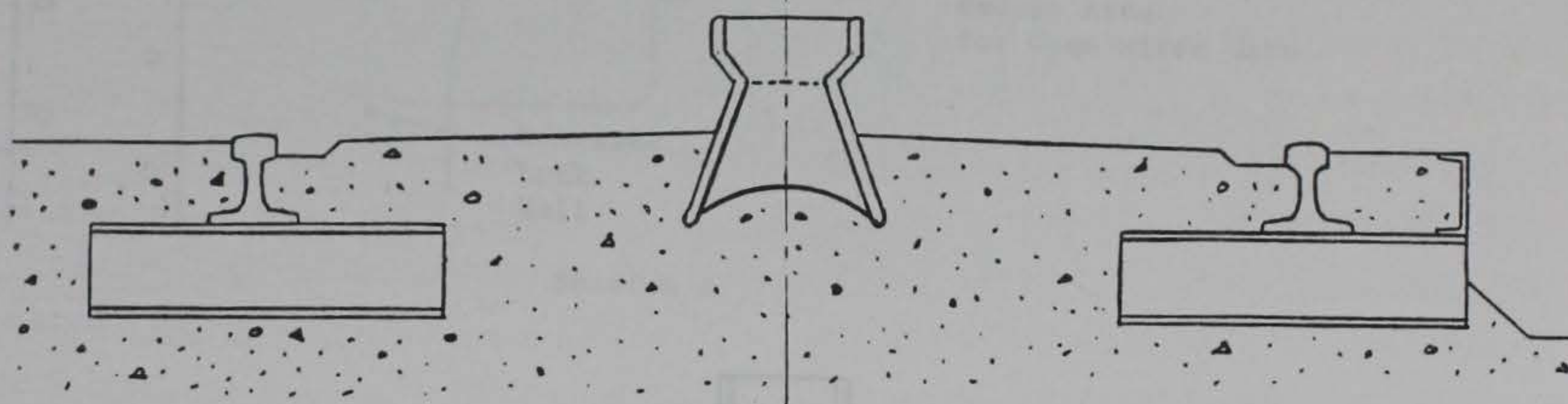
Figure 1. Cutaway sketch of typical concrete foundation tow track section

of 35,000 lb of sustained cable tension, pay out through pulley arrangements which revolve freely to allow any appropriate combination of horizontal and vertical cable angles. These cable exits are 10 ft apart, about 3-1/2 ft above rail elevation. All locomotive features are symmetrical about the mid-length, so that operations are unaffected by the direction of travel. Electric power is conveyed through pickup shoes which move along live conductor channels in the below-grade "conductor slot" adjacent to the landside rail (Figure 1). The dead weight of each locomotive is about 110,000 lb.

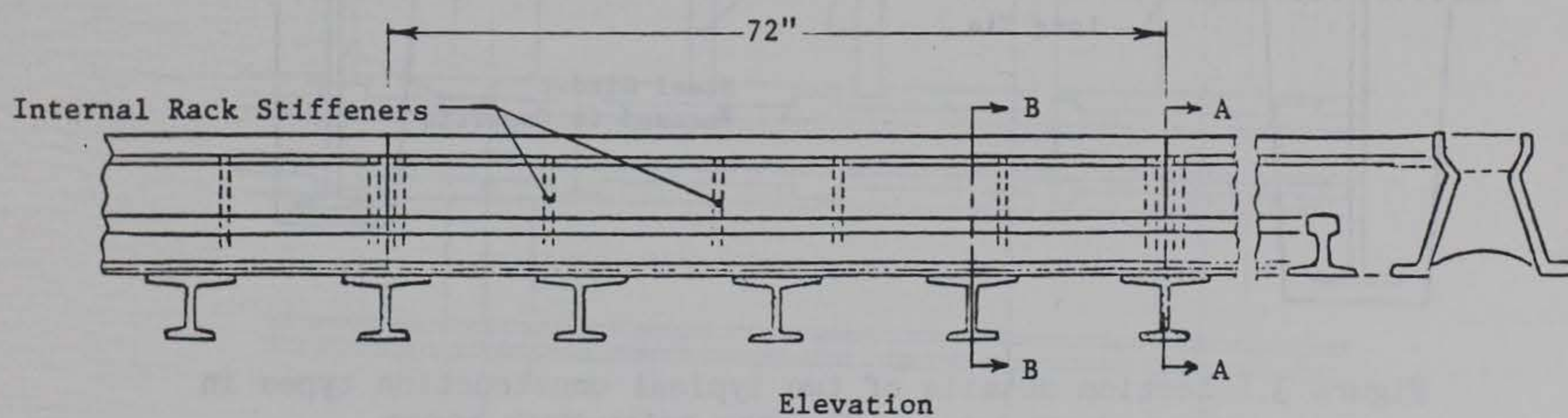
10. Each locomotive is independently operated by an on-board driver, who controls the direction and speed of travel as well as the disposition of each windlass. The operators receive coordinating instructions from a "lock-master" who relies on the continuous input of PCC pilots and observers stationed at the extremes of each ship. Four to eight locomotives are used with each ship, depending on its size, and both windlass cables of each locomotive are secured to the ship. Maximum towing speed is about 3 mph, although larger ships are usually moved more slowly. It is often necessary to assist the locomotives with the ship's own propulsion to overcome the tremendous inertia of



Section A



Section B



Elevation

Figure 2. Construction details of the concrete foundation tow track

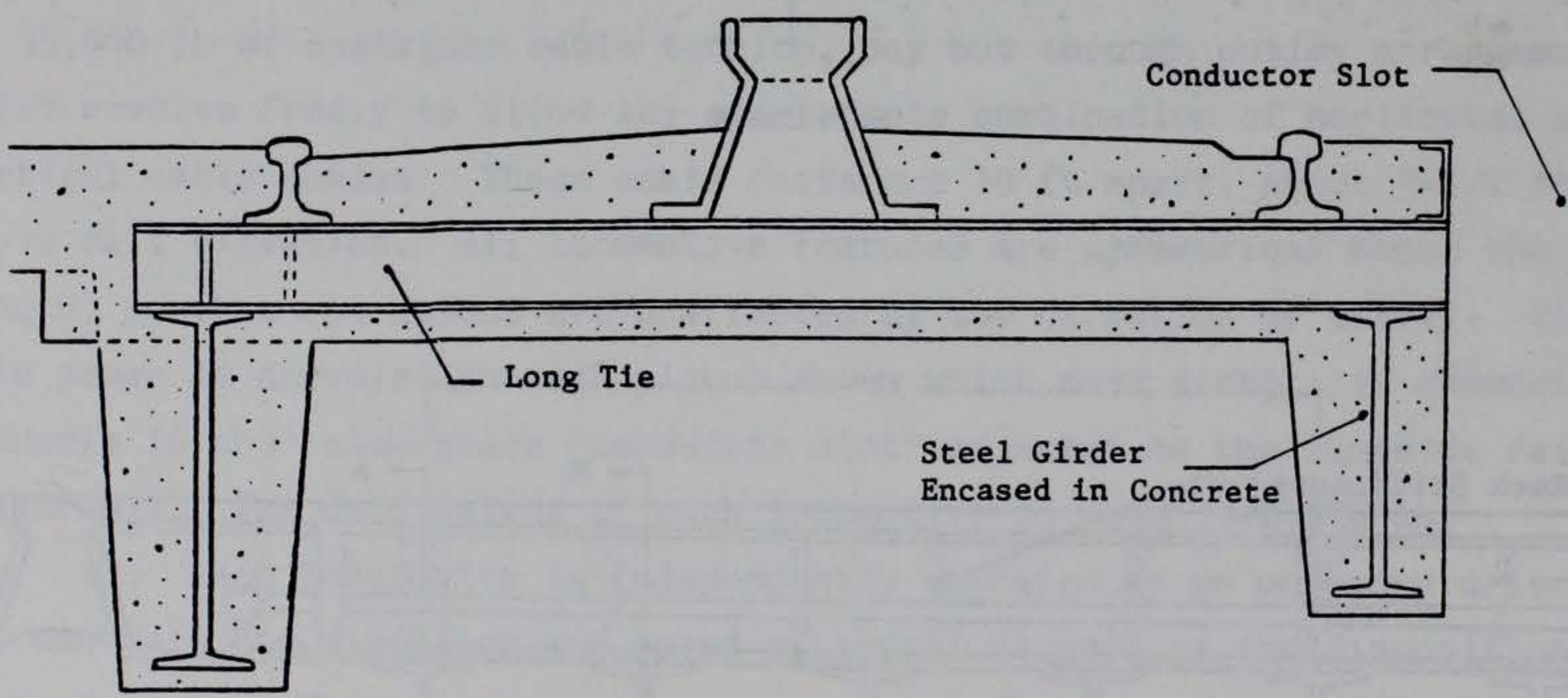
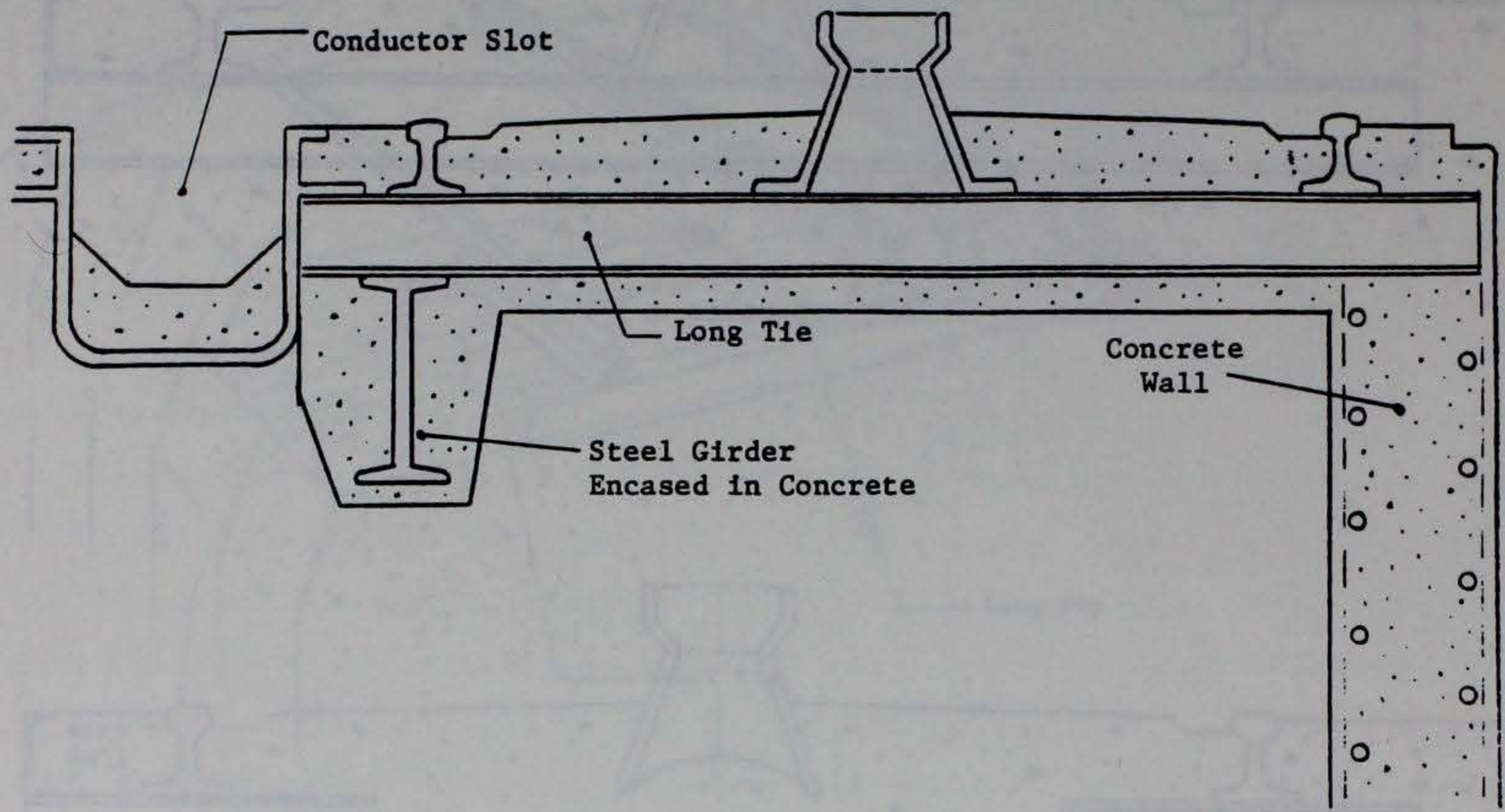
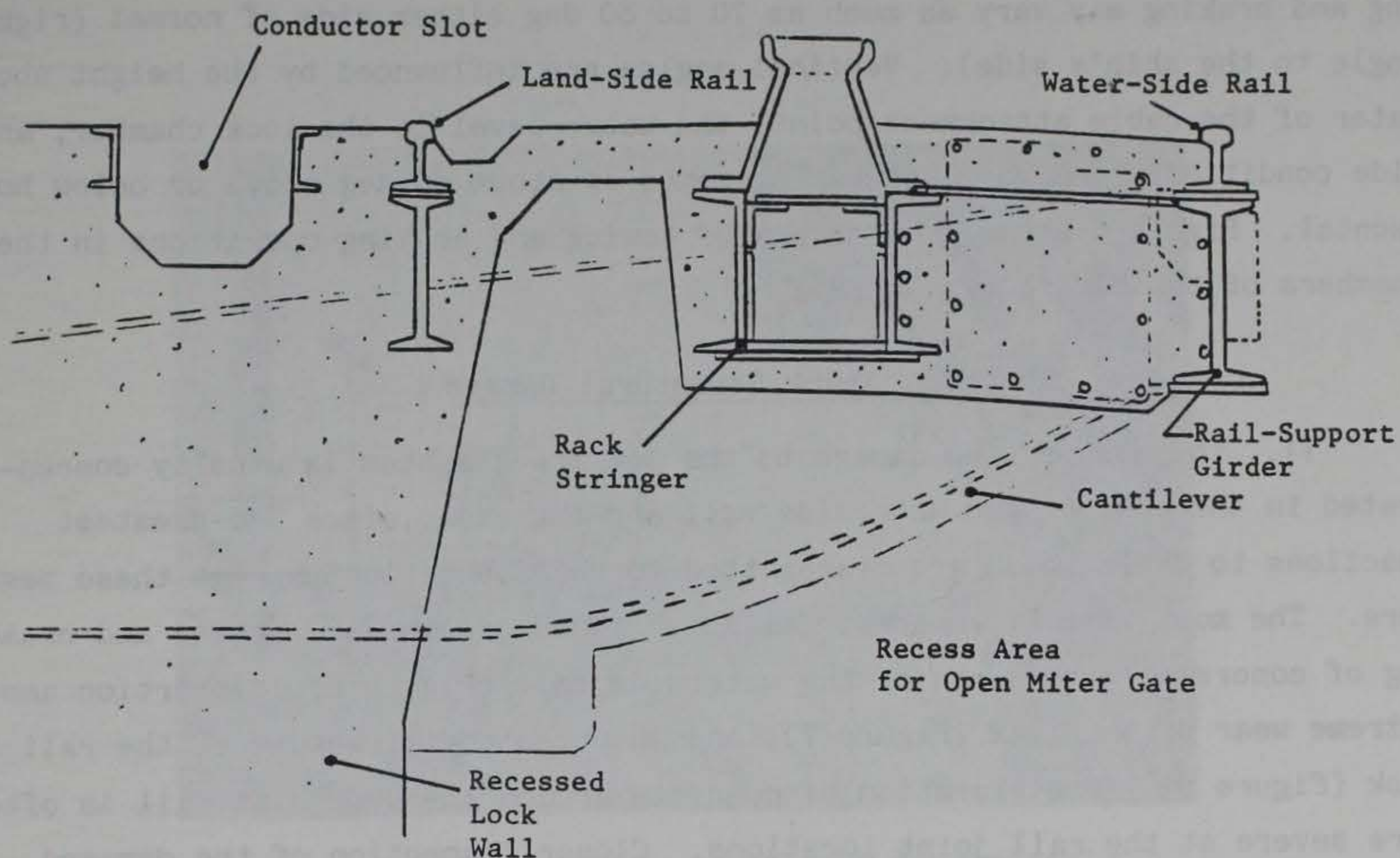
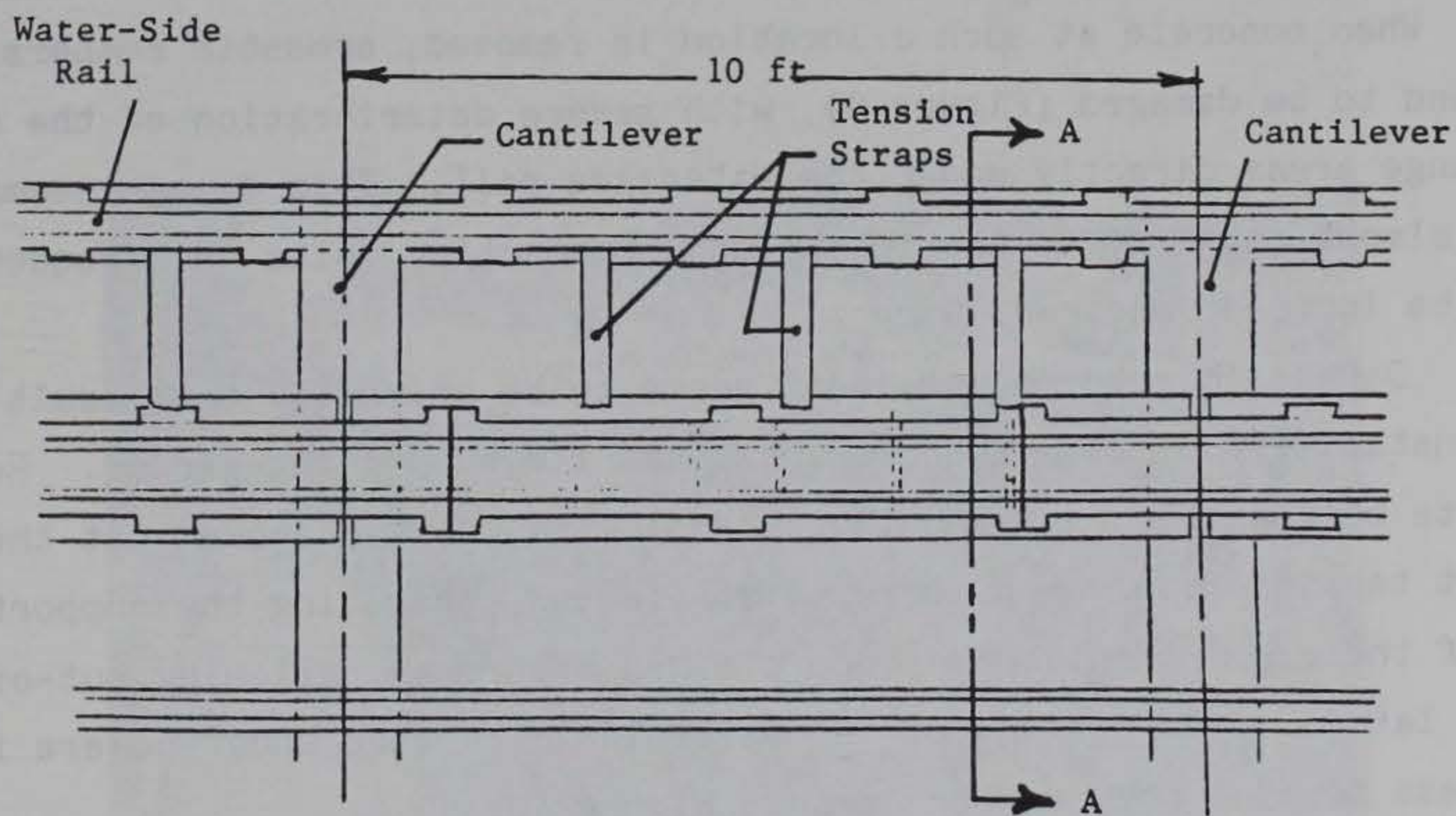


Figure 3. Section details of two typical construction types in areas where tow track spans below-deck rooms



Section A



Plan

Figure 4. Plan and section views of gate recess tow track construction

the larger vessels. The horizontal angles of the windlass cables during towing and braking may vary as much as 70 to 80 deg either side of normal (right angle to the ship's side). Vertical angles are influenced by the height above water of the cable attachment point, the water level in the lock chamber, and tide conditions, and vary between extremes of about 80 deg above or below horizontal. Figure 5 shows photographs of towing and braking operations in the chambers of the Miraflores Locks.

Tow Track Structural Damage

11. The most severe damage to the tow track system is usually concentrated in the area of the waterside rail and the rack, since the greatest reactions to cable loads are transmitted to the foundation through these members. The most visibly apparent damage includes excessive cracking and crushing of concrete in the area of the waterside rail (Figure 6), distortion and extreme wear of the rack (Figure 7), and an occasional fracture of the rail or rack (Figure 8). Deterioration of concrete around the waterside rail is often more severe at the rail joint locations. Closer inspection of the damaged area usually reveals significant settlement and misalignment of the rails (primarily the waterside rail) and the rack with respect to the rails. Such misalignment has apparently been the cause of some derailments of towing locomotives. When concrete at such a location is removed, crosstie members are often found to be damaged (Figure 9), with severe deterioration of the web and upper flange areas directly under the waterside rail. This damage seems to be confined almost entirely to the long ties. Connecting bolts are frequently found to be loose or sheared.

12. Damage in gate recess areas seems to be primarily the result of lateral instability of the waterside rail and its supporting girder. Removal of concrete between the rack and the waterside rail often shows that the intermittent tension rods which serve as stiffeners connecting the supporting members of these components have been yielded or broken, allowing out-of-tolerance lateral deformations of the waterside structure under severe loadings. These tension rods can be seen in Figure 10.

Repair Procedures--The "Alternate Tie" Method

13. The "alternate tie" method is the procedure developed by PCC for the rehabilitation of the tow track system. The repairs are made section by



a. Locomotive cable angles vary considerably



b. Cable angles such as this cause the most severe loadings of the waterside rail

Figure 5. Typical towing operations (Continued)

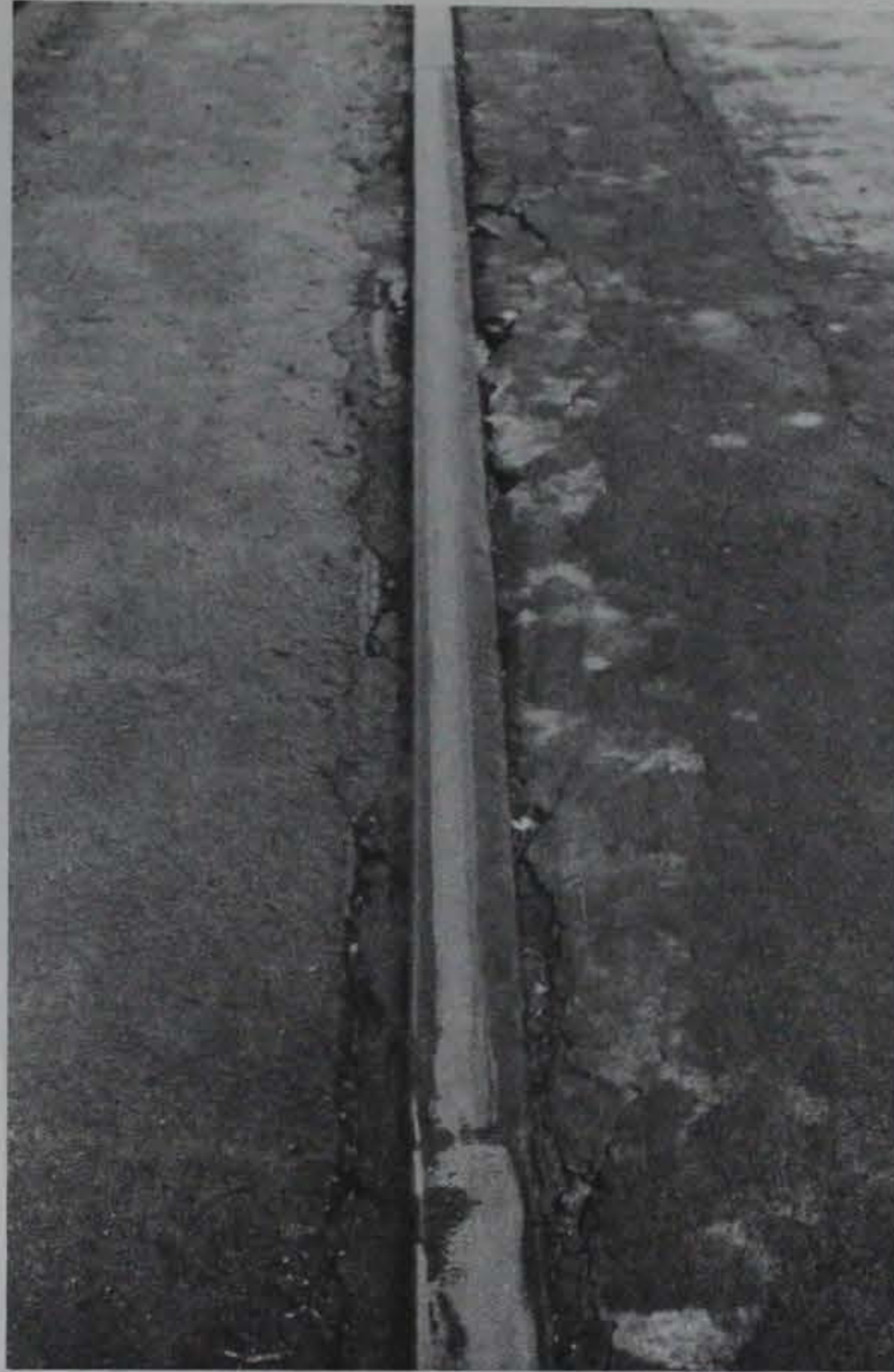


c. Many of the larger vessels have only inches of clearance in the 110-ft-wide chambers

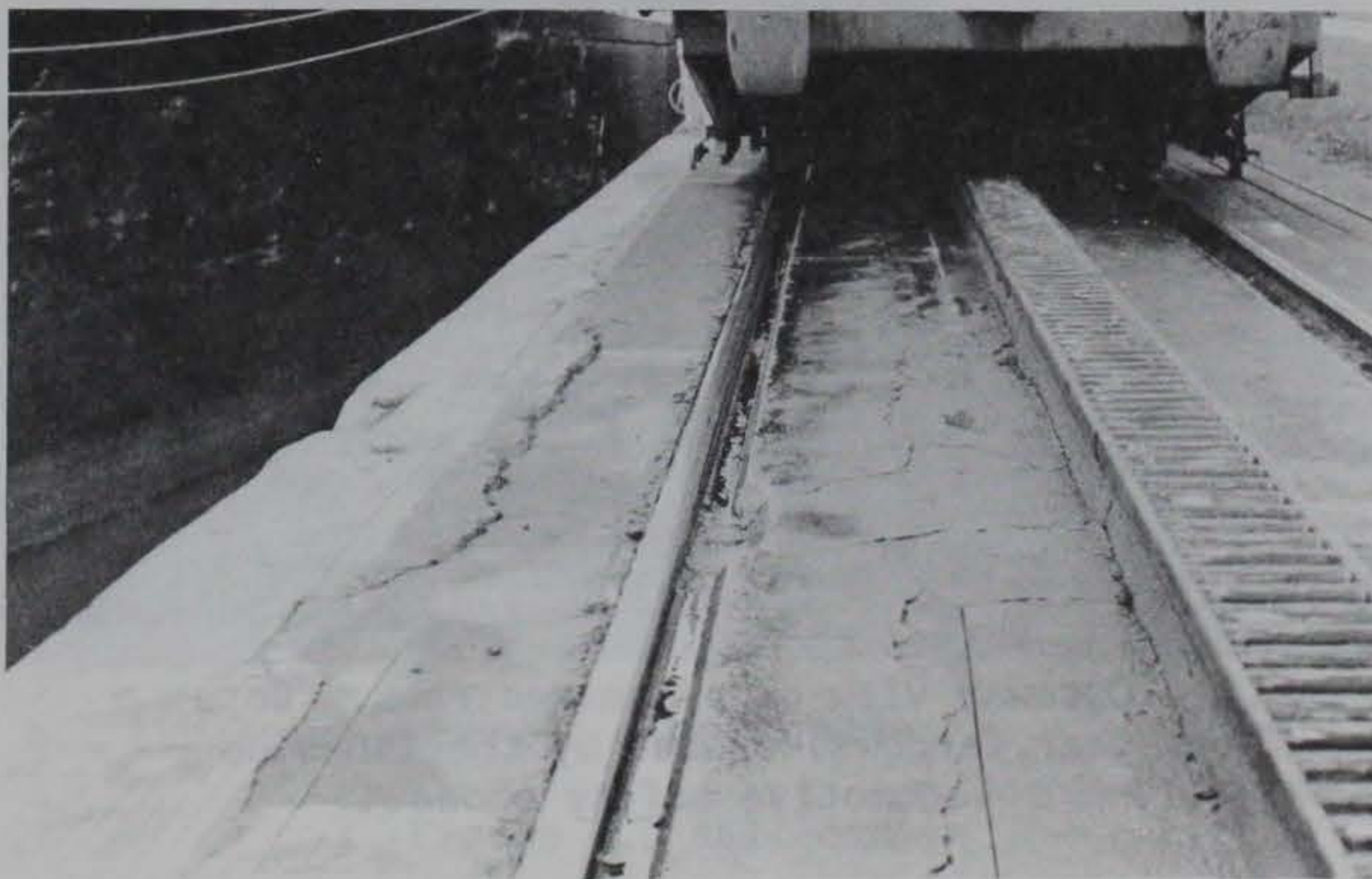


d. The Queen Elizabeth 2 is the largest passenger ship that uses the canal

Figure 5. (Concluded)

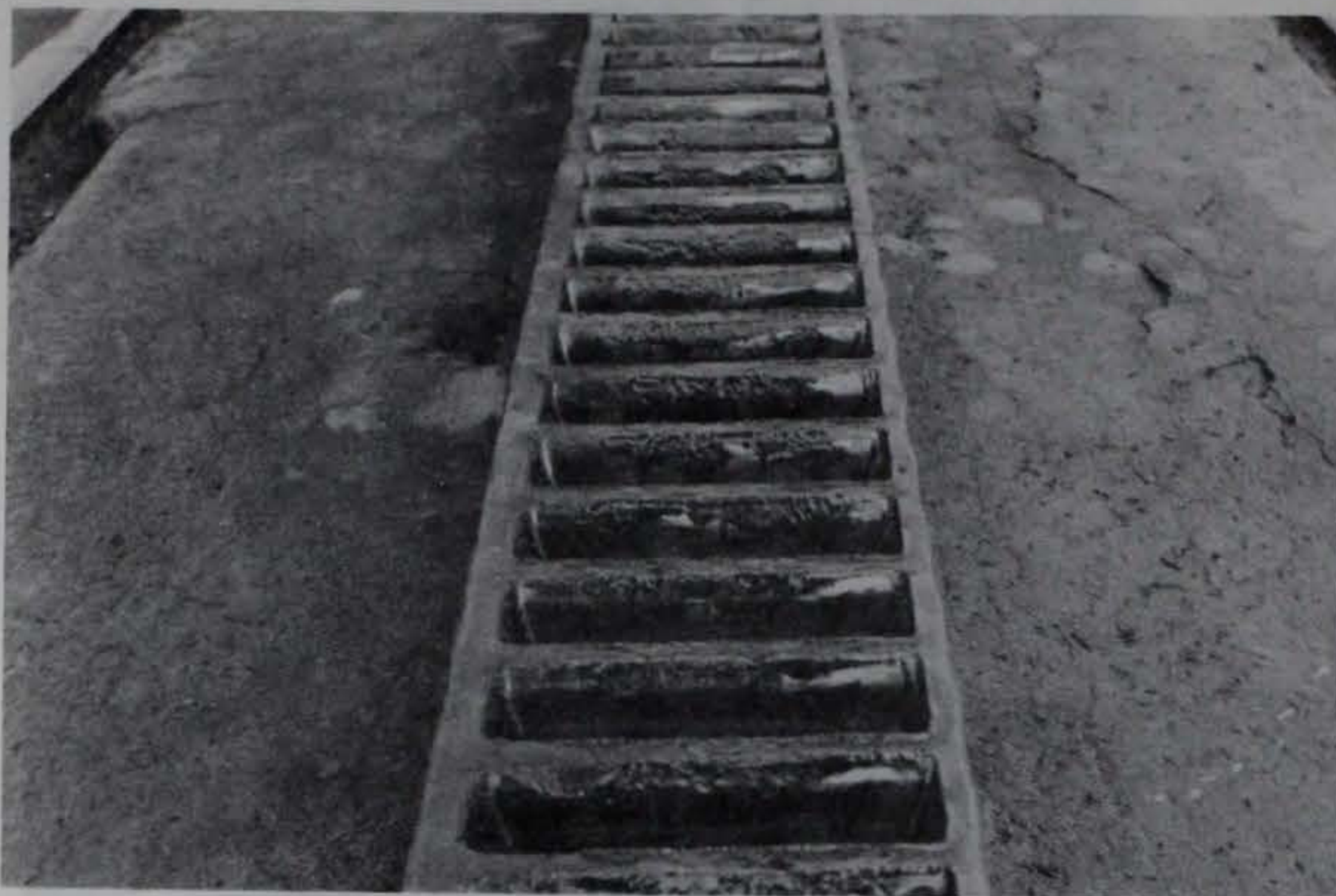


a. Typical concrete damage along the waterside rail

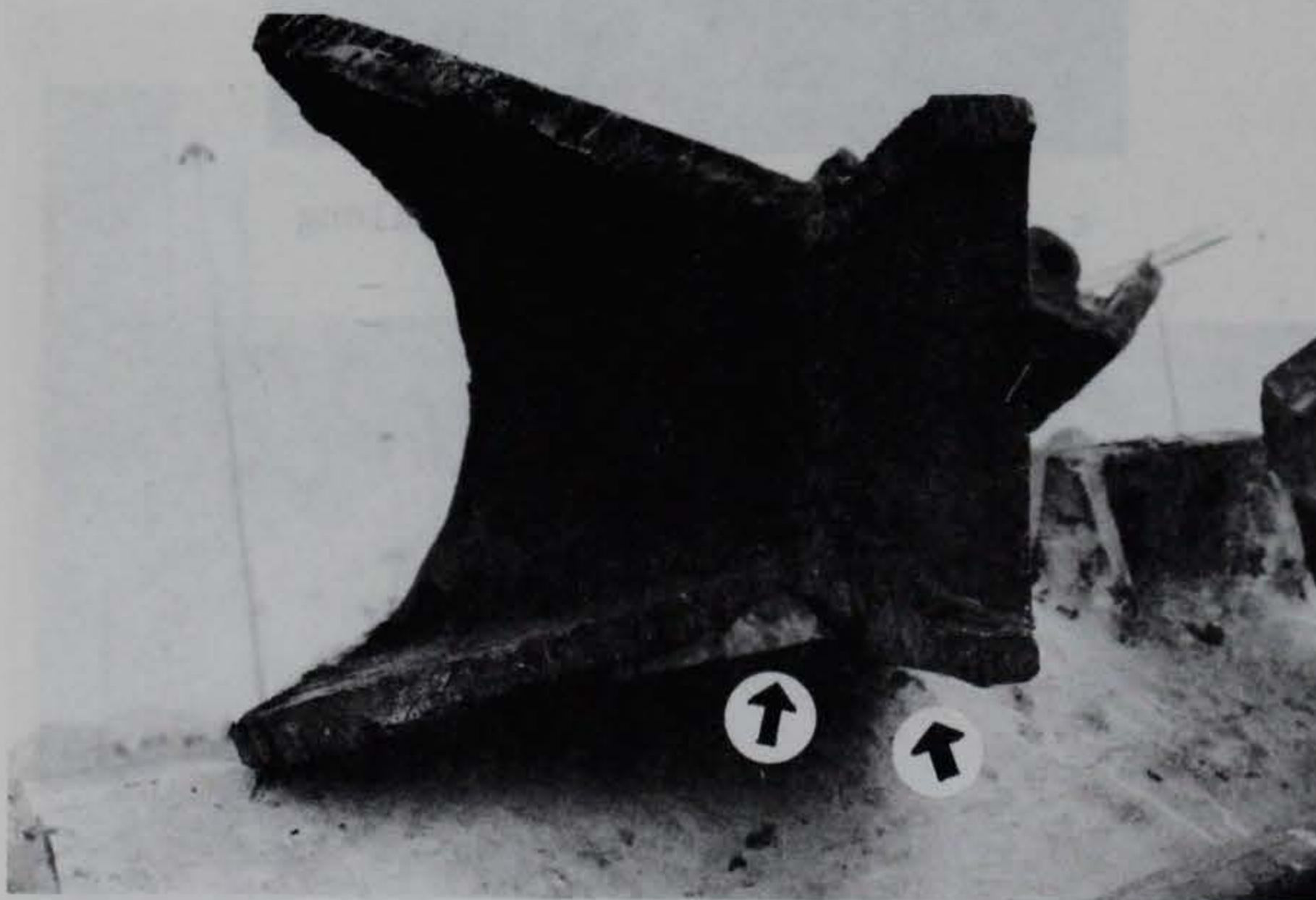


b. Damage is sometimes evident along the tie ends

Figure 6. Deterioration of surface concrete

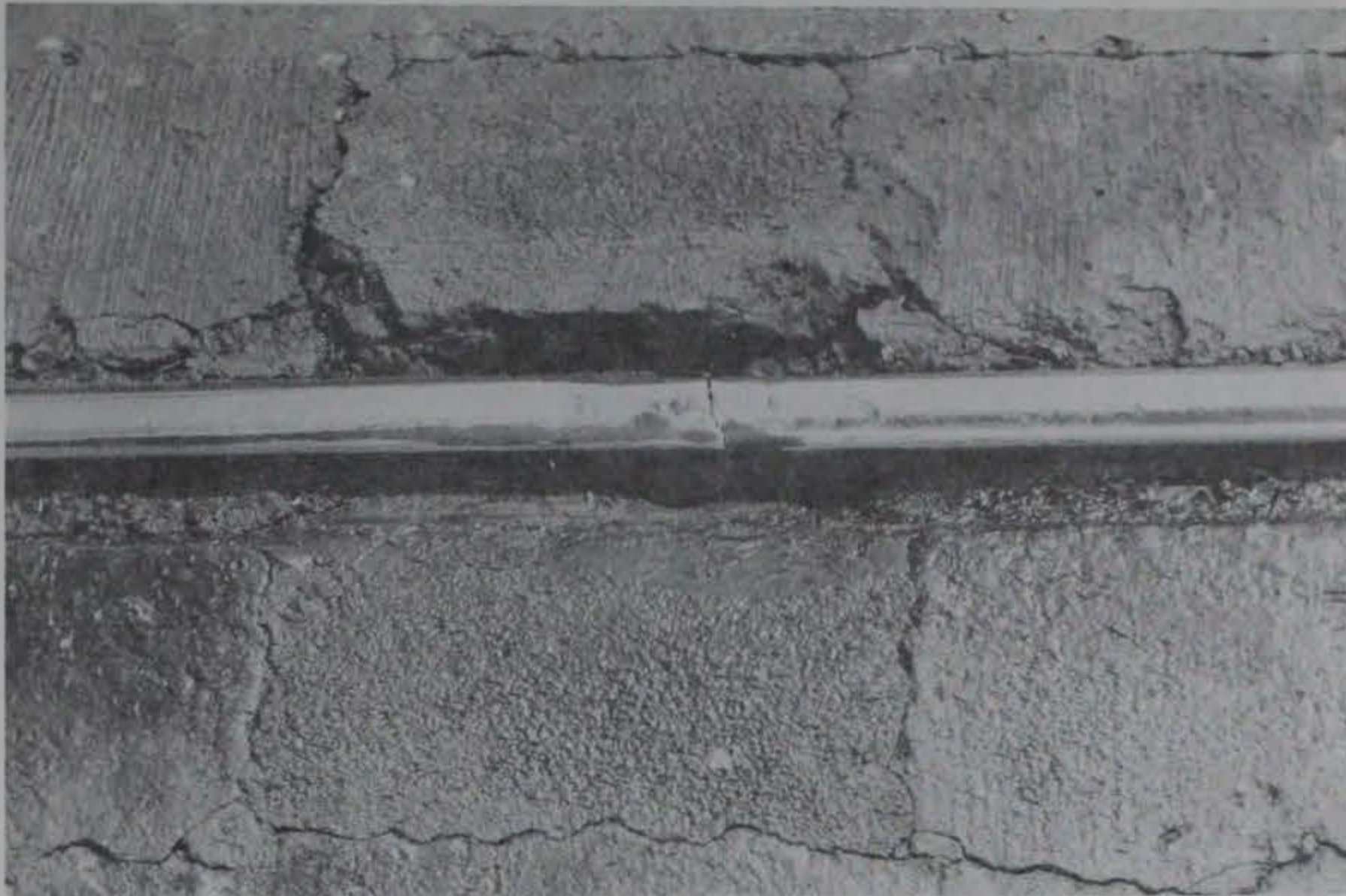


a. A worn rack section. Note the damage to the waterside (right in photo) flange caused by locomotive drive gears

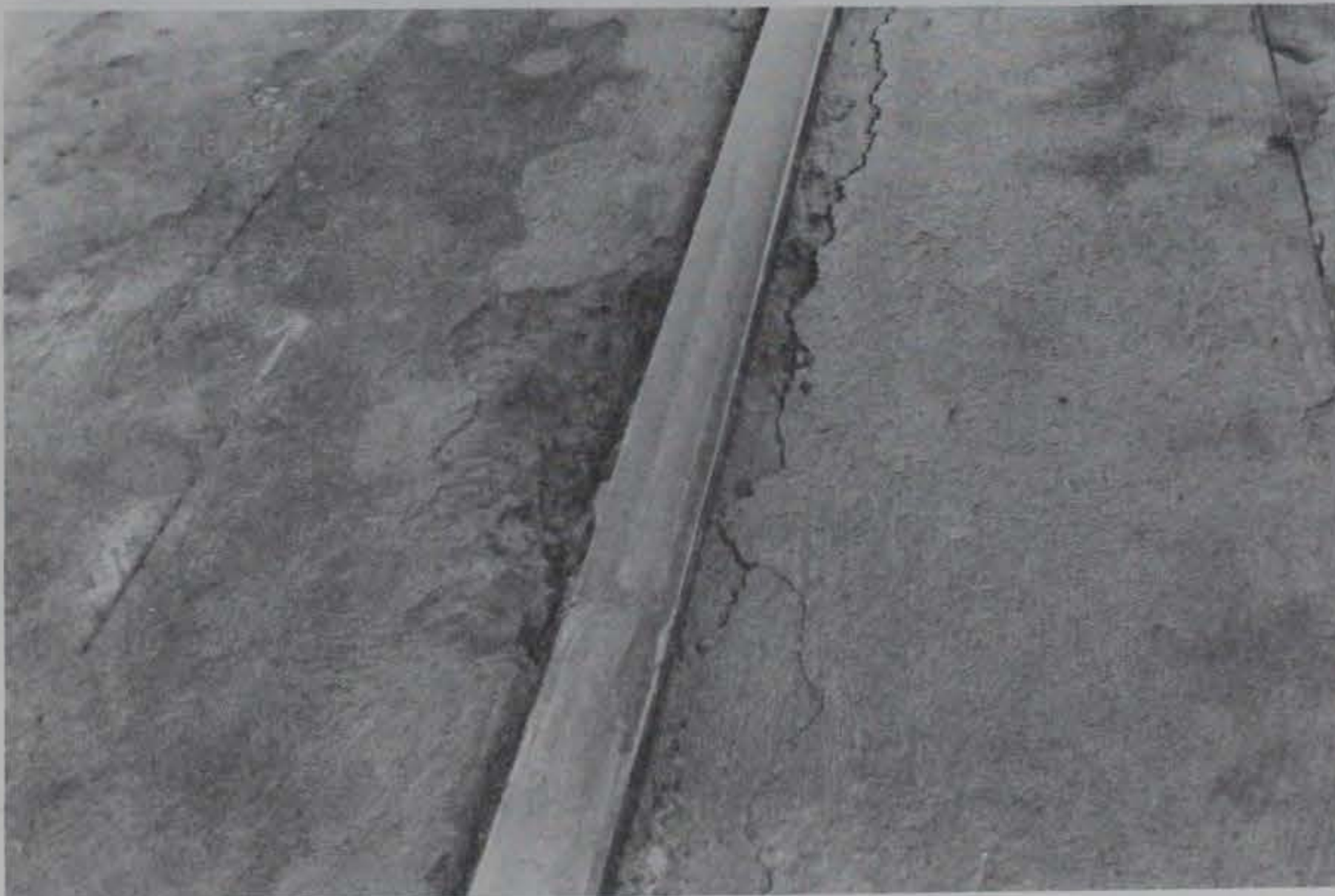


b. Cutaway view of a damaged rack. Note the wear (arrows) caused by the landside locomotive safety shoes

Figure 7. Damage to the rack



a. A typical rail fracture. Most such failures are located at the welded joints



b. Excessive concrete deterioration at a rail joint

Figure 8. Rail damage

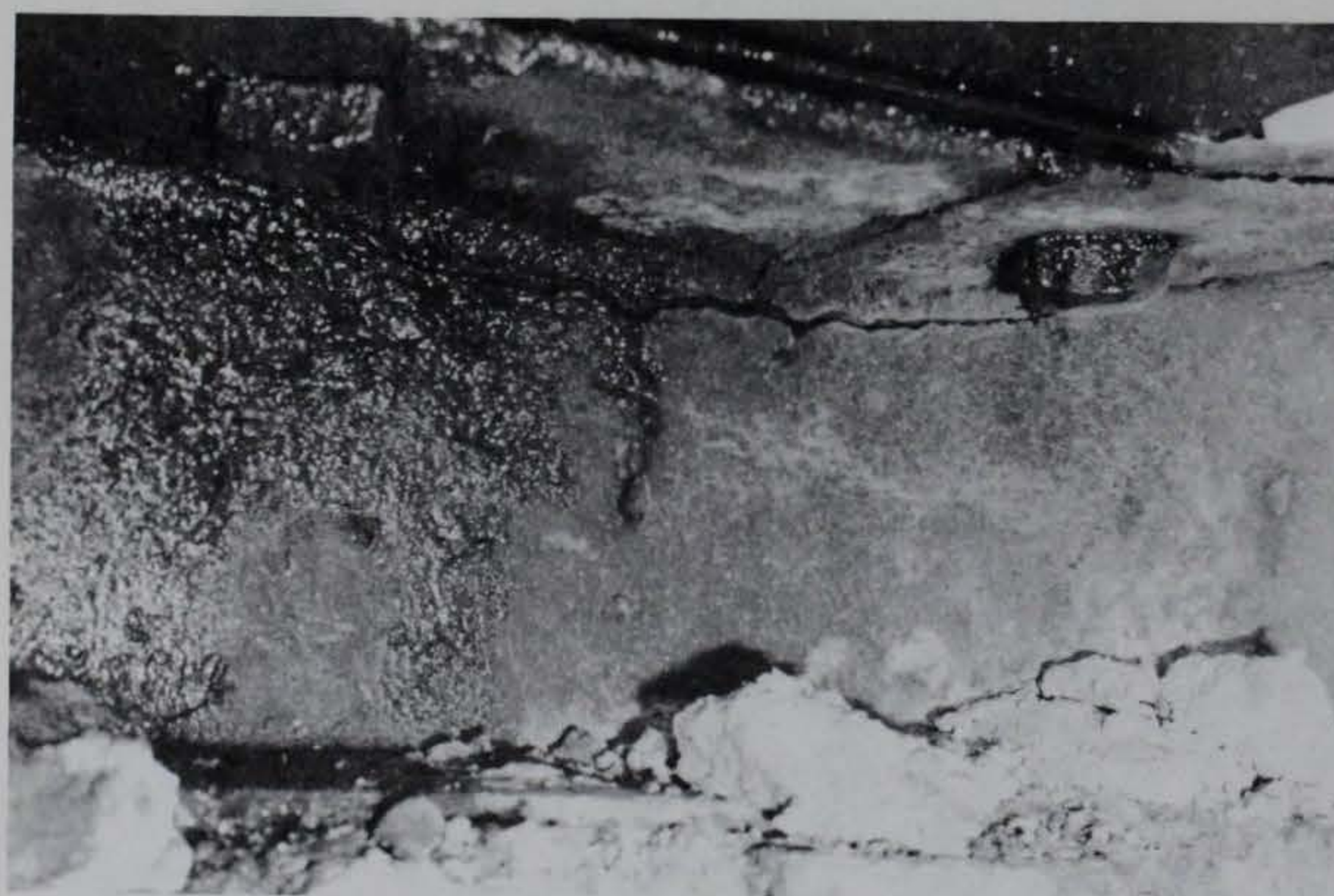


Figure 9. Views of two different long ties showing severe damage to the web under the waterside rail. Photos were taken immediately after the removal of concrete. Note also the damage to upper flanges



Figure 10. Gate recess area after removal of concrete between waterside rail and rack. Note the rods which serve as lateral stiffeners of the rail-support girder

section and are designed to be accomplished without any interruptions of lock traffic. Actual hardware replacement is done during the 1-1/2- to 3-hr midday period known as the traffic window, when there are normally no ships in the locks due to the shift in traffic direction. (Both traffic lanes run in the same direction at all times; traffic enters both ends of the canal during morning hours and begins to exit in the afternoon when the first entering ships have crossed Lake Gatun.)

14. Repairs of a section are begun by removing the concrete around the waterside rail down to the lower flanges of the ties. All short ties in the area are then completely removed and long ties are closely inspected for damage (Figure 11). Long ties that are found to be damaged only under the waterside rail are cut off about halfway to the rack, and a new, heavier section is attached to the old using butt welds and splice plates (Figure 12). When a tie is more extensively damaged, concrete is excavated along its complete length so that it can be removed and replaced. Many of the original ties (more than half) do not appear to be damaged and are not replaced. Since sections identical to the original ties are no longer available, replacements are usually lengths of a standard W6 x 20 I-beam section. Limited supplies of a new heavier tie design are kept on hand for use where special details

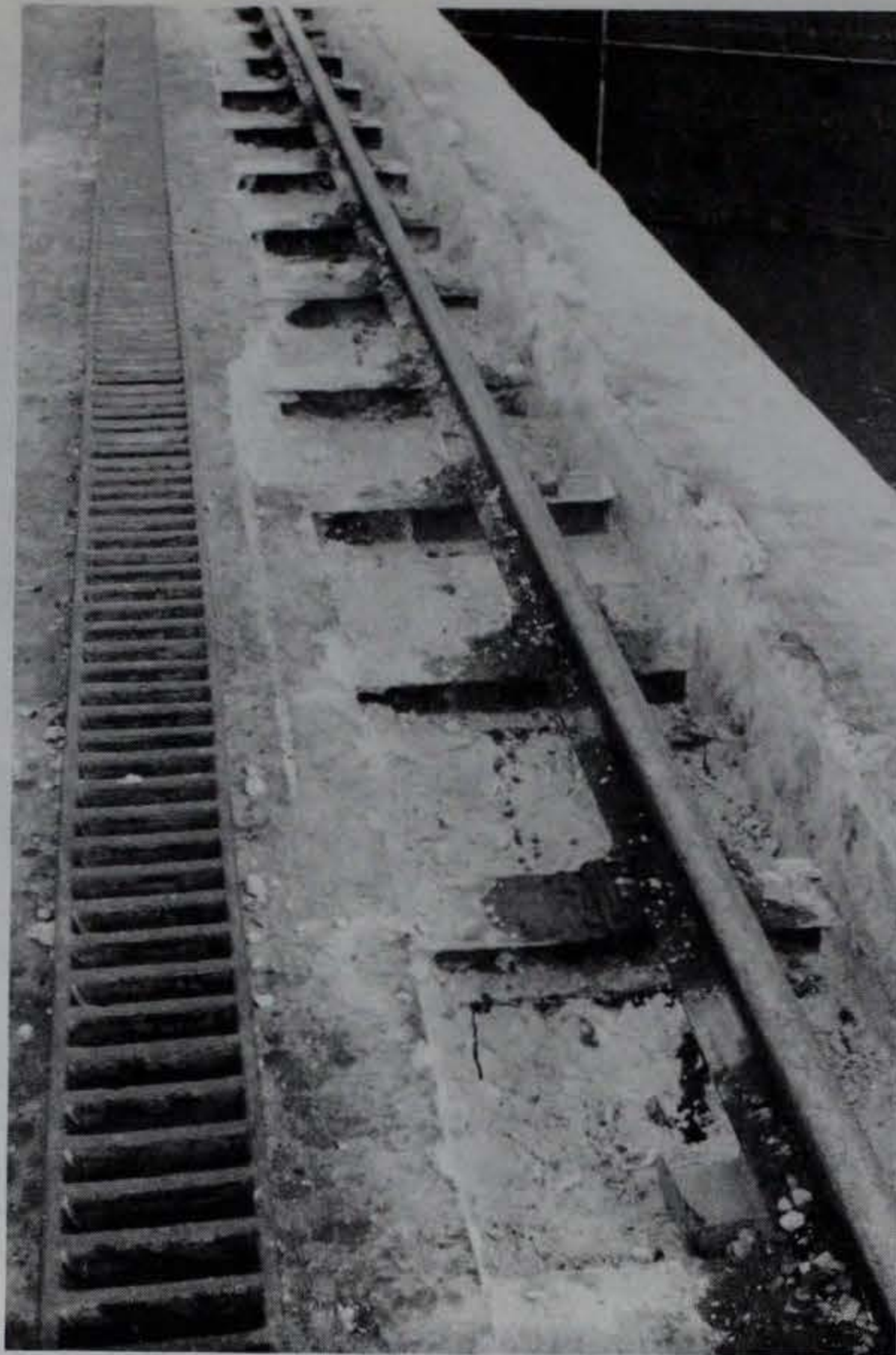


Figure 11. Repair area after the initial concrete excavation and removal of short ties

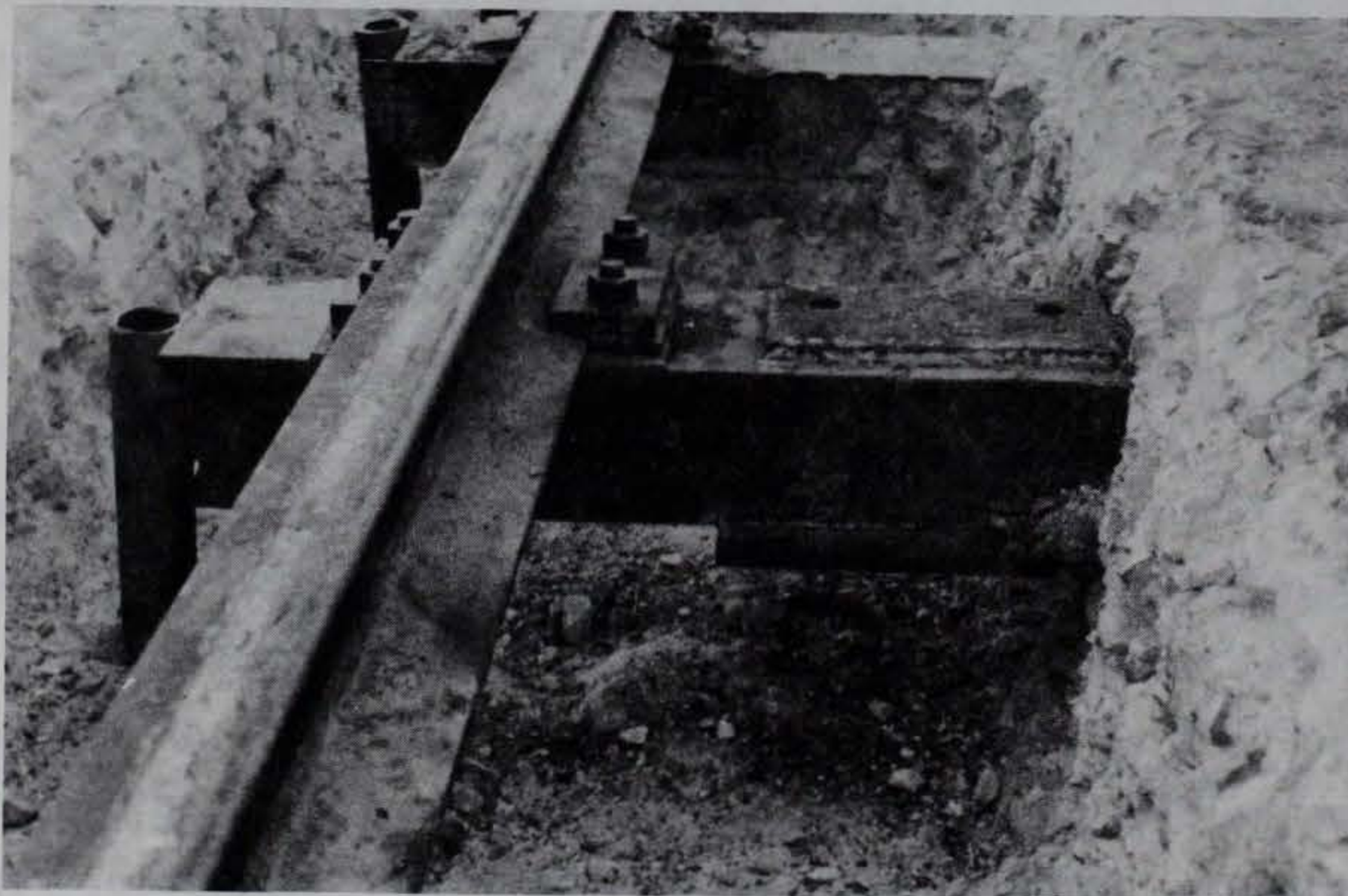
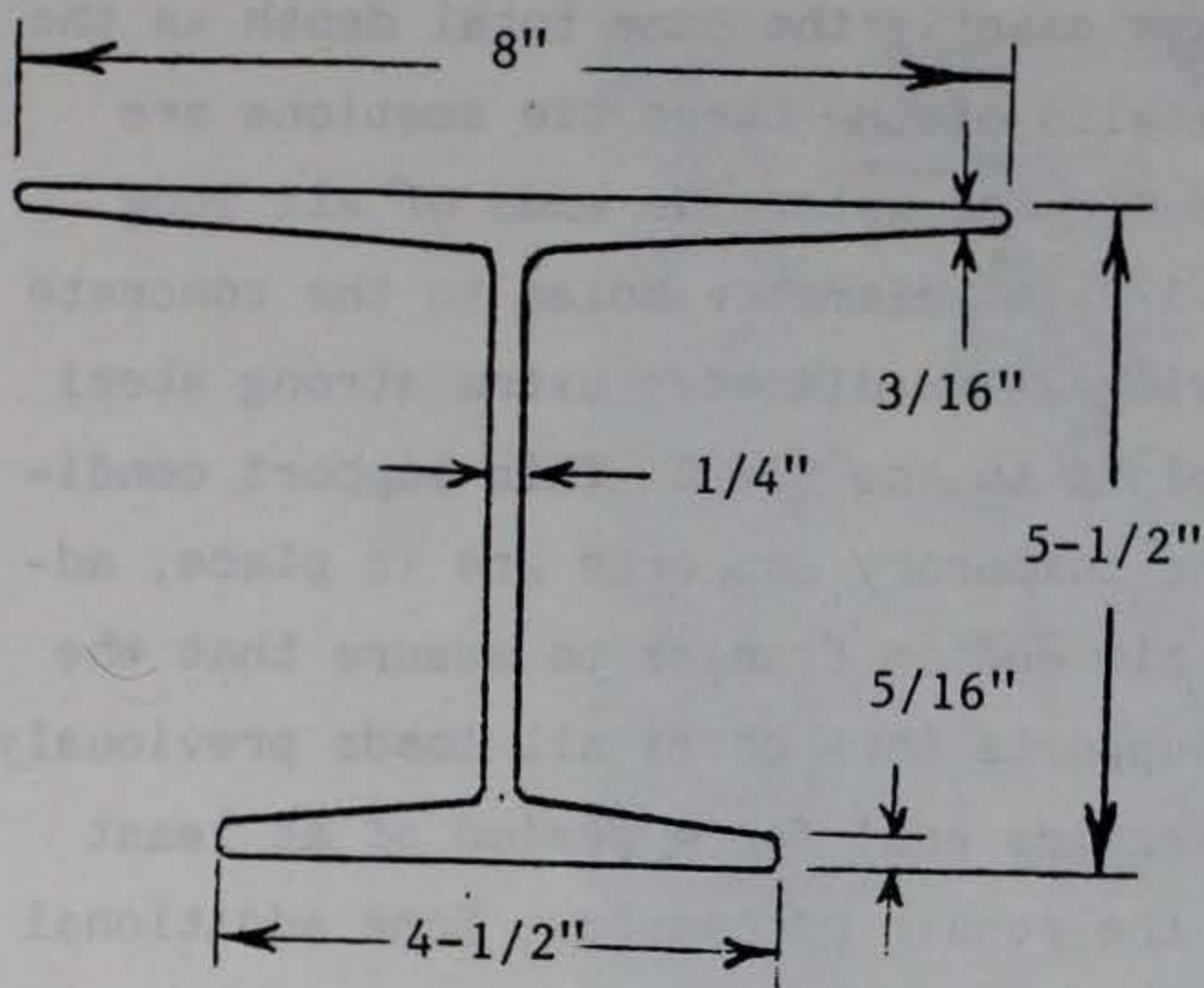


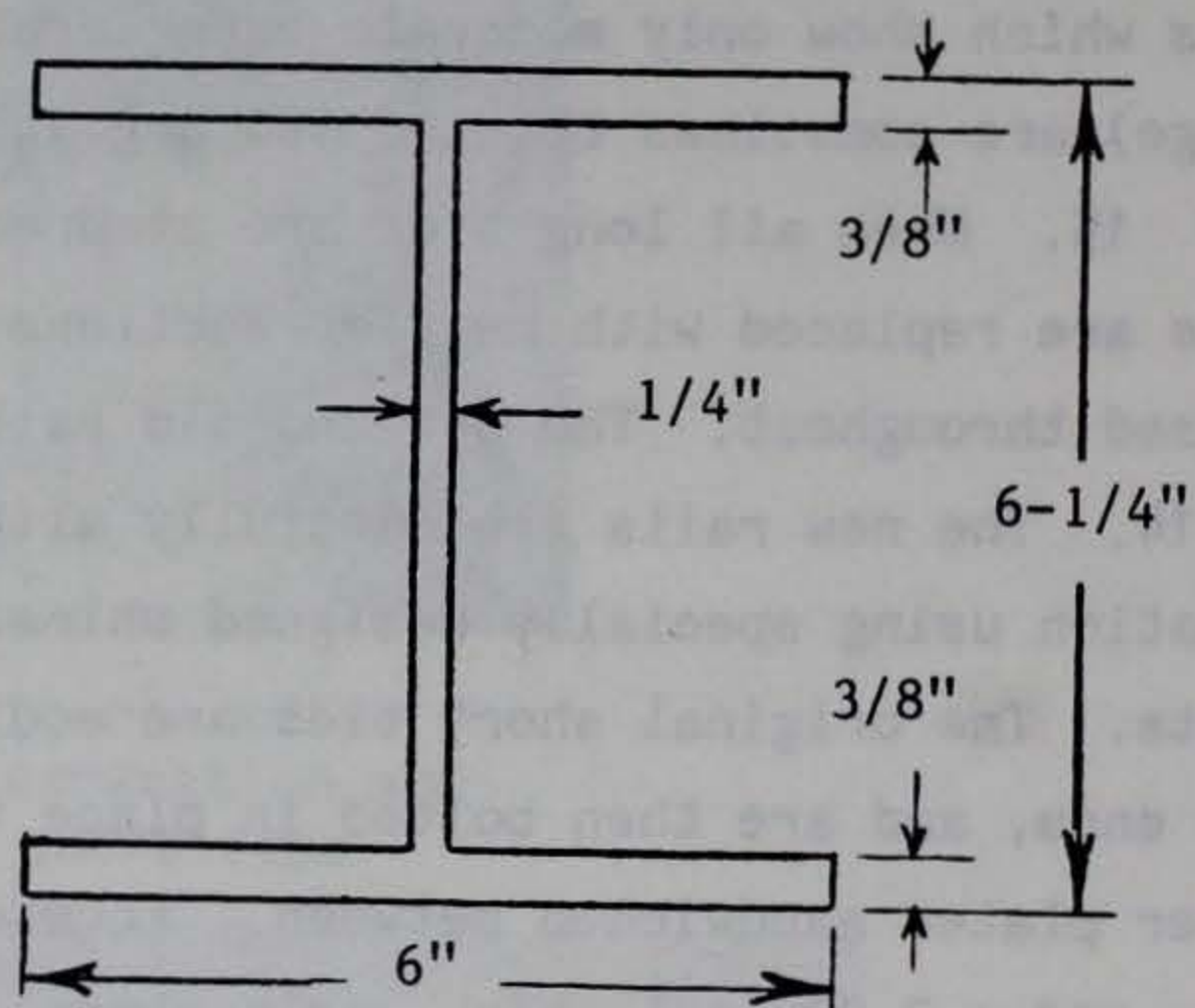
Figure 12. Splice-repair of a damaged long tie. Pipes welded to the tie ends carry loads after the supporting concrete has been removed

require that the replacement section have exactly the same total depth as the original-style tie. Cross-sectional details of the three tie sections are shown in Figure 13. Temporary supports for the waterside ends of all long ties are made by drilling 2-ft-deep, 2-1/2-in.-diameter holes in the concrete foundation at the end of each tie, driving 2-in.-diameter extra strong steel pipes into the holes, and welding the pipes to the ties. This support condition can be seen in Figure 12. When the temporary supports are in place, additional concrete is removed below the tie bottom flanges to assure that the repair foundation is sound. The pipe supports thus carry all loads previously borne by the tie foundation (at the waterside end) for a period of at least several days, during the next steps of the repair procedure. Some additional concrete is removed when a damaged rack section must be replaced. Rack sections which show only moderate deterioration of the wear surface (landside flange) are sometimes rotated 180 deg and reinstalled.

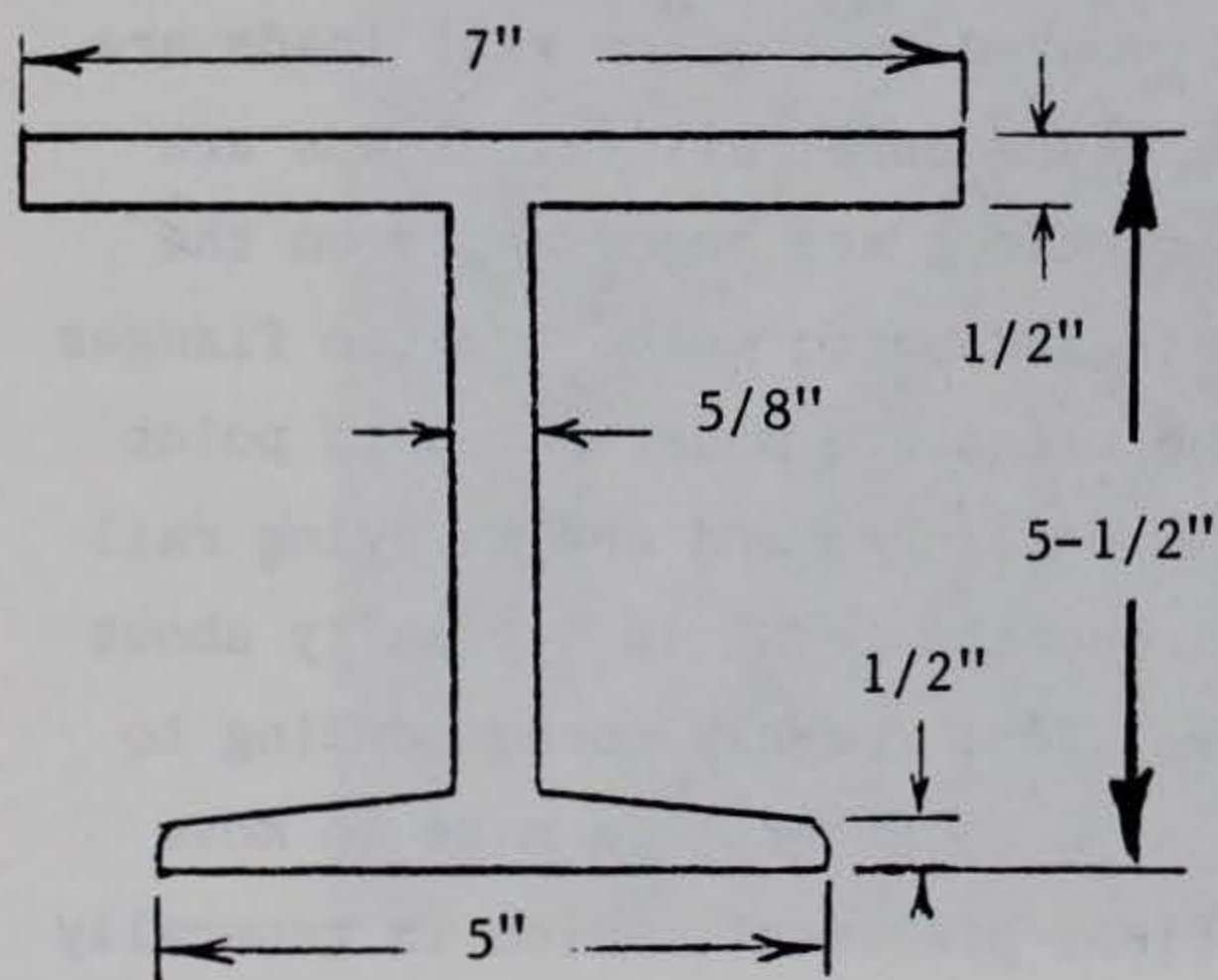
15. When all long ties are secured by pipe supports, the waterside rails are replaced with heavier sections and upgraded connection hardware is used throughout. The new and old rail sections are detailed in Figure 14. The new rails are carefully aligned and brought to the appropriate elevation using specially designed shims. Thermit welds are used at rail joints. The original short ties are modified by welding plates on the landside ends, and are then bolted in place to the new rails, with removable spacer plates sandwiched between. Formwork is constructed around the short ties, and a 3,000-psi, high early strength concrete is cast up to the top flange of the suspended short ties only (Figure 15). After an initial set (no-traffic period), the spacer plates are removed so that no rail loads are transferred to the fresh concrete. After a 24-hr cure, all rail loads are transferred to the short ties and final connections are made; shims on the long ties are removed. Concrete is then cast and cured up to the top flanges of the long ties (Figure 16) and final connections are made. At this point all ties are encased in concrete up to the top flanges and are carrying rail loads, but the rail is still exposed. The concrete level is typically about 1/4 in. below the rail bottom flange between ties, roughly corresponding to the thickness of shims at the tie connections. No attempt is made to move concrete under the rail flange during the final placement, which is generally regarded to function only cosmetically. The repair is complete when the final concrete is cast to the original surface level and crack control joints are



a. Original ties
(long and short)

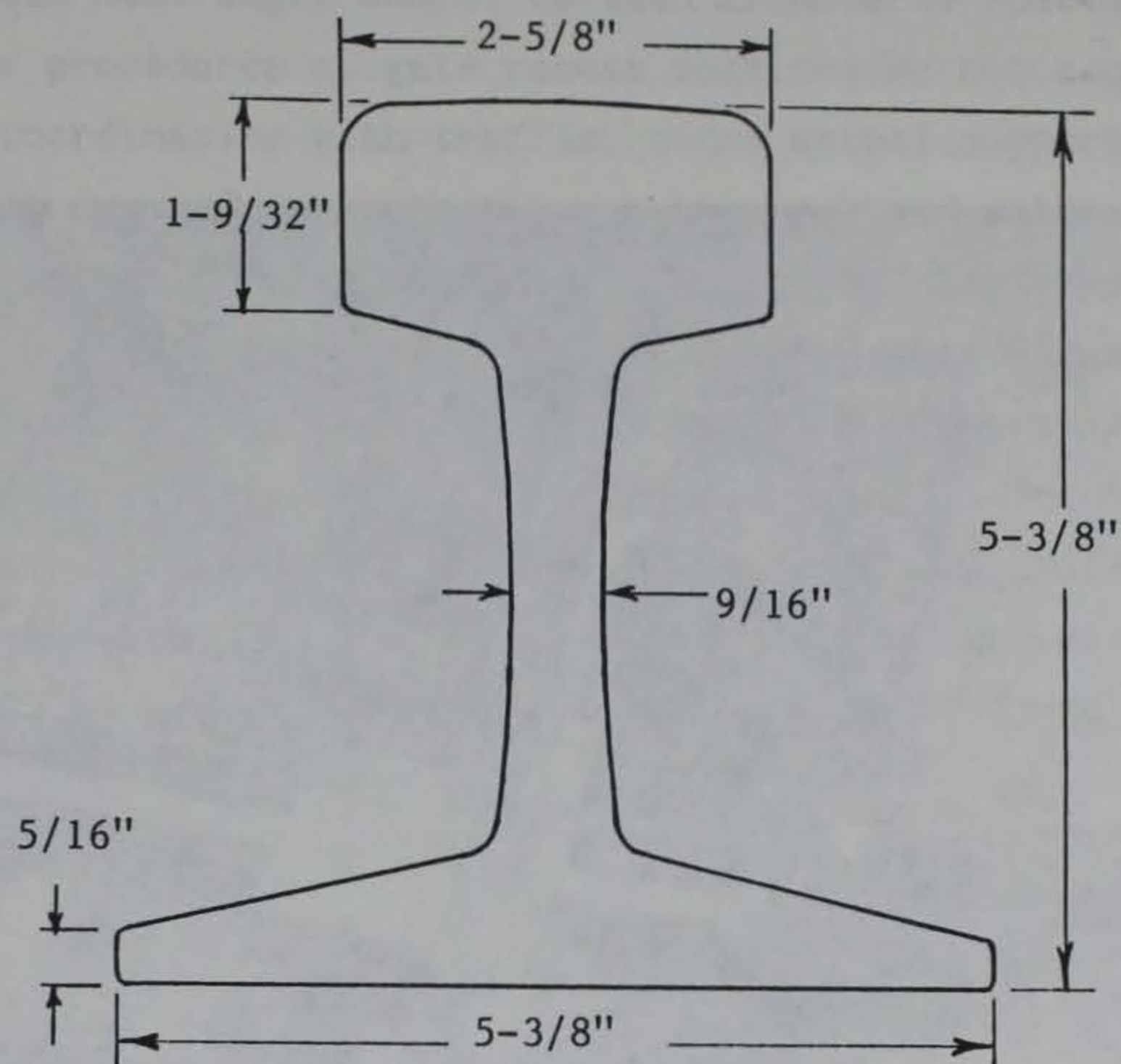


b. Typical long tie replacement section
(W6 x 20 I-beam)

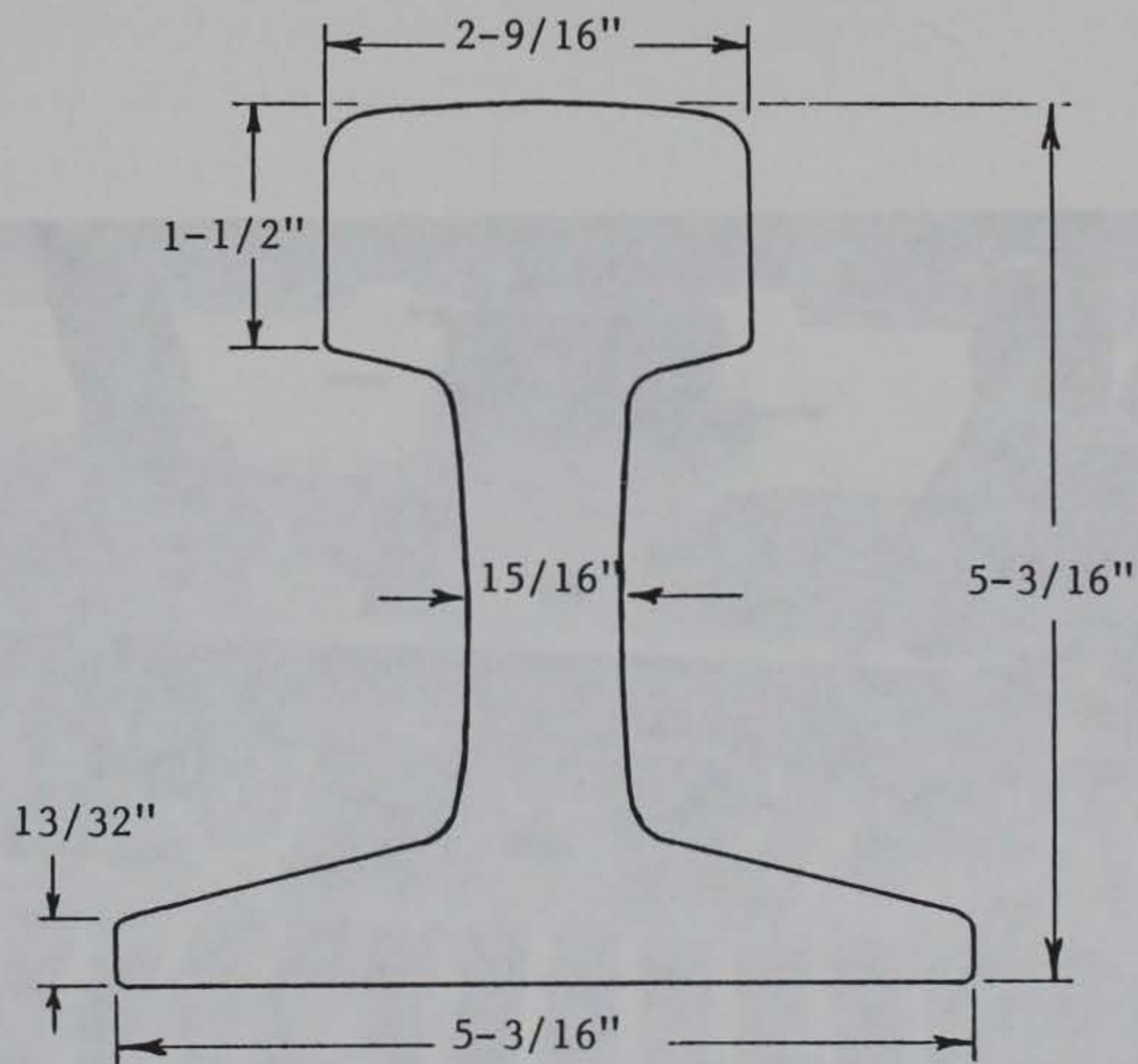


c. Long tie replacement section for special depth-critical locations (inverted ST5 x 17.5 with welded top flange)

Figure 13. Sectional details of crossties



a. Original rail, 90 lb/yd



b. Replacement rail, 105 lb/yd

Figure 14. Cross-sectional details of original and replacement rails

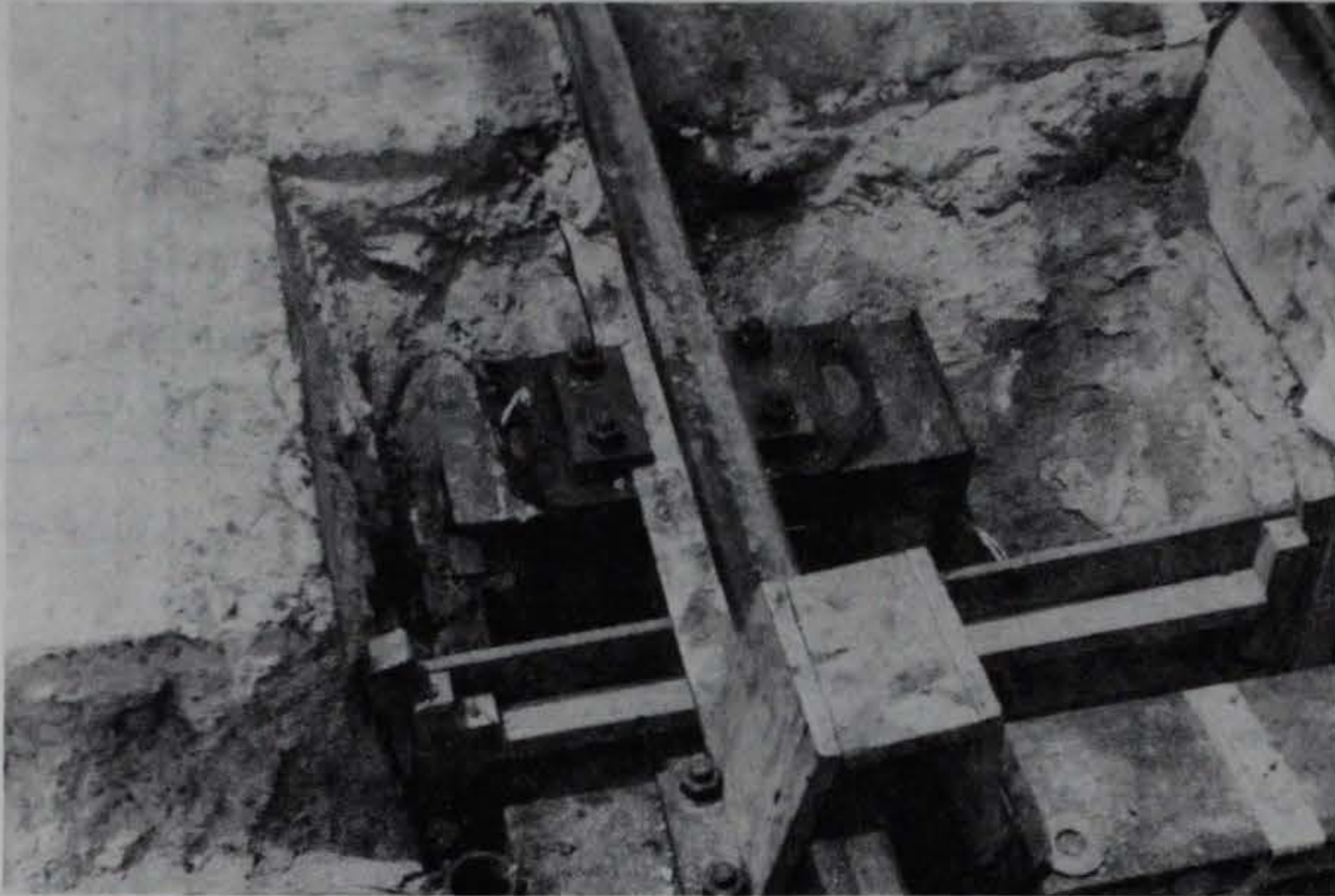


Figure 15. Formwork is constructed around a short tie

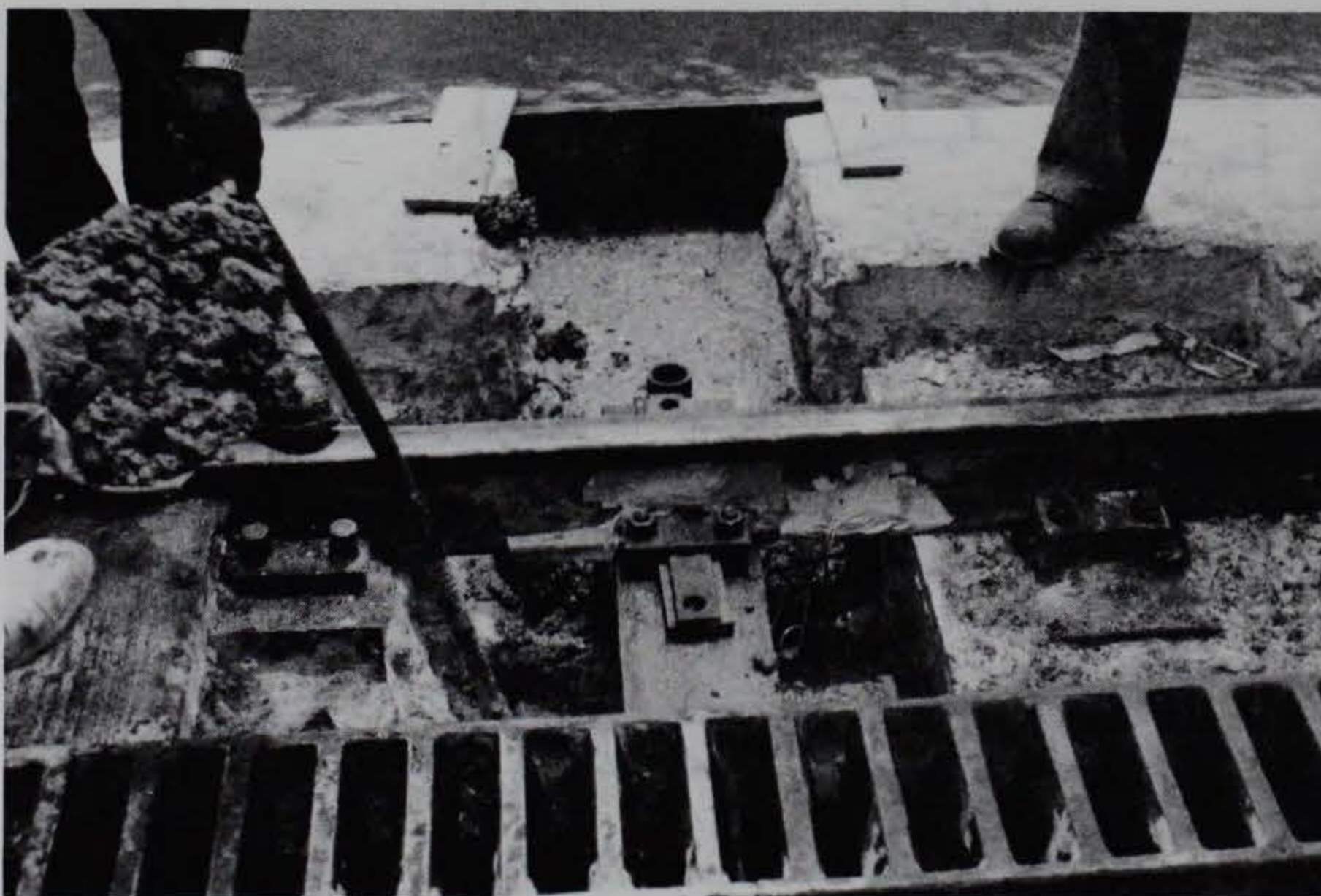


Figure 16. Concrete is cast around a long tie

made along the rail head edges and at certain transverse spacings.

16. Repair procedures at gate recess sections do not require such critical timing and coordination with traffic, since actual support members are not replaced. All damaged concrete between the rack and waterside rail is removed, and the waterside rail is replaced using the heavier section detailed in Figure 14 and upgraded connection hardware. Any damaged rack sections are replaced or rotated, and the tension rods connecting supporting members of the rack and waterside rail (Figure 10) are replaced with 3/8-in.-thick by 4-in.-wide steel straps, which are welded in place. Additional stiffener plates are added to the I-beam which supports the rail. Alignment and elevation of the new rail is carefully adjusted, and new concrete is cast up to the original surface level.

PART III: TESTING PROCEDURES

17. Specific test plans were devised with the primary objectives of obtaining strain data from tow track components at three representative repaired sections under a wide variety of accurately defined locomotive loadings, including actual towing and braking operations. Original plans called for placing strain gages on the component members being used in repair procedures at each site and installing those components during the actual repair of the track section in which that test site was located, with as little departure from normal repair operations as possible. Component sections being replaced at each site were to be strain-gaged under laboratory conditions before being transported to the site for use. Repairs to the track section spanning a test site were to be performed according to normal repair procedures and schedules. Tests were to begin at a site as soon as that track section was completed and returned to normal service, and were to include a preplanned array of loading conditions.

18. On-site testing is usually done under circumstances which are less ideal than those in the laboratory, but work on the tow track structure posed some particularly unusual problems. A locomotive passes any given track location an average of 12 times per hour except during the traffic window periods. Any test procedures which could not be accomplished around the steady traffic were reserved for the brief midday window period. The passing of each locomotive left fresh deposits of grease and hydraulic fluid on tow track components, and seasonal afternoon rainshowers had to be contended with. A few unexpected details required some modifications to original test plans. It was not discovered until construction of test sections was near completion that the ties provided for strain gaging and testing were not those typically used in repairs. Also, repairs had already been completed at two of the three track sections to be strain-gaged, each with an open space in the new construction left to accommodate the strain-gaged components. The insertion of one or two tie supports and placing of concrete within a previously repaired section was, of course, a nontypical detail with respect to normal repair procedures.

19. The three test locations were along the east wall of the lower, eastside chamber of the Miraflores Locks. Site 1 was near the north end of the chamber and was characterized by the typical crosstie-supported, concrete

foundation construction. Site 2 was in a gate recess area at the south end of the chamber. Site 3 was near the center of the chamber and was identical in construction to site 1. Some consideration had been given to the selection of the third site in an area where the tow track spanned a below-deck opening. The specific details of this construction type vary among locations, however, and the observed structural damage to rails, racks, and ties in these areas resembled that in concrete foundation areas. The selection of a test section identical to site 1 was favored, considering the statistical value of duplicate tests and the importance of test data from this construction type. Over 85 percent of the damaged tow track throughout the locks is of the concrete foundation construction type.

20. Instrumentation included up to 48 channels of active electronic measurements which were recorded on analog tape during testing at each site. The gages used were primarily strain gages placed on tow track structure components, but also included pressure transducers which monitored the hydraulic pressure of the windlass drives (as a measure of cable tension), a tension load cell (for verification of theoretical hydraulic pressure-cable tension relationships), accelerometers mounted on locomotives, and deflection gages on the gate recess cantilever girders. Strain gage locations were chosen with the objectives of obtaining data which would help identify deformation and quantify strain levels in each of the concerned track components. Most gages could not be located exactly at the points of anticipated maximum strains due to the proximities of connection hardware and wheel contact and the constraints of gage placement techniques.

Preparation of Test Sections

21. Gage layout details for each of the three test sites are shown in Figures 17 through 22. When new component sections were available for instrumenting prior to installation, adhesive-type strain gages were placed under controlled conditions (Figures 23 through 25). These components included the ties at sites 1 and 3 and the rail and rack at site 2. Adhesive strain gages could not be used on those components already in place due to insufficient no-load time periods and the inaccessibility and surface conditions of the gage locations. Weldable strain gages were used for these applications (Figure 26).

22. Preparation procedures were quite similar at test sites 1 and 3

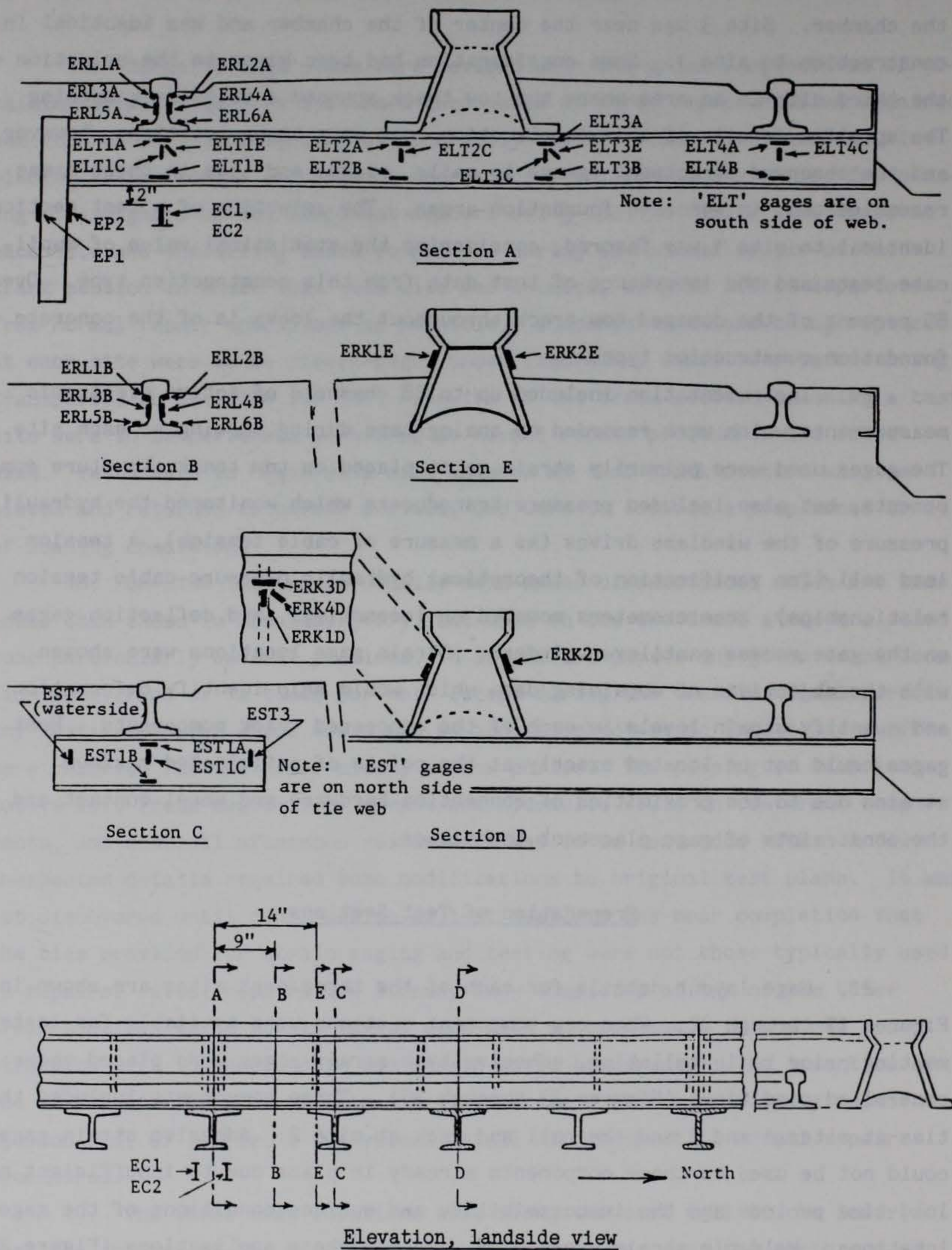


Figure 17. Gage locations, site 1

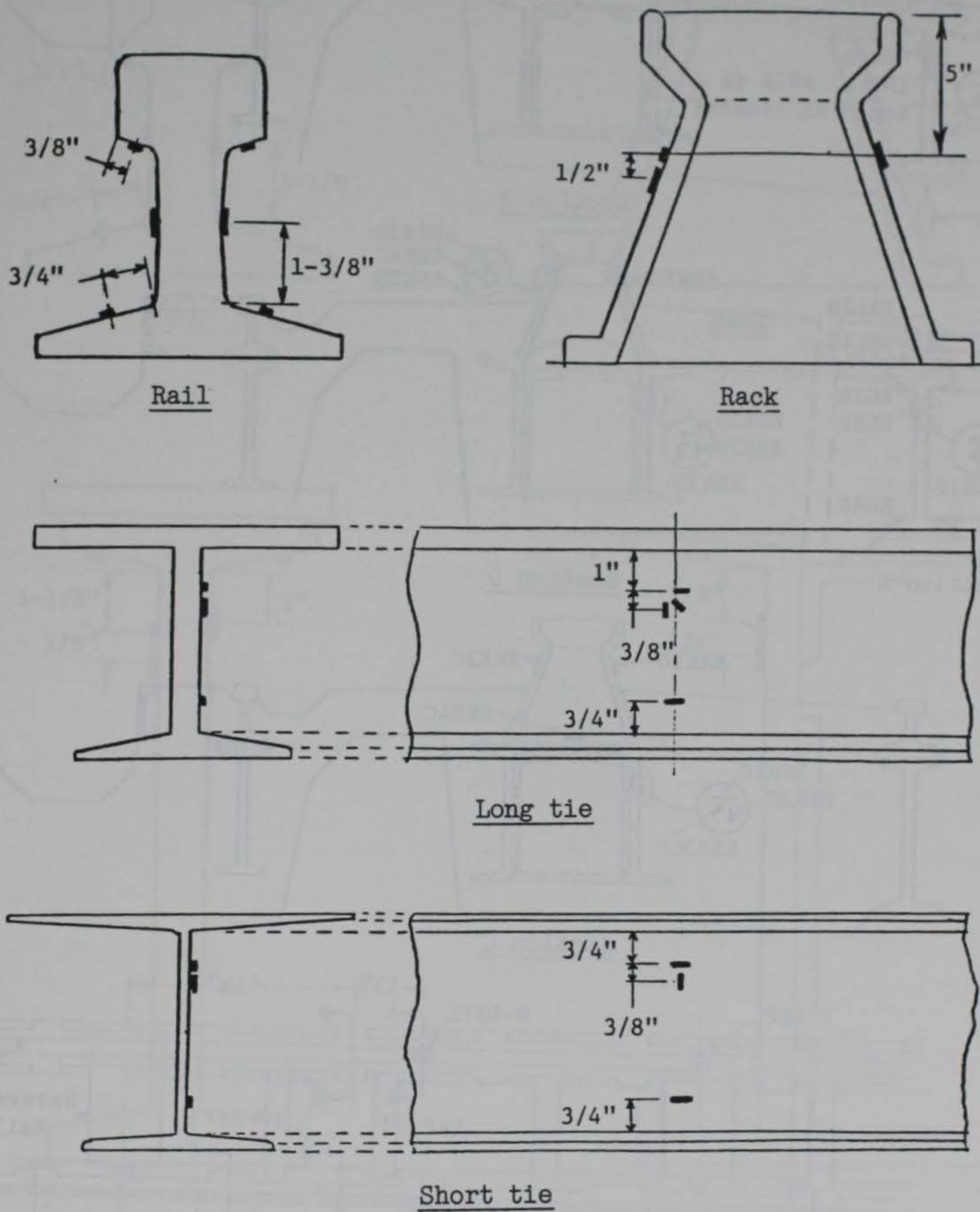


Figure 18. Strain gage location details, site 1

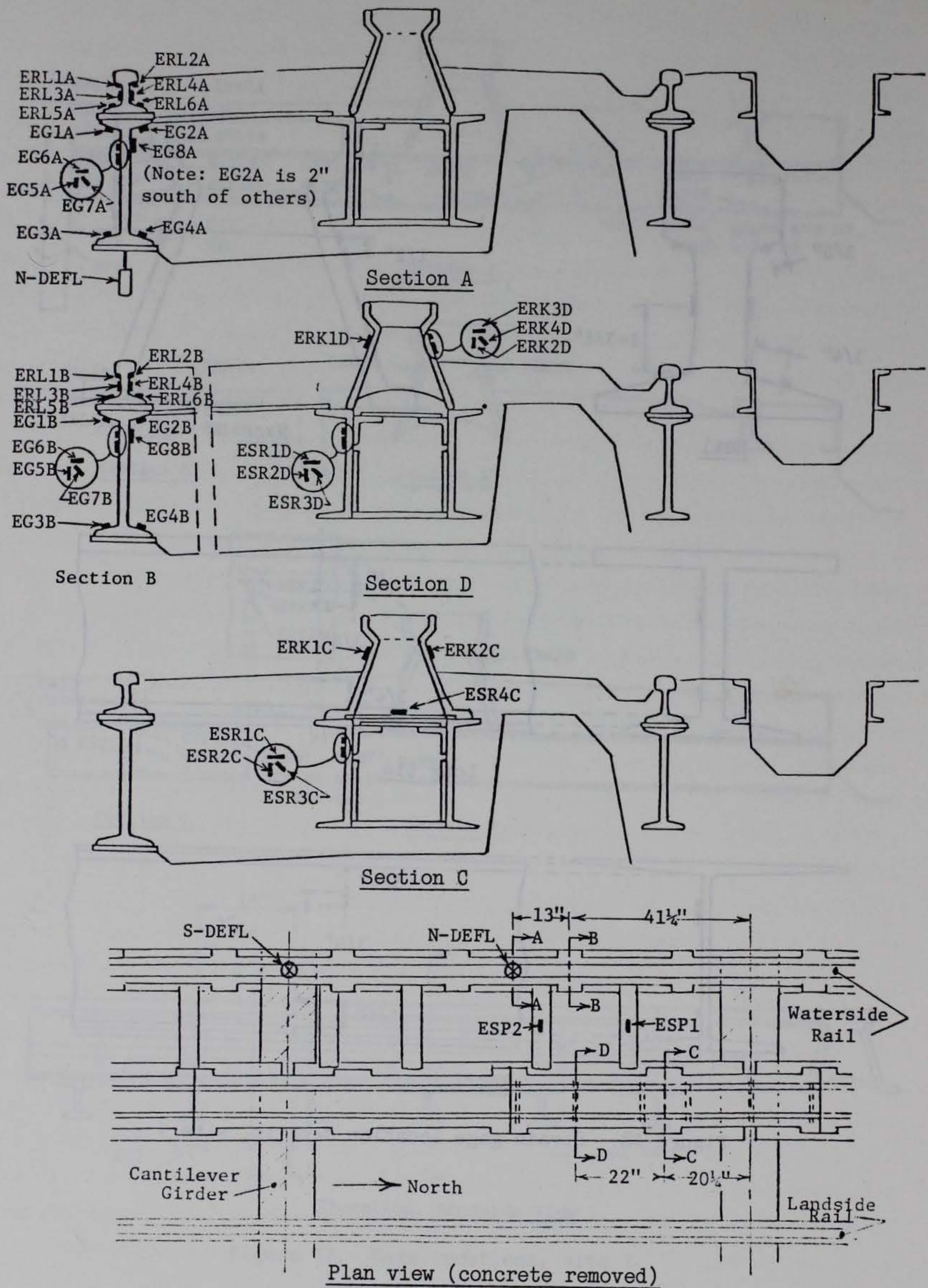
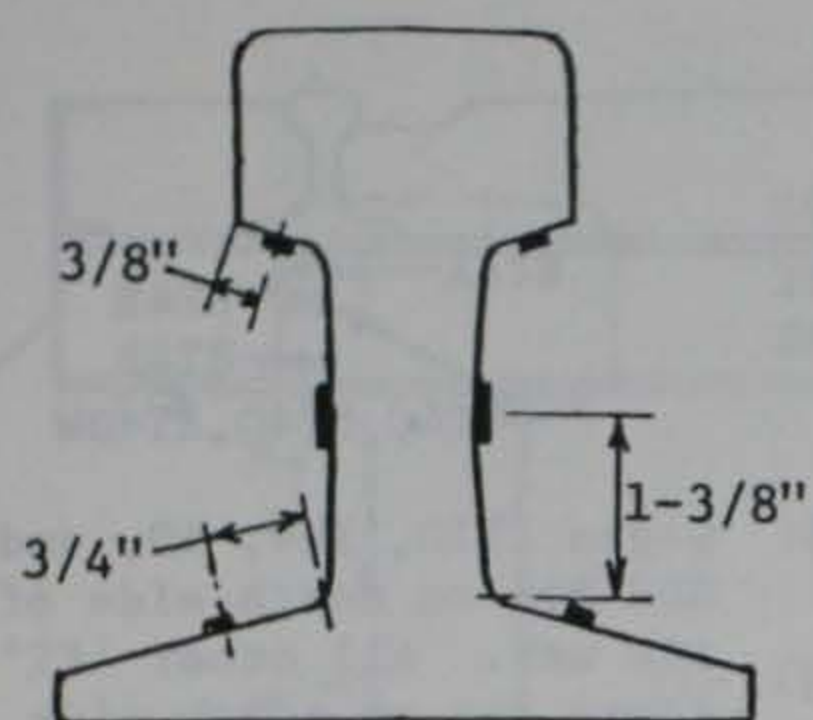
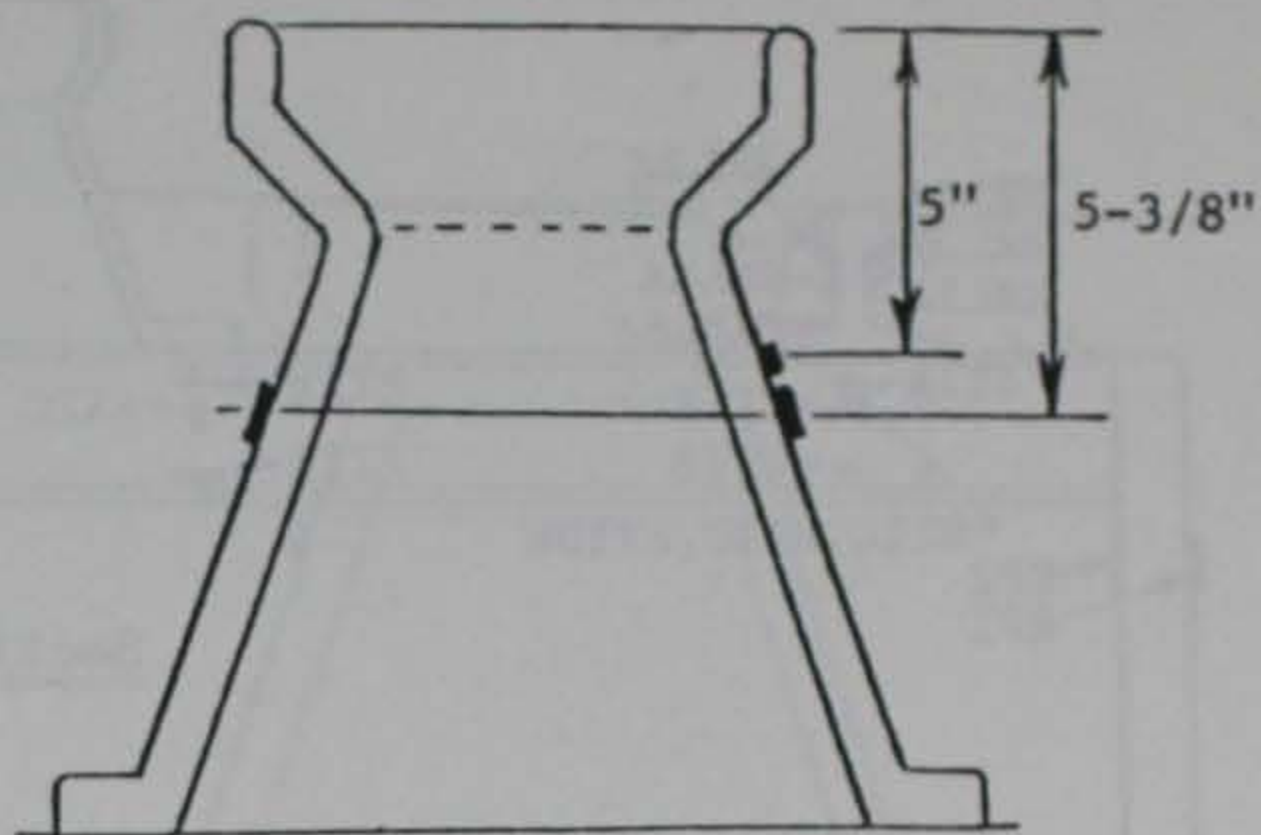


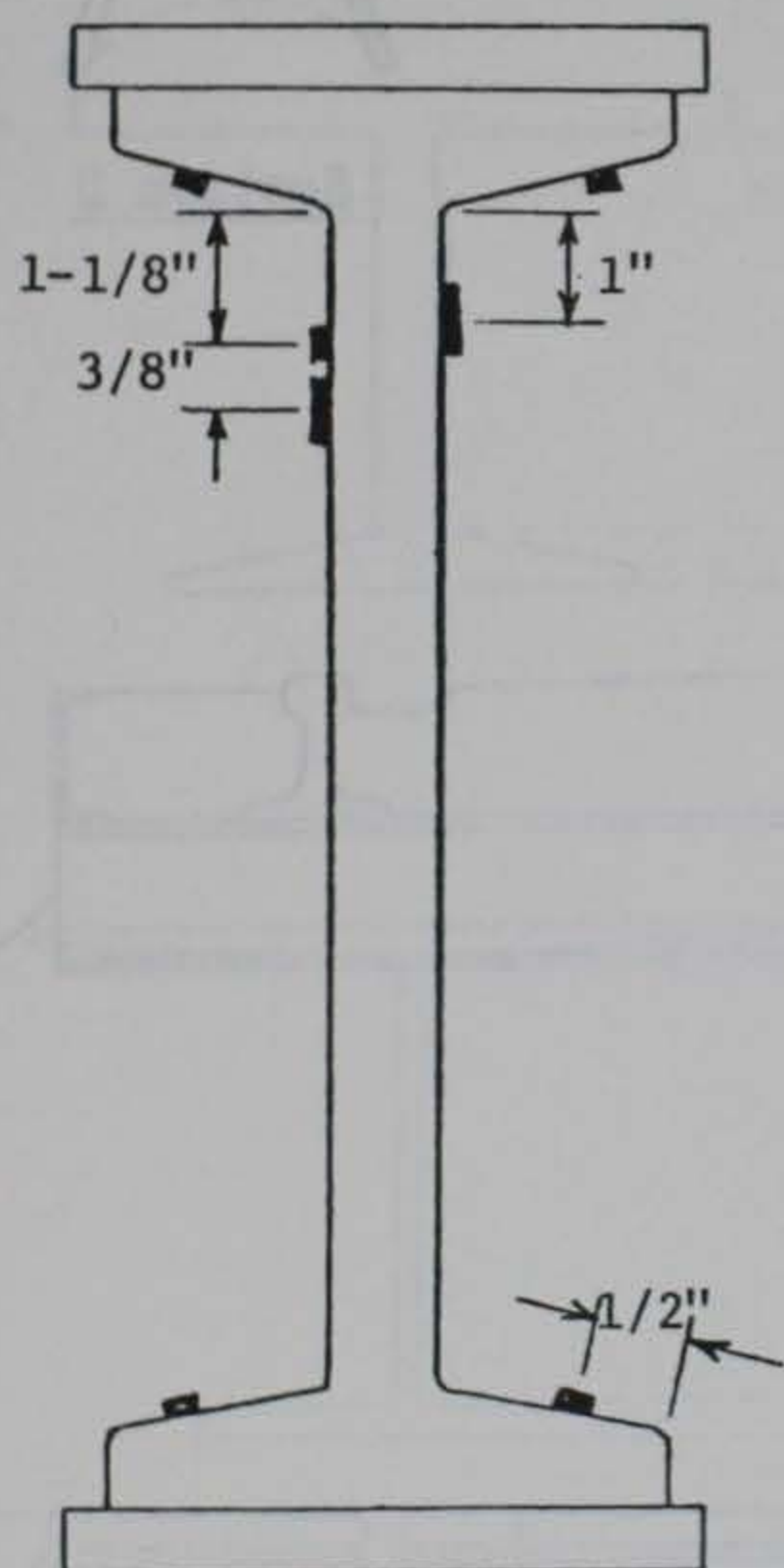
Figure 19. Gage layout, site 2



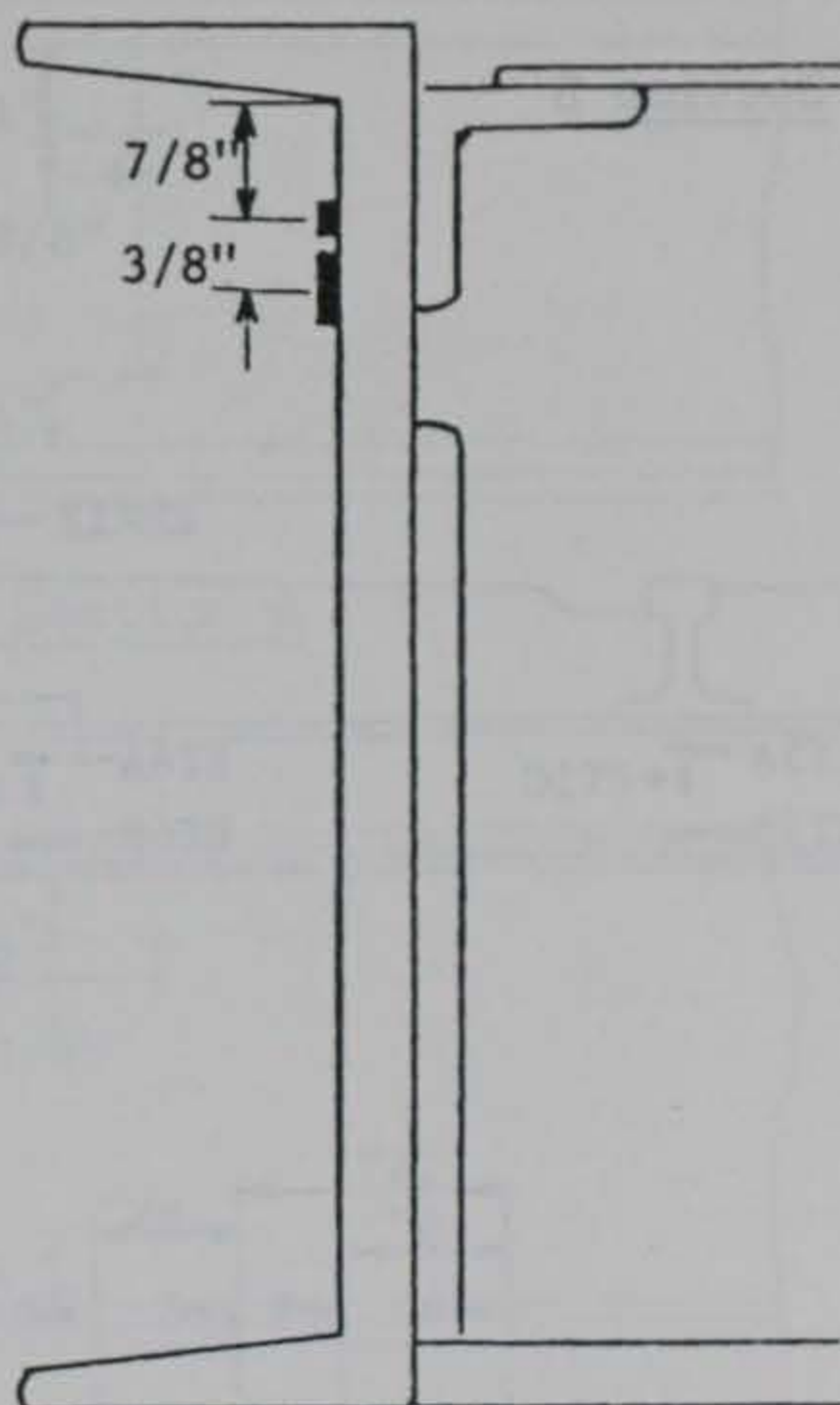
Rail



Rack



Girder



Stringer channel

Figure 20. Strain gage location details, site 2

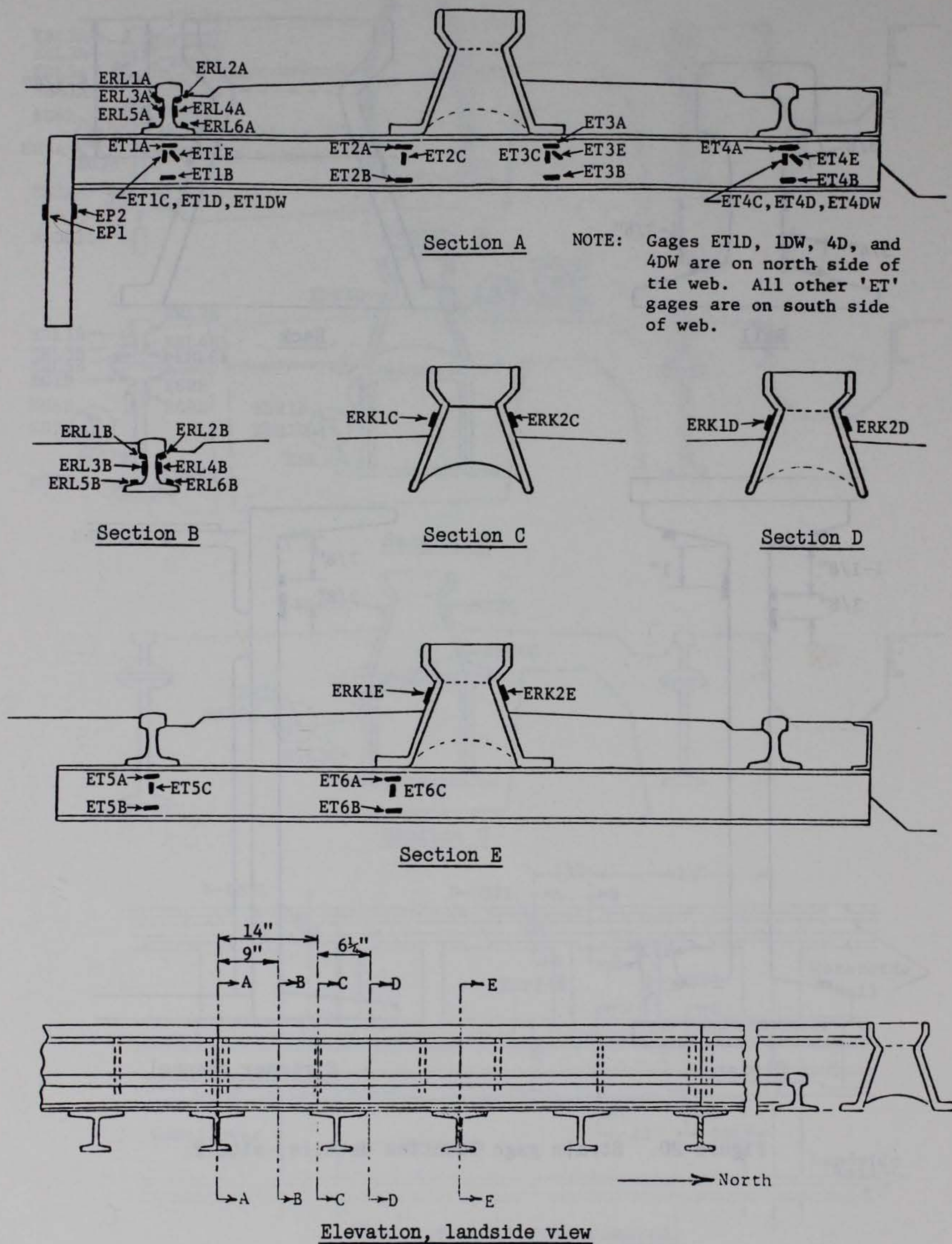
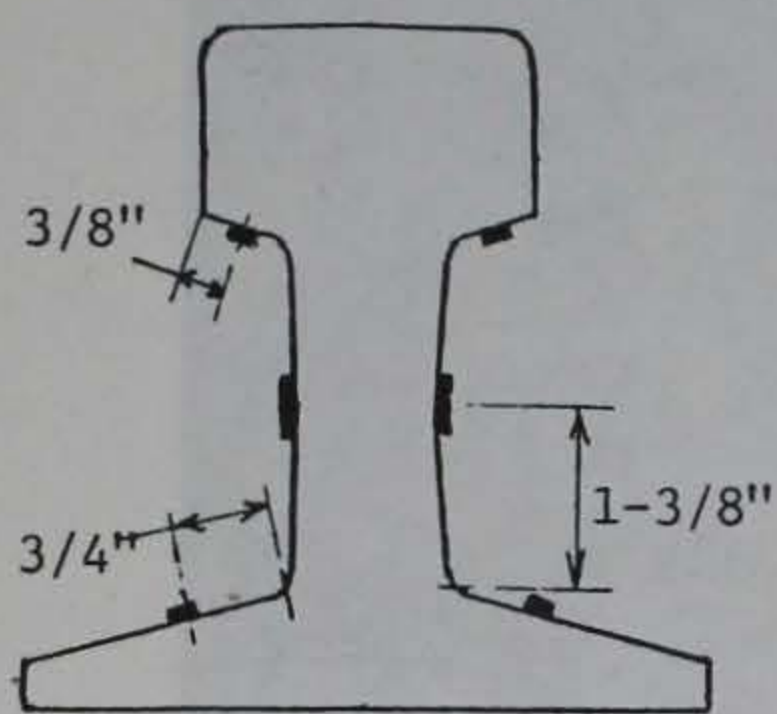
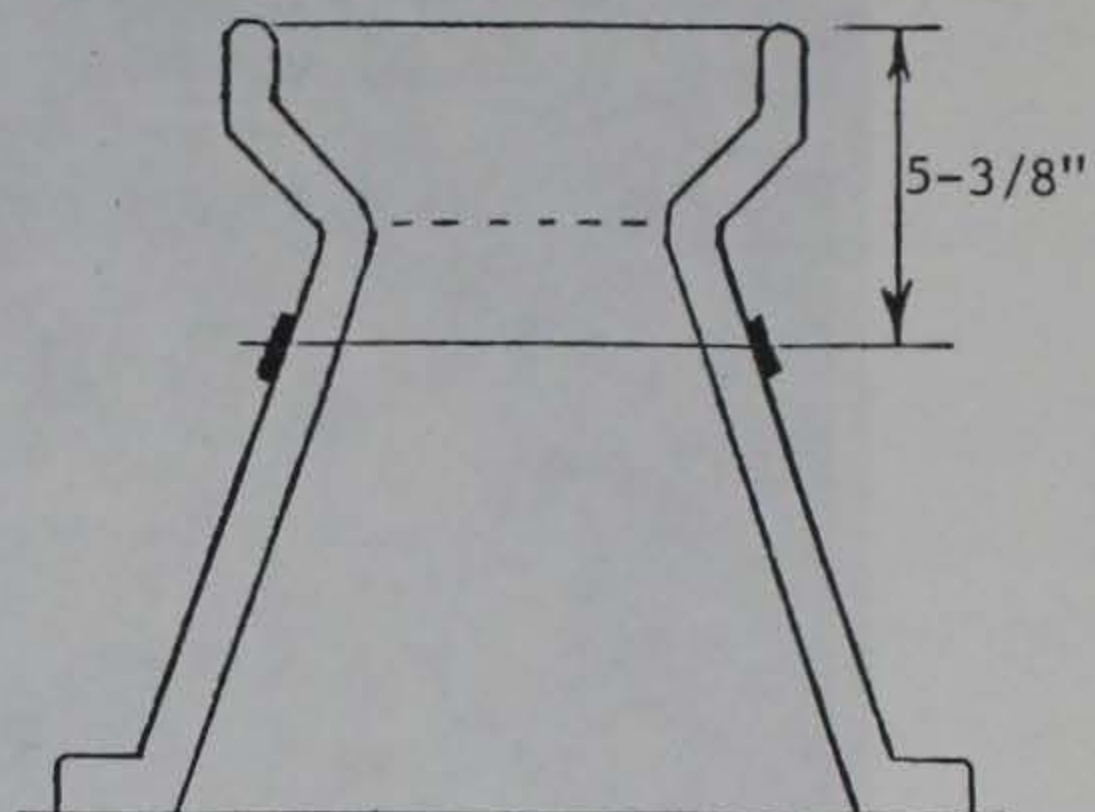


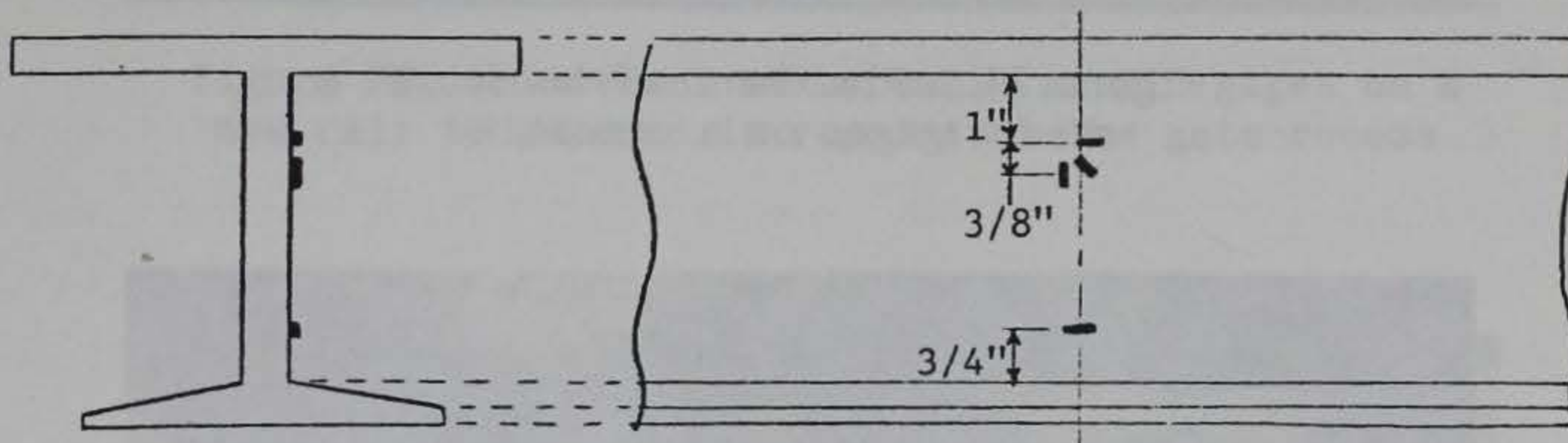
Figure 21. Gage layout, site 3



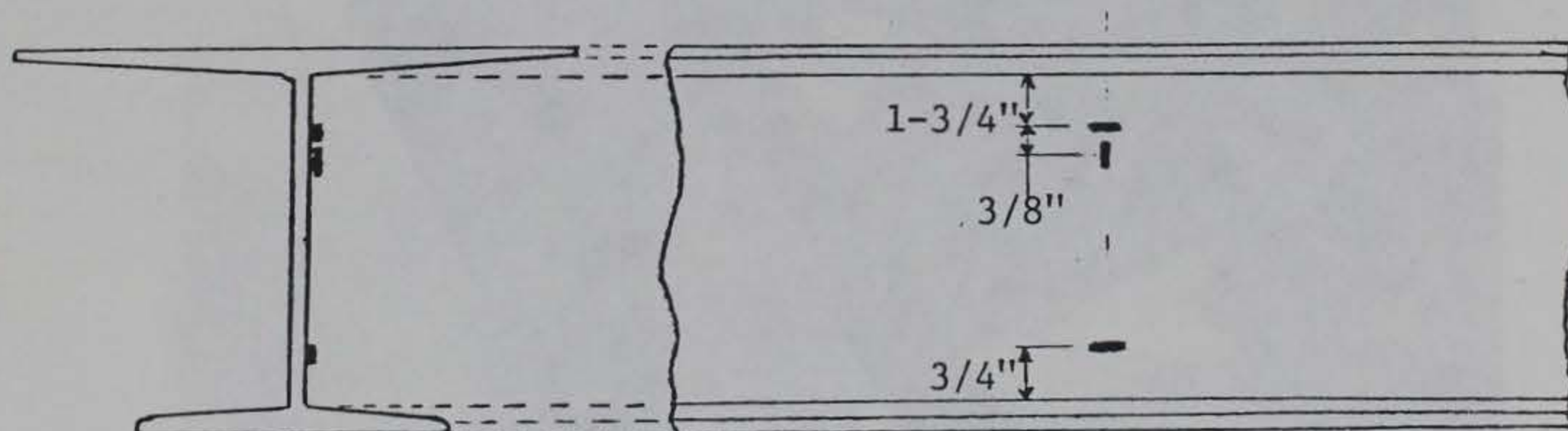
Rail



Rack



Tie - Section A



Tie - Section E

Figure 22. Strain gage location details, site 3

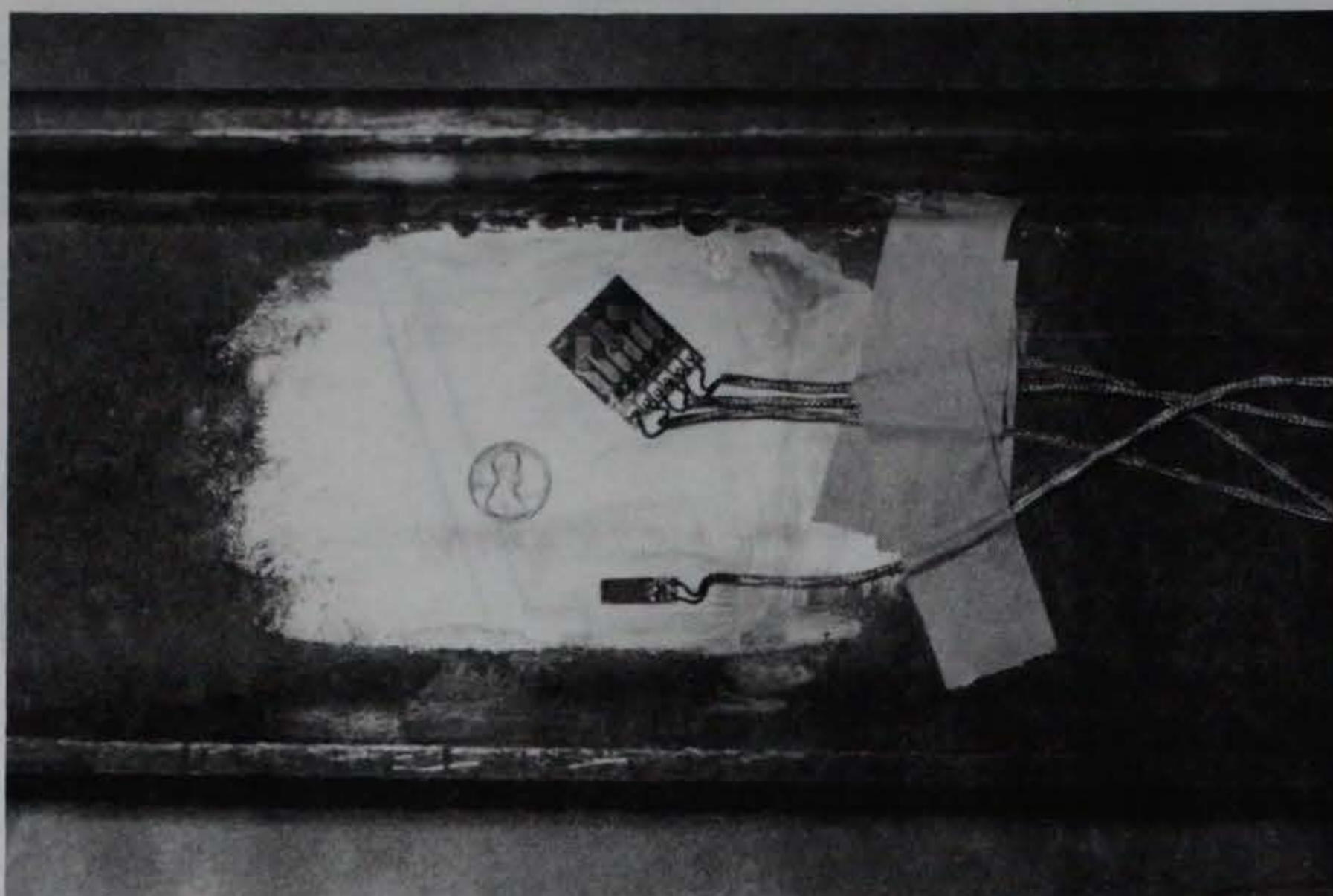


Figure 23. Placement of bondable strain gages on a crosstie



Figure 24. Application of protective coatings on strain gages and cables

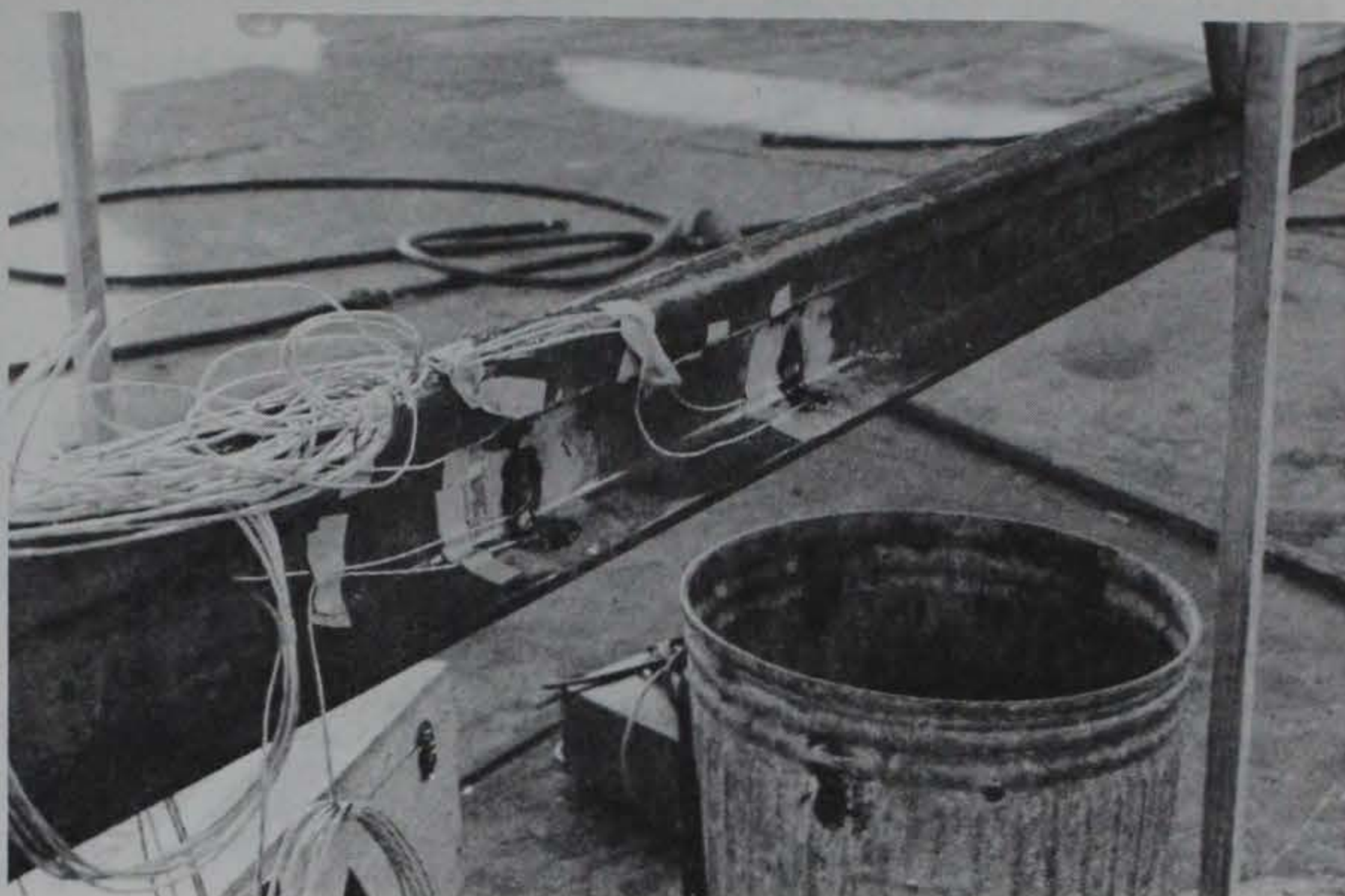


Figure 25. Placement of bondable strain gages on a new rail to be used in repairs at the gate-recess

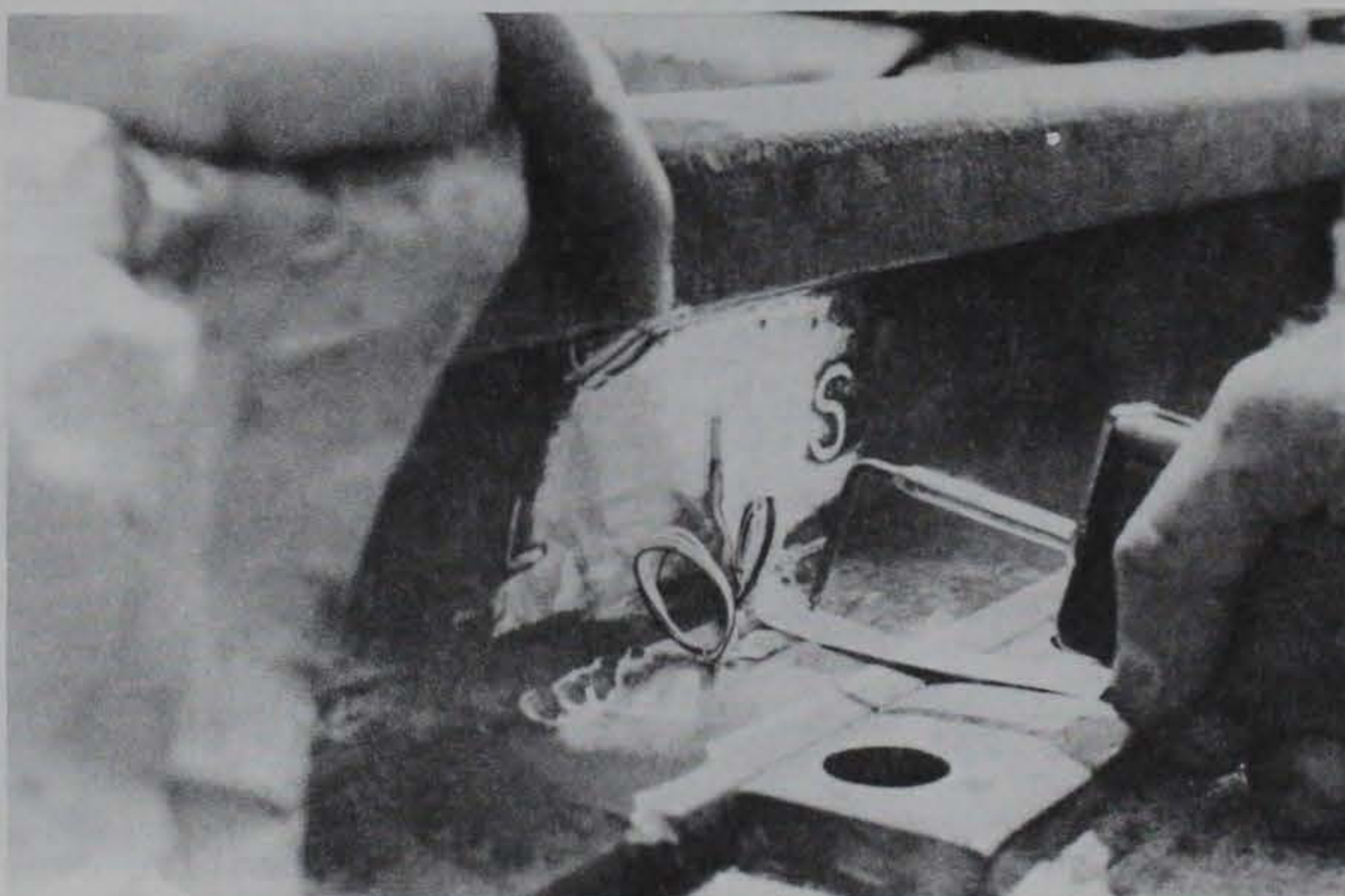


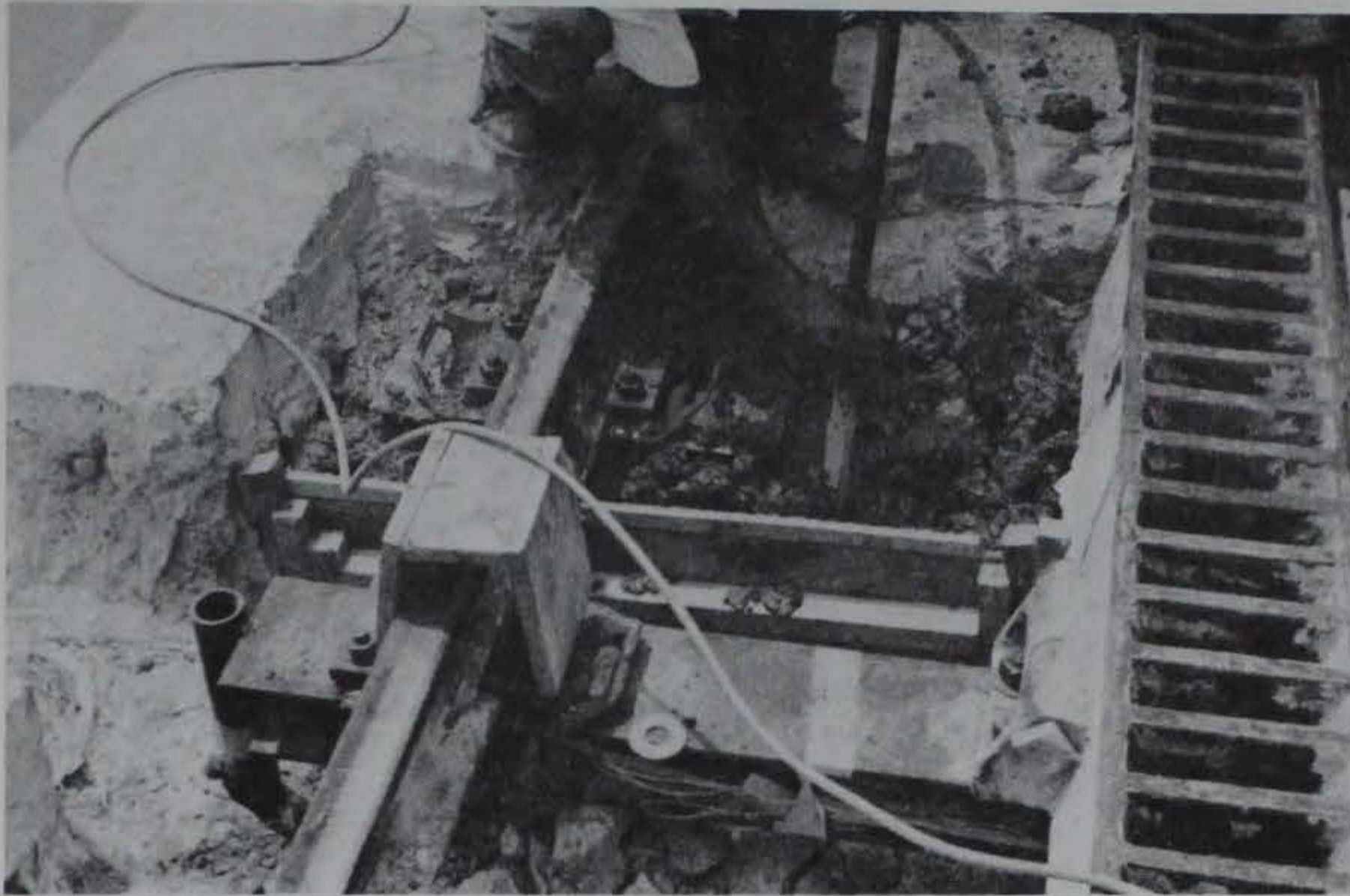
Figure 26. Placement of weldable strain gages on a rail already in service

since the structural details were identical. Assembly of the components and placing of concrete were done by the PCC repair crews in accordance with the established repair procedures. One long tie at each site and one short tie at site 1 were replaced with new sections which had been strain-gaged in a nearby workroom. Gage layouts at the two sites were essentially the same except that weldable strain gages on the web of an adjacent original long tie were used at site 3 in place of the gages on a short tie at site 1. All gage cables were routed through conduits under the conductor slot first to nearby junction boxes which contained Wheatstone bridge completion circuits, and in turn to the shelter which housed the data recording equipment. Hardware connections and concrete placement at site 1 were made in accordance with alternate tie procedures (paragraphs 14 and 15). All ties adjacent to the new one at site 3 (including short ties) were already encased in concrete and carrying loads, so only one placement was required to bring all concrete in the test section to the upper tie flange elevation. Photos of the assembly and construction at sites 1 and 3 are shown in Figures 27 and 28.

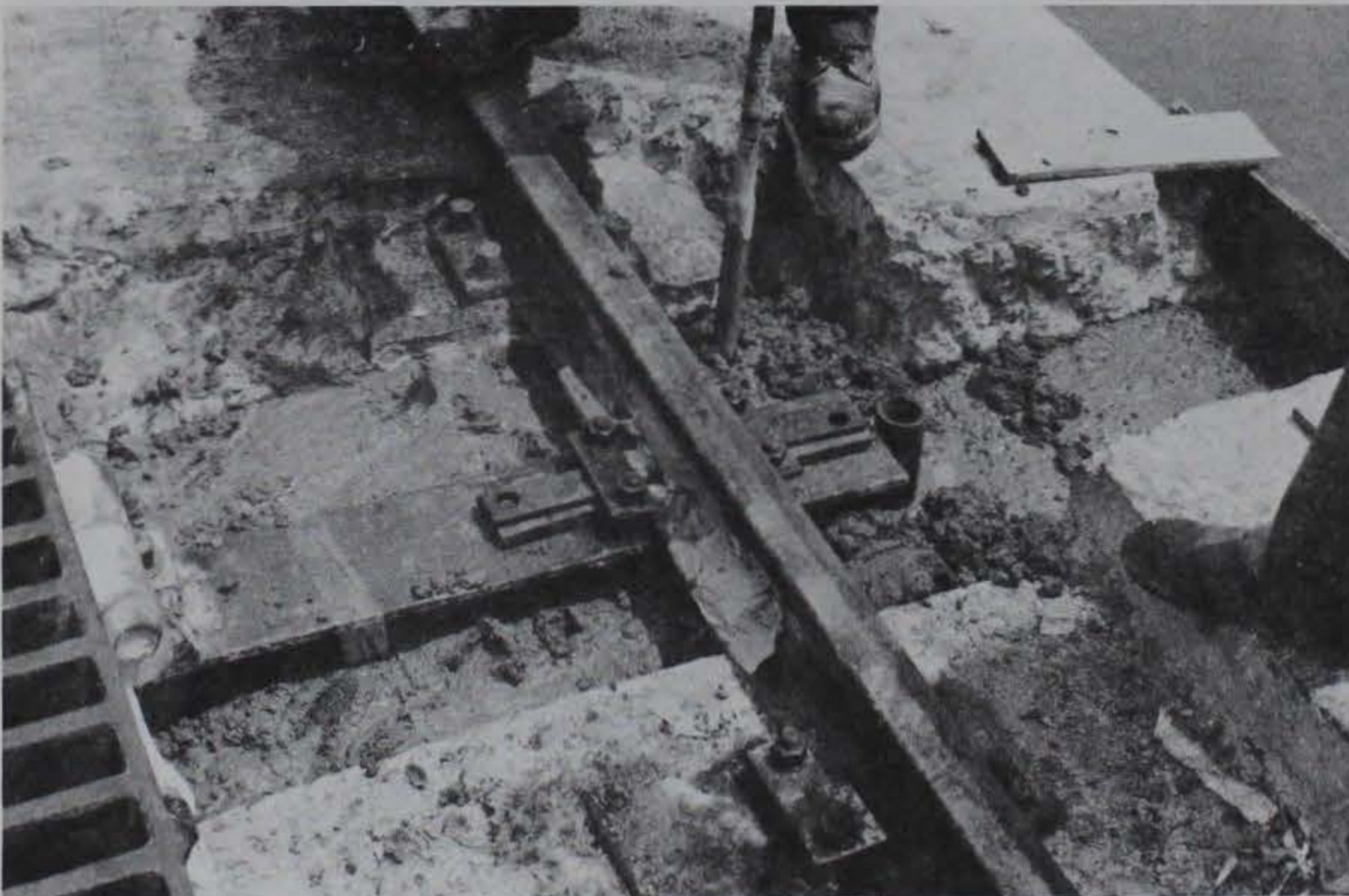
23. Test site 2 was prepared for testing during the actual repairs of the entire gate recess section. The new waterside rail, rack section, and tension straps to be used were strain-gaged with adhesive-type gages prior to installation. Weldable strain gages were placed on the rail-supporting girder and stringer channel (part of the built-up structure which supports the rack) after the confining concrete was removed. Deflection gages for monitoring any movement of the cantilever girders were attached to specially constructed steel supports which were anchored into the lock wall. All new concrete in the gate recess section was cast at one time, completing the repair. Figure 29 shows views of the gate recess repairs and test site preparation.

Test Methods

24. For purposes of recording and identifying data, each individual test consisted of the passing of both axles of one locomotive over the test section. Data signals were continuously recorded on magnetic tape during each test, beginning a few seconds before the arrival of an approaching locomotive and ending when the locomotive had gone a short distance past the instrumented area. A total of 74 individual tests were conducted, including 37 at site 1, 20 at site 2, and 17 at site 3.



a. Concrete is cast around instrumented short tie while pipe-supported long tie carries rail loads

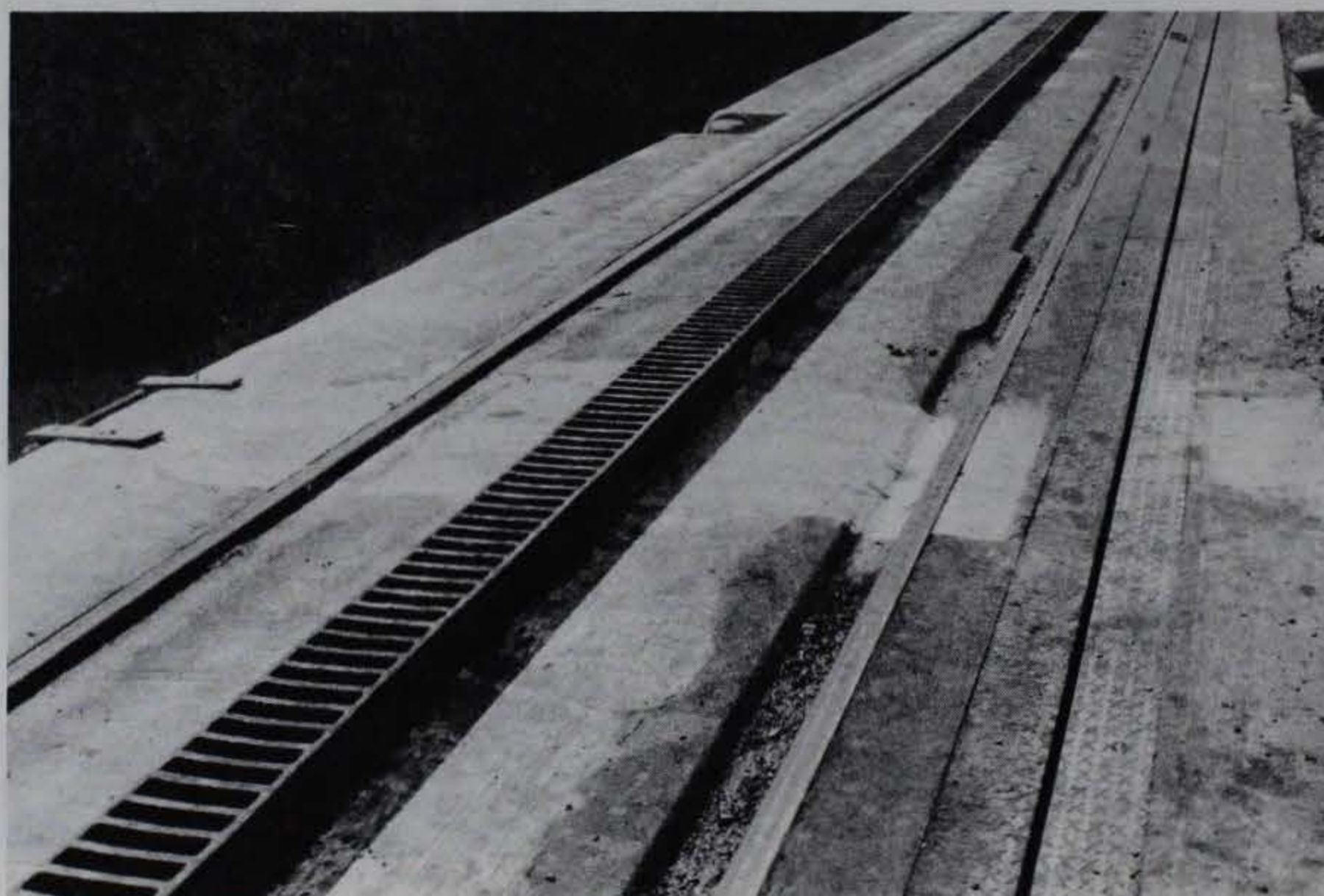


b. Load is transferred to short ties (next day) and concrete is cast around instrumented long tie

Figure 27. Construction at test site 1 (Continued)

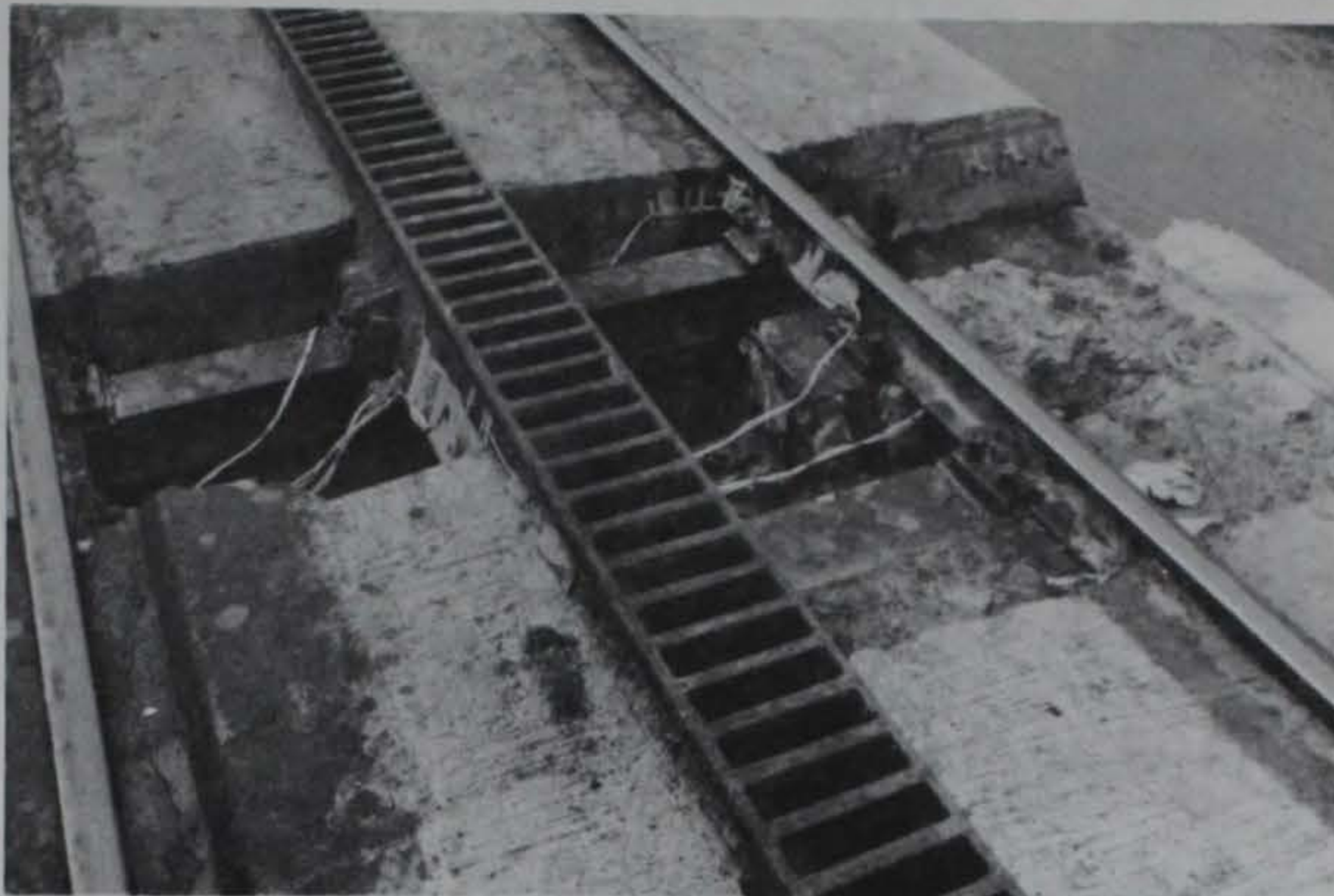


c. After a 24-hr cure, final connections are made at all ties, and surface concrete is cast

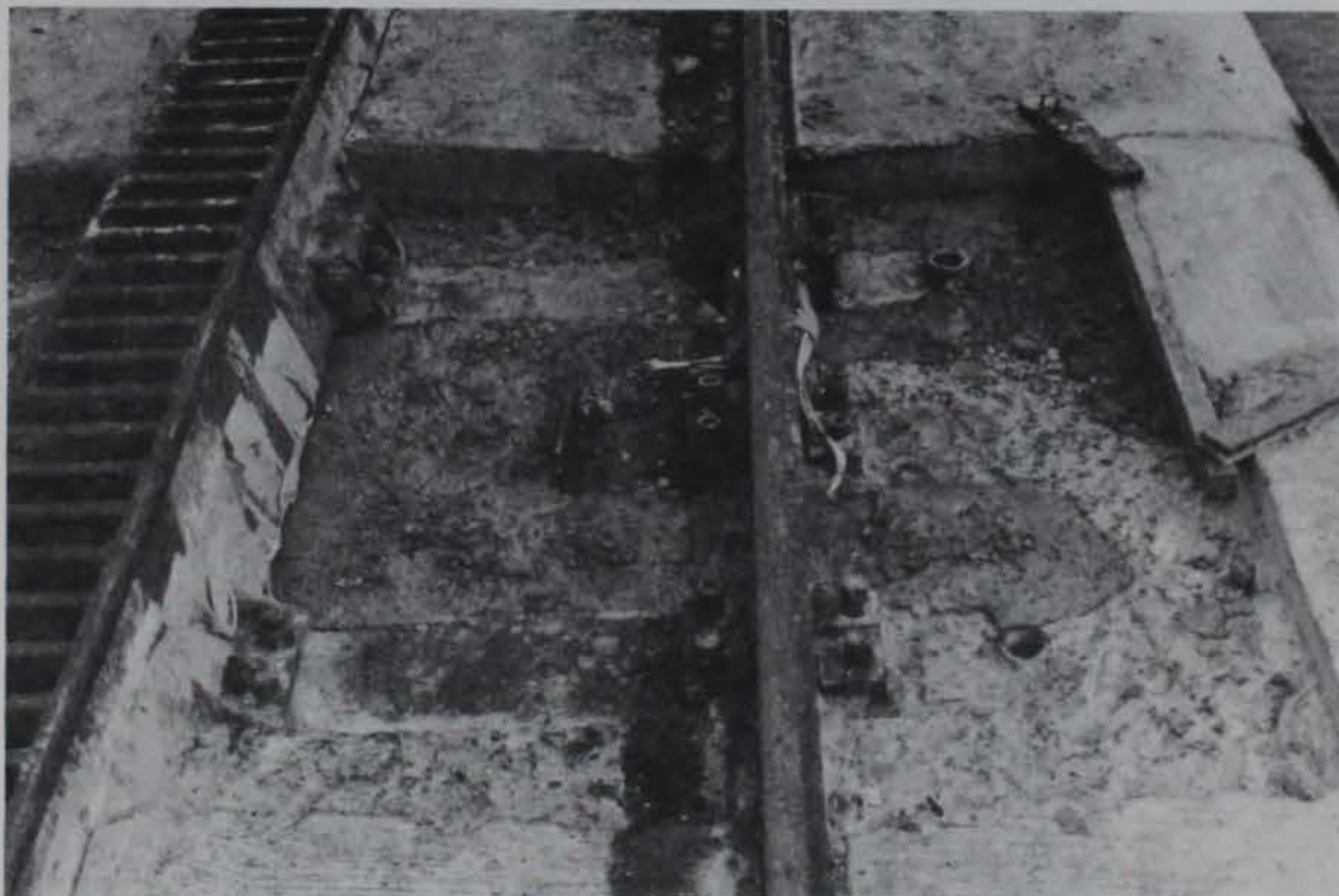


d. Completed repair

Figure 27. (Concluded)

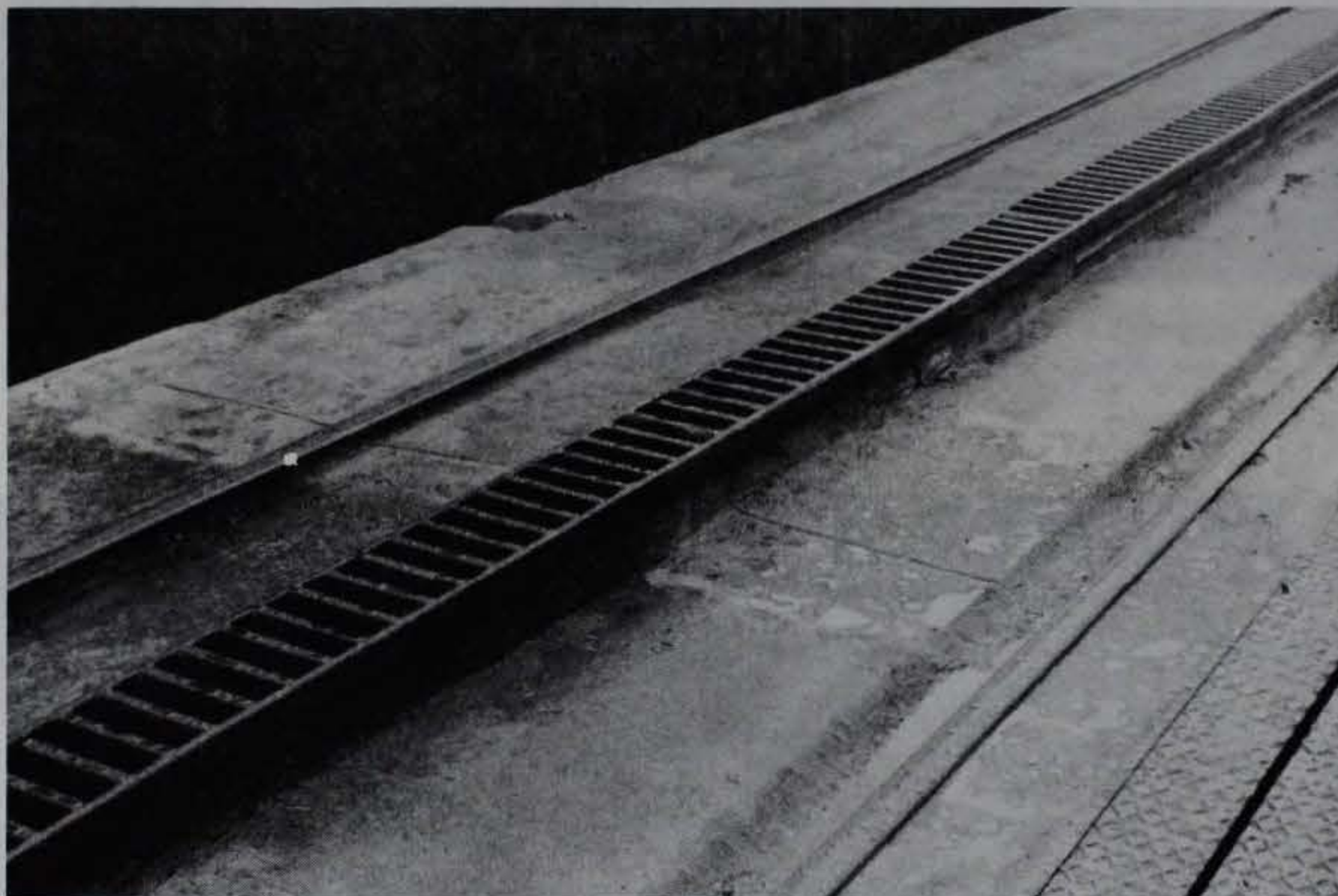


a. Instrumented long tie is installed



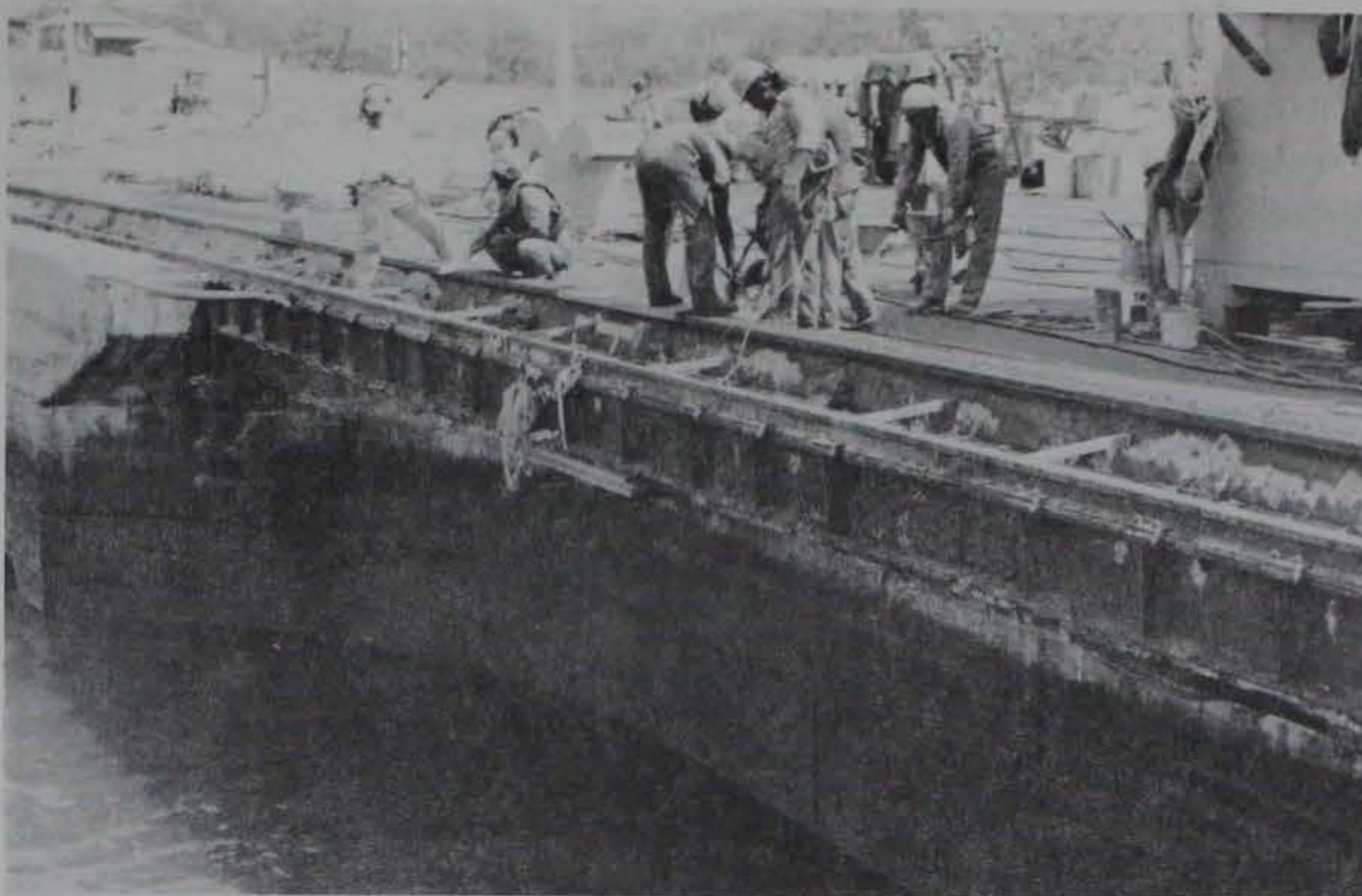
b. Concrete is cast to the top flanges of ties. The instrumented long tie carries no loads until shims are inserted and connections made after a 24-hr cure

Figure 28. Construction at test site 3 (Continued)

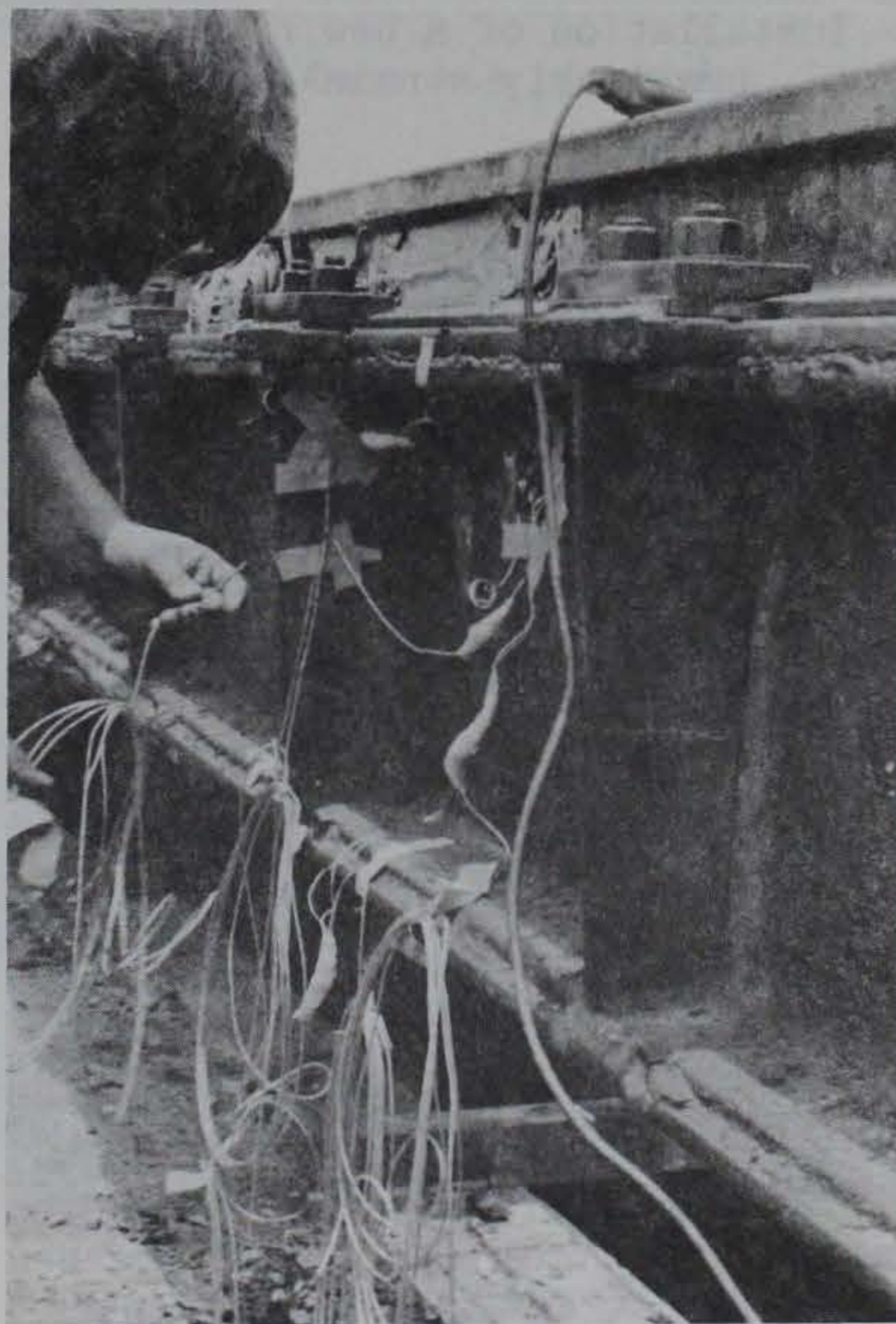


c. Surface concrete is cast, completing the repair

Figure 28. (Concluded)

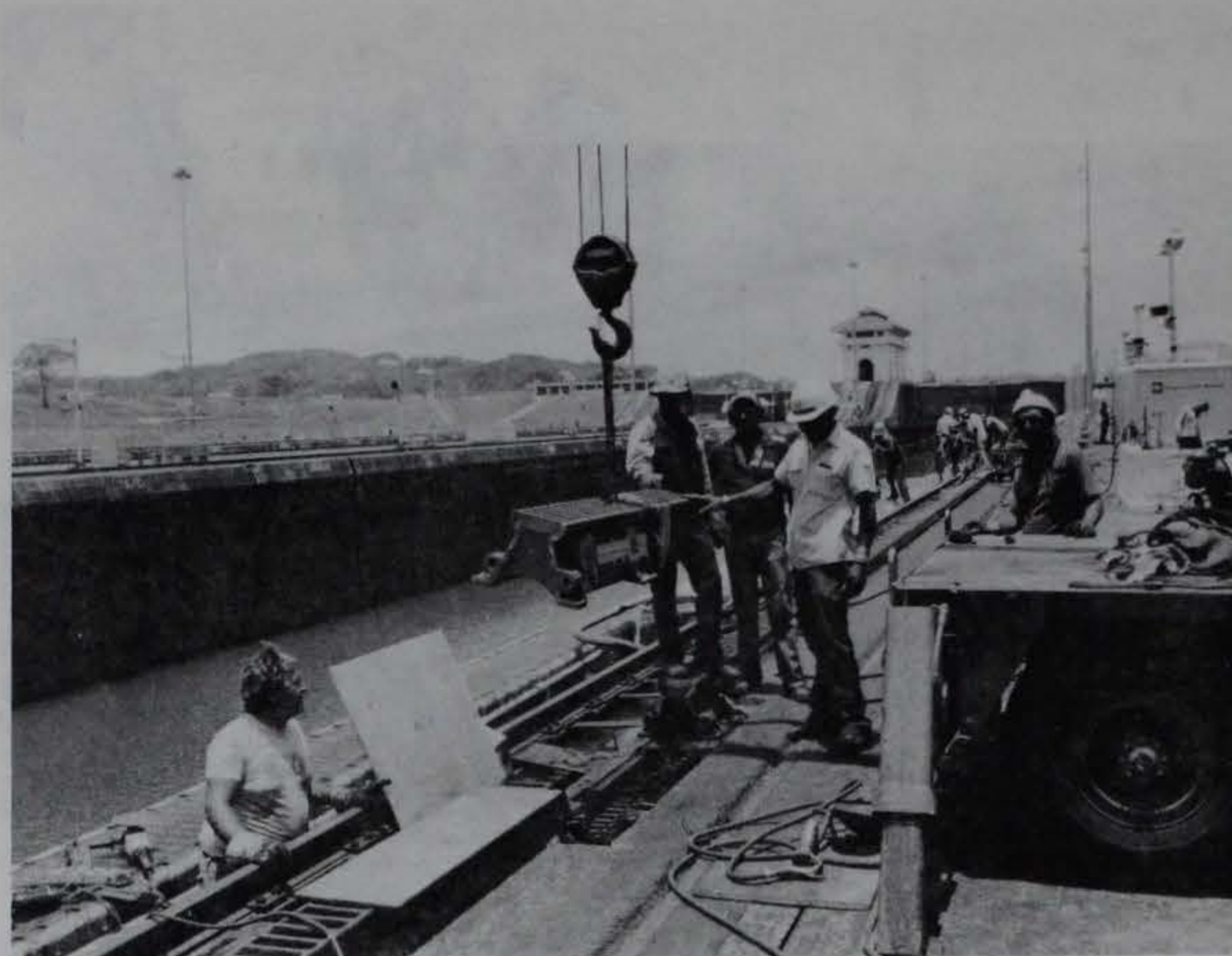


a. View of construction work from atop the closed miter gate

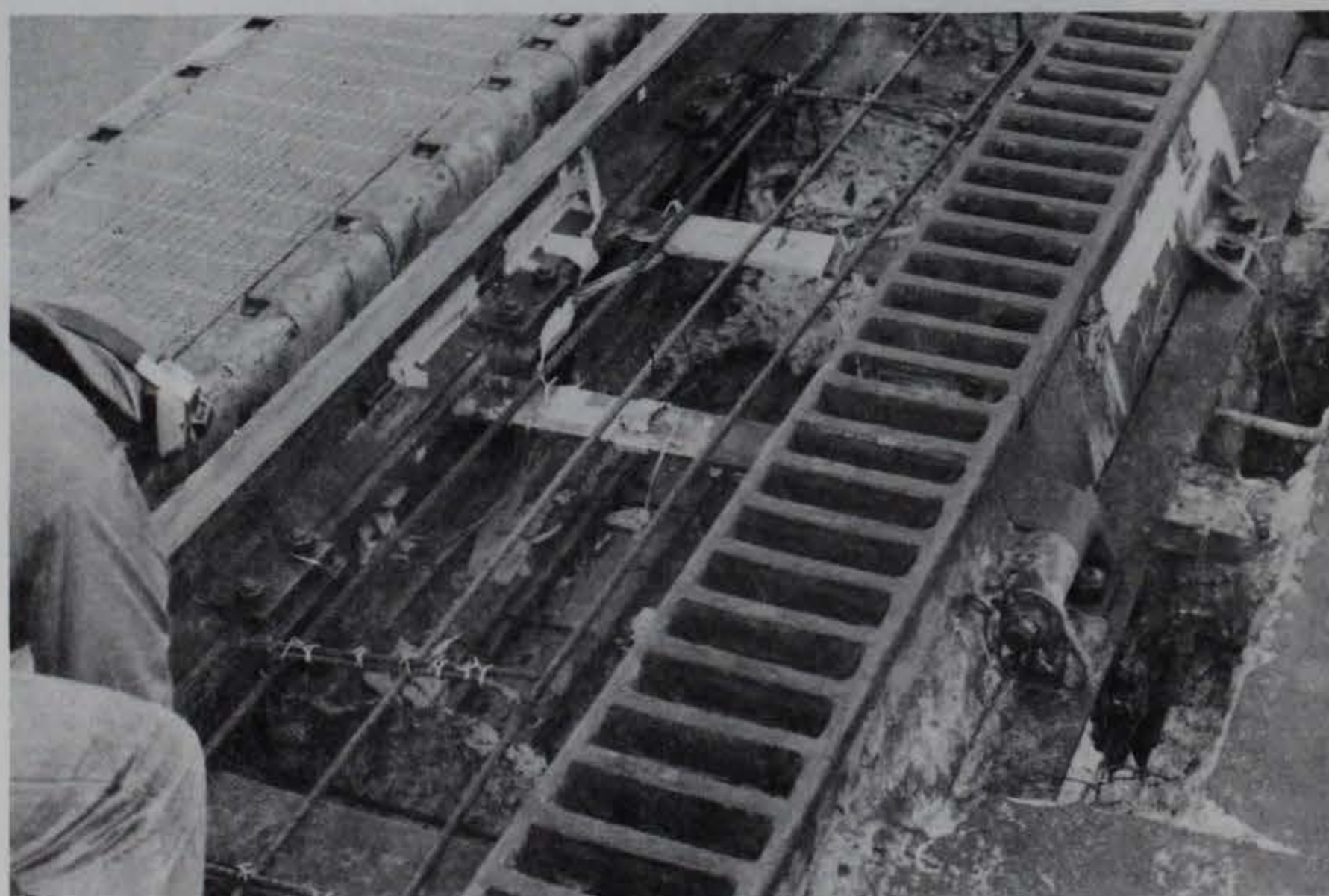


b. Placement of strain gages on the rail-support girder

Figure 29. Construction at the gate recess, test site 2
(Sheet 1 of 3)

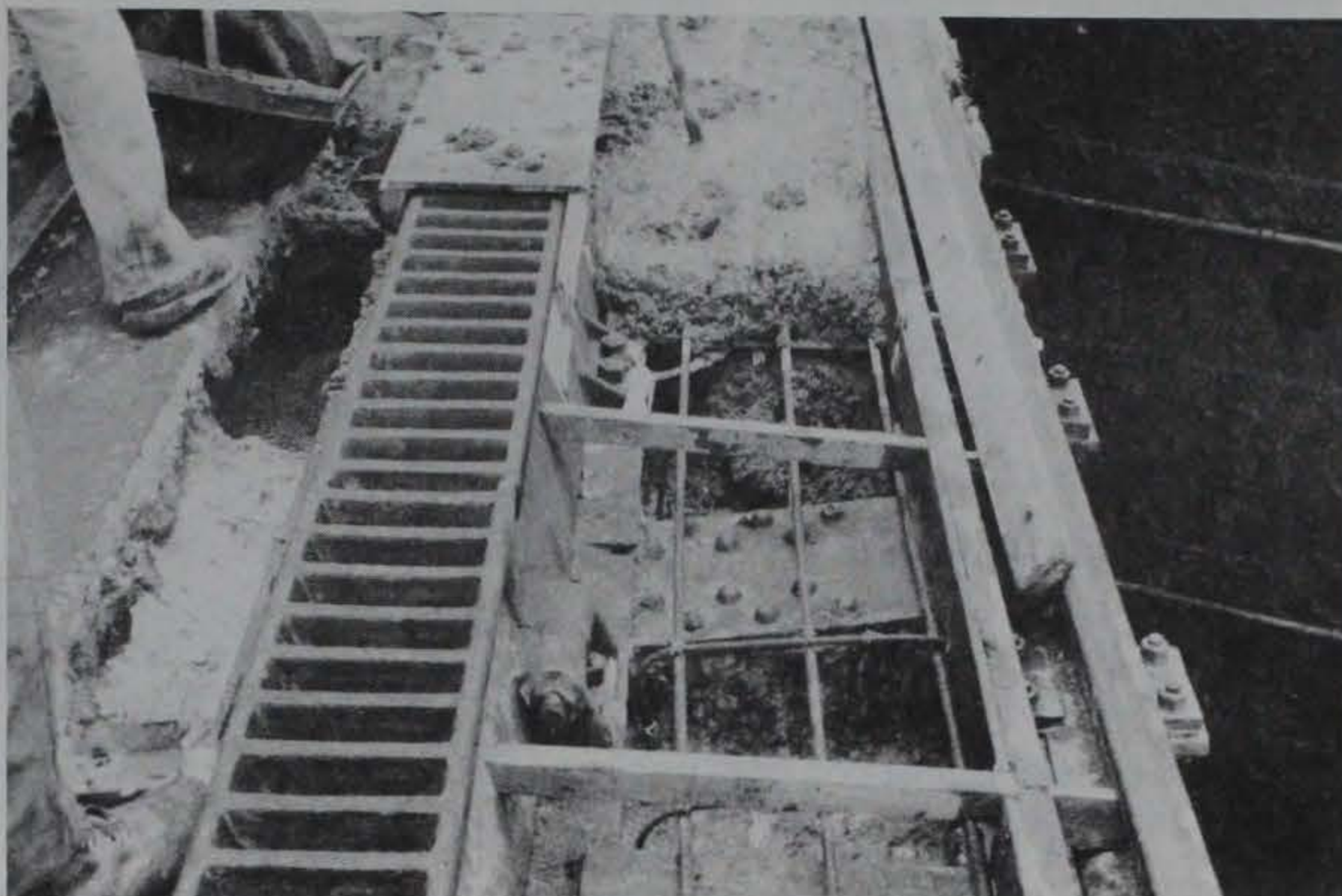


c. Installation of a new rack section,
previously strain-gaged

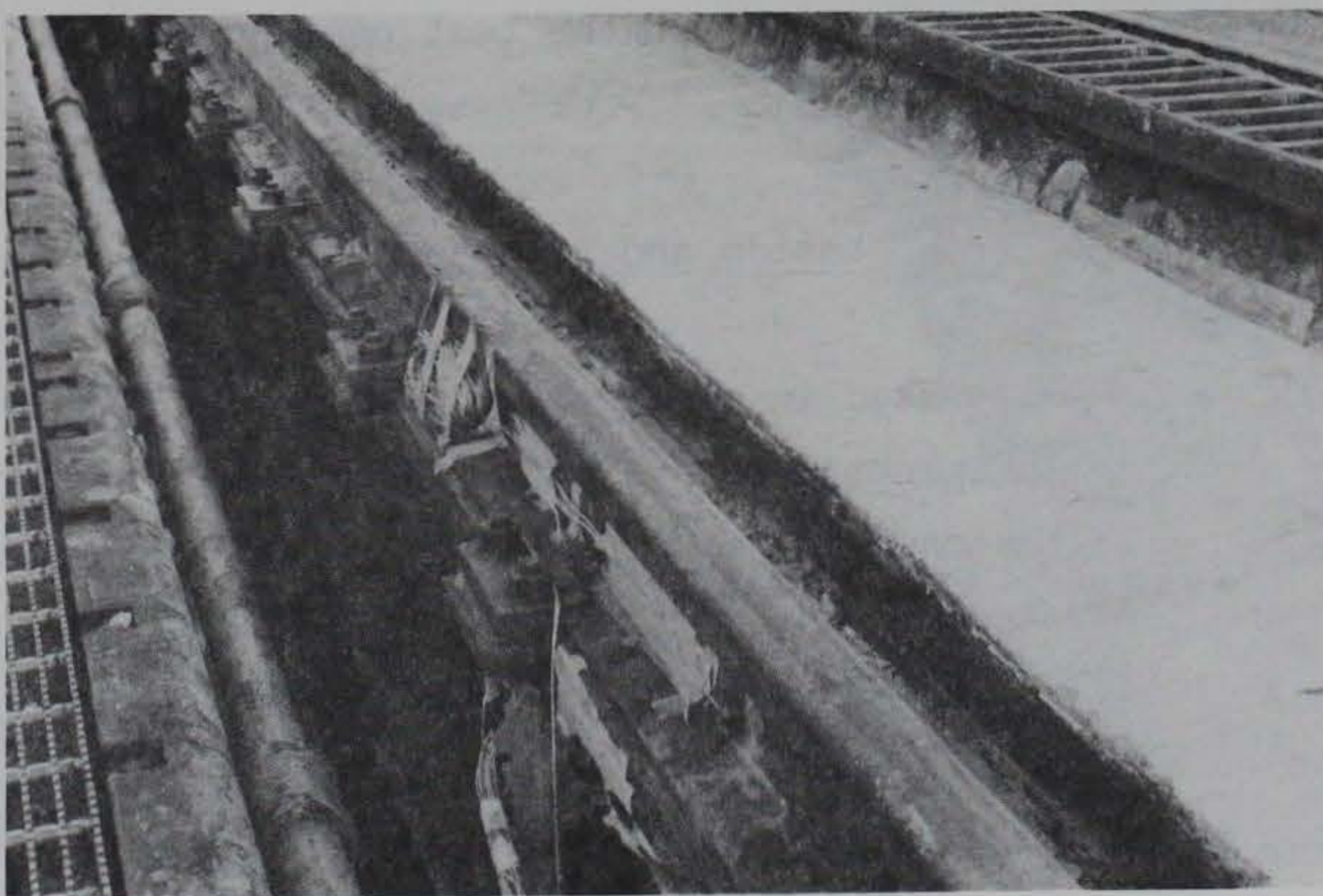


d. Placement of gages and component
assembly are complete. Note the new
"tension strap" girder stiffeners

Figure 29. (Sheet 2 of 3)



e. Concrete placement



f. Completed repair

Figure 29. (Sheet 3 of 3)

25. The tests conducted at each site included both actual towing situations and controlled tow simulations. The simulations were made by securing the locomotive windlass cables to stationary anchors on the opposite lock wall. Locomotives then moved across the test area at the desired speed with one or both of the windlasses exerting a prearranged (usually maximum) cable tension. The simulation conditions allowed more precise measurement of loadings over a limited range of cable angles. Data which reflected effects of the most extreme cable angles had to be obtained in actual towing tests. Since locomotives were not always fully loaded when passing a given section and extremely severe cable angles occurred only occasionally, a large number of tests were conducted in hopes of obtaining data from a representative variety of severe loading conditions. One test in which windlass cables were completely unloaded was conducted at each test site for reference purposes.

26. In addition to electronic instrumentation measurements, other information collected from each test included ship name, length, beam, and draft (for towing tests), measured horizontal and vertical angles of windlass cables, readings of locomotive cable tension meters, and position and function (towing, braking, or guiding) of the locomotive. Summaries of the individual tests can be found in the draft data report referred to in paragraph 3. Photography was used to document many of the test configurations (Figures 30 and 31).

Instrumentation and Data Reduction

27. The strain gages used in all testing were 1/4-in., 350-ohm gages made by Micro Measurements Company, rated for strains up to 5 percent (50,000 μ in./in.). Wheatstone bridge completion circuits constructed at WES were used in junction boxes no further than 10 ft from gage locations. Instrumentation shelters which housed all recording equipment were located up to 100 ft away from the junction boxes. Data signals were multiplexed and direct-recorded using Schlumberger MA-1142 multiplexers and a Racal Store-7 analog tape recorder. Amplifiers and other signal-conditioning electronics were specially constructed at WES. A galvanometer oscilloscope was used to check the recorded data after each test.

28. Immediately prior to each test or test group, a "calibration step" was recorded for each data channel. This is a generated electronic signal

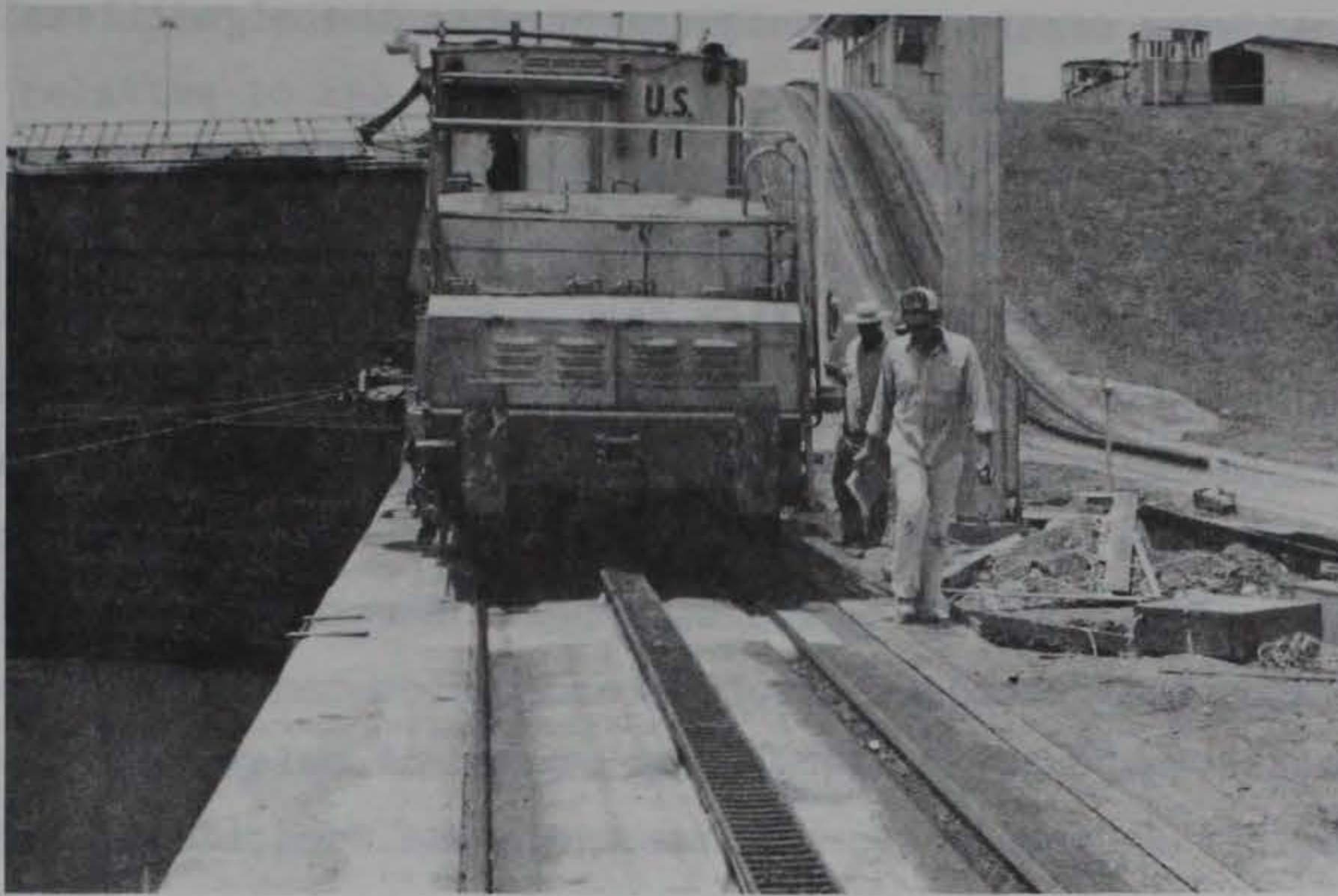


Figure 30. Controlled tow simulation tests were made by moving the locomotive over the test site with windlass cables anchored to the opposite lock wall

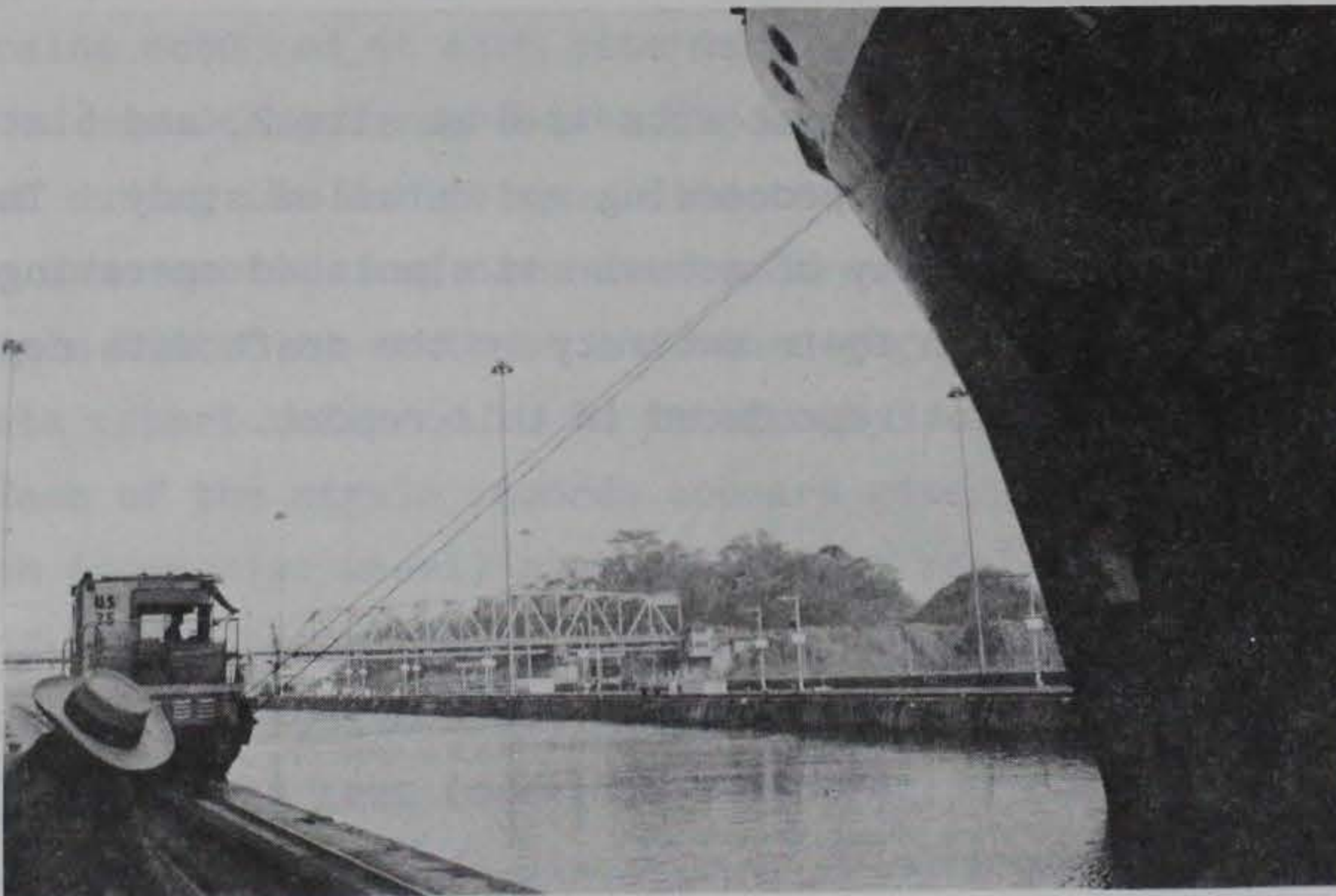


Figure 31. Tests which involved actual towing or braking of ships were made during normal operations

whose constant voltage level corresponds to that associated with the maximum predicted measurement for that channel. The calibration signal facilitates accurate quantifying of the data measurement when the signal level is compared to the known calibration level.

29. Data reduction and final processing were done at WES. Analog tapes were played back through decoding circuitry so that multiplexed signals were restored to individual channels. Each data signal and its associated calibration step was converted from analog to digital form so that special-purpose computer codes could be used to further process the data. Once in digital form, each signal was automatically analyzed for frequency content. It is common for unwanted electrical noise to appear on recorded data signals, especially when gages and recording electronics are located near high-voltage power and electric motors. A significant amount of this noise was present on the data tapes. The frequencies of unwanted noise were identified and digitally filtered, leaving only the frequencies of actual data signals. The computer codes were used to quantify the data signals by comparing them with the assigned values of corresponding calibration steps. Finally, each data signal was automatically plotted to an appropriate scale versus time. The digitally stored records can easily be replotted to a common scale or superimposed to facilitate visual comparisons.

30. Twenty-seven tests (13 at site 1, 8 at site 2, and 6 at site 3) were selected for complete data processing and detailed study. These tests represent an appropriate variety of actual and simulated operating loads. The data records are presented in their entirety in the draft data report referred to in paragraph 3 and are not reproduced in this report.

PART IV: RESULTS OF TESTING

31. Test data indicate that significant tow track component strains are quite local relative to the exact positions of locomotive wheels at any instant in time. Measurable strains are rarely found more than about 3 ft away from a wheel, and significant strains are confined to those areas within a few inches.

32. The instrumented component sections in which significant strains were measured included all parts of the rails at all sites, tie web sections directly beneath rails at sites 1 and 3, and the girder webs and tension straps at site 2 (gate recess). The measured strains at other sections of ties and in other instrumented components were relatively insignificant.

33. The maximum strains measured in the high-strain locations for each site are listed in Table 1. Positive strains are tension by sign convention. These strains are not necessarily the most severe strains present in each respective section, since the gages were not located at the extremes of section geometries. For example, it can be shown that strains at rail section extremities could theoretically reach as much as 2.5 times the measured strains, depending on the biaxial bending conditions present. The tests in which the greatest strains occurred at each site were all controlled tow simulations. Each tabulated measurement represents the maximum strain encountered at that gage location during the entire specified test; the strains shown for various gages at the same section may not have occurred during the same wheel pass. Complete strain histories at these and other gage locations are included in the draft data report referred to in paragraph 3.

34. Each of the strain records appears generally as a pair of pulses (one for each locomotive wheel) plotted against real time in milliseconds. The amount of time between the pulses varies somewhat between tests, according to differences in locomotive speed. Since locomotive speeds were usually constant through any given test (especially controlled simulations), an approximate relationship of the actual distance of wheel travel to any time period of interest can easily be determined by comparing the time between pulses to the locomotive wheel span (180 in.). This method can be used to determine the strain at a gage location when the locomotive wheel is at an adjacent tie or midspan point, etc.

35. Hydraulic pressures of the locomotive windlass drive systems were

monitored during all controlled simulation tests and whenever possible during actual towing tests. The records are presented along with all other test data in the draft data report referred to in paragraph 3. The theoretical relationships between hydraulic pressures and cable tension (supplied by PCC) are shown in Figure 32. Cable tensions determined using these plots compared very well with actual cable tensions measured with a tension load cell which was attached between a windlass cable and a stationary mooring anchor in several of the first controlled-simulation tests.

36. An accelerometer was attached to a locomotive axle and was monitored during several of the initial tests. The accelerations measured were extremely small, and it was concluded that there are no significant dynamic loadings imparted to the tow track by the locomotives. No effects on component strains or responses resulted from changes in locomotive speeds, which varied from essentially a standstill to a maximum of about 3 mph.

Tests of the Crosstie-Supported Tow Track

37. Test sites 1 and 3 were of identical construction, characterized by crossties supported by solid concrete. Duplicate testing adds statistical significance to data, and also helps identify any inconsistencies in test conditions by allowing comparisons of data from otherwise identical tests.

Rails

38. The bending and torsional response of a rail is much like that of a beam subjected to vertical and horizontal loads. The horizontally oriented strain gages on rail heads and lower flanges were positioned so as to measure those strains caused by bending of the rail section about its horizontal and vertical centroidal axes. Those gages oriented vertically on the rail webs are sensitive to web compression resulting from wheel loadings and can be used to identify bending of the web and the associated twisting of the rail section caused by horizontal wheel loads and/or eccentric vertical wheel loads. Biaxial bending in the rail results in differences in measured strains on opposing sides of the head and lower flange. Bending about the rail's horizontal centroidal axis (vertical bending) resulting from the vertical component of wheel loading can theoretically be quantified using an average of the measured strains in the lower flange and/or the rail head and beam flexure theory. Since the strains measured in the rail head appear to be significantly

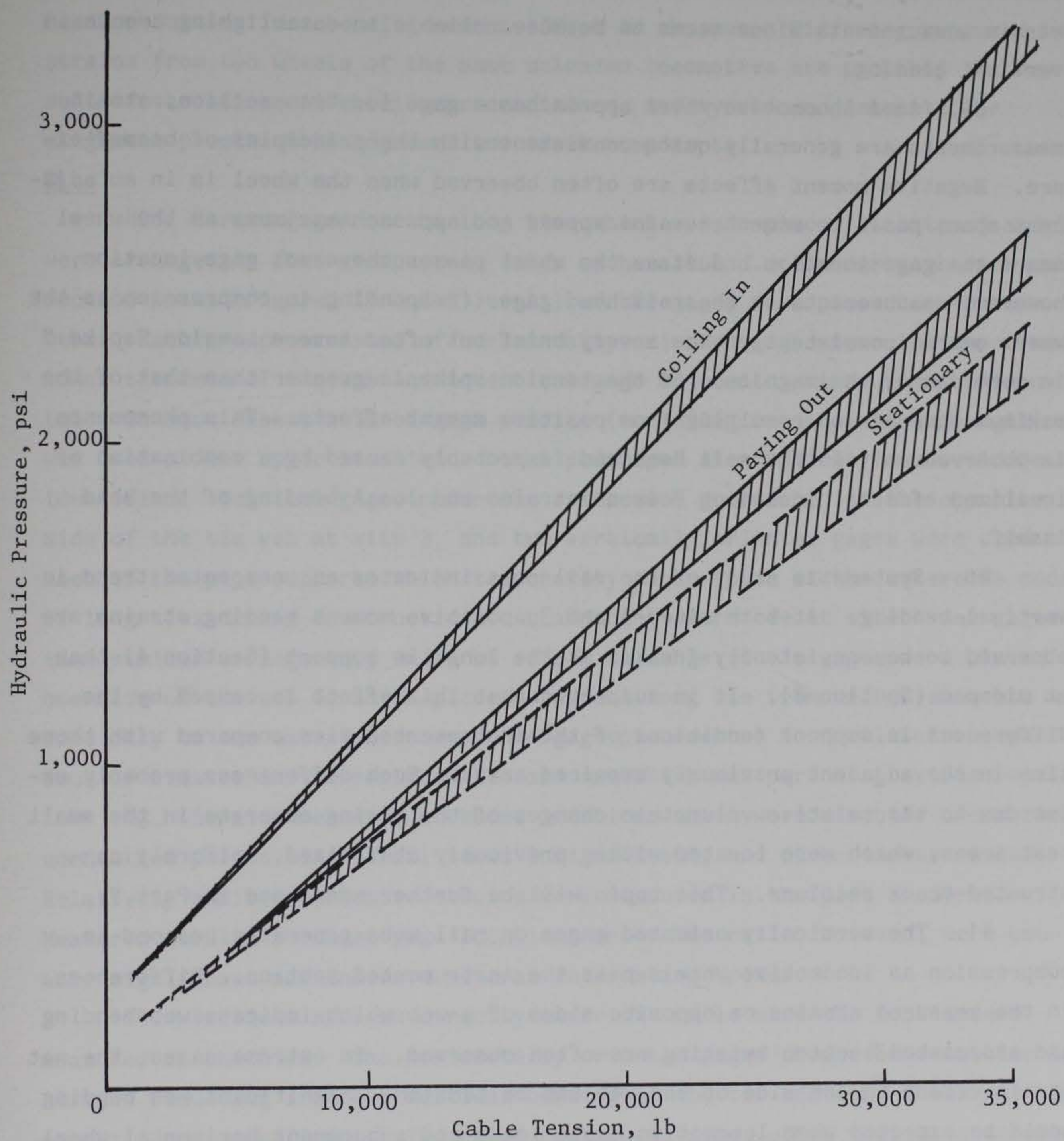


Figure 32. Relationships between cable tensions and windlass hydraulic pressures

influenced by the local effects of locomotive wheels, the use of lower flange strain measurements alone seems to be more reliable in establishing trends in vertical bending.

39. As a locomotive wheel approaches a gage location section, strain measurements are generally quite consistent with the principles of beam flexure. Negative moment effects are often observed when the wheel is in an adjacent span; positive moment strains appear and approach maximums as the wheel nears the gage location. Just as the wheel passes the exact gage location, however, measurements at the rail head gages (responding in compression as the wheel nears) consistently show a very brief but often severe tension "spike." In some cases, the magnitude of the tension spike is greater than that of the maximum compression resulting from positive moment effects. This phenomenon is observed only in the rail head and is probably caused by a combination of localized effects, including Poisson strains and local bending of the head itself.

40. Systematic study of the rail data indicates an unexpected trend in vertical bending. At both sites 1 and 3, positive moment bending strains are observed to be consistently greater at the long tie support (Section A) than at midspan (Section B). It is suspected that this effect is caused by the differences in support conditions of the instrumented ties compared with those ties in the adjacent previously repaired areas. Such differences probably exist due to the relative volumetric changes of the curing concrete in the small test areas, which were located within previously stabilized, uniformly constructed track sections. This topic will be further addressed in Part V.

41. The vertically oriented gages on rail webs generally respond in compression as locomotive wheels pass the instrumented section. Differences in the measured strains on opposite sides of a web which indicate web bending and associated section twisting are often observed. In extreme cases, the net strain effect on one side of the web can be tension. Significant web bending would be expected when locomotive cable loads and subsequent horizontal wheel load components are large, but such behavior can also be seen in those tests having no cable loads and theoretically no horizontal components of wheel loads. This may be caused by vertical wheel loads which are, in effect, eccentric relative to the rail's vertical axis of symmetry. Locomotive wheels wear in such a way that the bearing surface of a wheel conforms to the shape of the rail head. When wheel or rail alignments are for any reason slightly

irregular, a worn wheel may bear primarily to one side of center of the rail head, resulting in a bending moment effect in the web. Differing measured web strains from two wheels of the same unloaded locomotive are probably the result of variations in wheel wear conditions, safety shoe adjustments, or alignment precision in adjacent tow track components.

Ties

42. Strain gages on the long ties which were replaced at sites 1 and 3 were arranged in four groups, one under each rail and one under each rack connection point (Figures 17 and 21). All of the gages were placed on the tie webs. Each group consisted of horizontally oriented gages near the upper and lower extremes of the web and a vertical gage adjacent to the upper horizontal. In some cases, a three-gage rosette (including one at a 45-deg angle) was used at the upper location so that principal strain directions could be identified. Vertical gages under the rails were duplicated on the opposite side of the tie web at site 3, and two vertically oriented gages were used on each of the pipe supports which temporarily carry loads at the waterside ends of long ties during construction. An adjacent short tie at site 1 was gaged in a similar arrangement, while at site 3 weldable strain gages were placed on one side of the web of an in-place, original long tie (removal of concrete was done only to the extent necessary for gage placements) to facilitate comparisons of strains in the replaced tie and one which was part of previous repairs.

43. Strains measured at those locations which were directly under rack connection points were at all times insignificant, and often immeasurable. Relatively small compressive strains were measured in the pipe supports. Measured strains at those gage locations under the rails, however, were usually significant and indicate several interesting trends.

44. Vertical strains directly under the rails were the most severe measured in the ties. The horizontally oriented gages should be sensitive to strains resulting from any vertical bending of the tie section, which was apparently not significant. The upper horizontal gages often indicated tensile strains (vertical section bending alone should result in compression), presumably caused by the Poisson effects of the much more severe vertical strains in the area. The strain responses of the short tie at site 1 were similar to those observed in long ties.

45. The severity of measured vertical strains under the waterside rail increases with the severity of locomotive cable loads, as would be expected.

Likewise, those strains under the landside rail decrease, since wheel loads there can approach zero as cable loads maximize. However, when waterside and landside wheel loads are theoretically equal (no cable loads) the vertical strains under the two rails are typically observed to differ. This behavior could be caused by slight inconsistencies in assembly tolerances or quality of concrete placement in the repaired section.

46. Vertical strain gages were used on both sides of the tie web for those locations under rails at site 3. Any differences in the vertical strains measured on opposite sides of a tie web at a given time would indicate some bending of the web and associated twisting of the tie section. While almost no web bending is evident under the landside rail (strain records of the opposing gages are almost identical), the bending is severe under the waterside rail. This behavior is independent of the severity of wheel loads, and may be caused by inconsistencies in the condition of rail connection hardware or (more likely) variations in the quality of concrete placement under the upper tie flanges.

47. The long ties which were strain-gaged and used at test sites 1 and 3 were not those typically used in repairs of the concrete-supported tow track. The most distinct difference in the cross-sectional characteristics of the instrumented ties is a greater web thickness (Figure 13). Both original ties and those sections normally used as replacements have a web thickness of $1/4$ in., while the web of the instrumented tie section is $5/8$ in. thick. The strains measured in the tie web would no doubt have been greater (as much as 2.5 times greater, in theory) had the instrumented tie section been one of those having a thinner web.

Rack

48. Strain gage locations on the rack were chosen so as to measure local strains caused by the locomotive safety shoes as well as those strains associated with twisting of the rack section. Other than one three-gage rosette, the orientations were vertical. All gages were on the outer surfaces of the rack sides, near the upper flanges on which safety shoes bear. Selected locations along the length of the rack sections included points both directly over and halfway between the internal stiffeners (Figures 17 and 21).

49. The strains measured at all gage locations on the rack were negligible. Even when cable loads were extreme, the measured strains never exceeded about $65 \mu\text{in./in.}$ Based on these strain magnitudes, it appears

likely that severe, premature deterioration of the rack is caused by excessive wear conditions arising from component misalignment or improper hardware adjustment rather than overstressing.

Comparisons of tests at two identical sites

50. Although test sites 1 and 3 were identical construction and would theoretically be expected to have the same responses to similar loadings, the strain measurements differ noticeably in many cases. Certain trends in these differences appear to be the results of slight variations in the exact positioning and alignment of the components (construction tolerances). For example, all of the strains in the rail and long tie which are directly associated with vertical wheel loads (on the waterside rail) were consistently greater in no-load tests at site 1 than at site 3. This behavior suggests that the relative as-repaired elevation of the tie (at the waterside end) may be slightly higher or the quality of concrete placement around the tie greater at site 1. Other response tendencies which indicate possible variations in concrete-placement quality around the tie at site 3 were observed in measured strains of the tie web (paragraph 46).

Tests at the Gate Recess

51. Tow track construction at site 2 was typical of that in all gate recess areas throughout the locks, characterized by a special cantilever-girder support system (Figure 4). The components which responded significantly to the test loadings were the rail, the support girder, and the tension straps. All of the strains measured on the rack and its supporting structure (stringer) were insignificant. The vertical deflections measured at the cantilever and at midspan of the rail-supporting girder were extremely small, and those strain measurements on the girder which are associated with vertical bending of the section confirm that very little vertical movement was present.

52. Strains measured in the rail head showed local effects identical to those of sites 1 and 3. The strain magnitudes in the rail head and web were often slightly greater than those at sites 1 and 3, possibly because of the greater effective support stiffness (in the vertical direction) of the massive girder, as compared with the concrete-encased ties. Vertical bending of the

rail, as indicated by the lower flange strain gages, was minor and appeared to be largely controlled by the composite behavior of the rail and the support girder.

53. Horizontal bending and associated twisting were significant in both the rail and girder. Local horizontal bending in the rail head and bending of the rail web were more severe than at sites 1 and 3, probably due to the lack of any confinement (concrete) on the rail's waterside. Bending in the girder web was significant when cable loads were severe. Strains measured in the tension straps were significant, though not excessive.

54. Significant component responses at the gate recess test site were primarily those associated with the lateral (horizontal) components of rail loadings. Modifications made to some of the components in the repair procedures (increased area of tension straps and the addition of web stiffeners on the girder) no doubt have reduced the severity of these tendencies, and none of the related strain measurements were considered excessive or critical. The tolerances of component assembly precision are likely much closer in the gate recess areas, since the final alignment of supporting components is not controlled by concrete placement and curing. Based on the strains measured at test site 2 and assuming correct alignment and adjustment of all components and hardware, it appears unlikely that accelerated deterioration due to component overstressing will be a problem in the repaired gate recess tow track sections.

PART V: ANALYSES

55. The tests summarized in previous parts have indicated that certain localized component areas regularly experience significant (but not necessarily excessive) stresses. Results of some of the tests and observations of tow track repair procedures have suggested that variations in the precision of component assembly and the consistency of concrete placement may affect component response tendencies and relative stress levels. The general objectives of these analyses are to investigate in greater detail those component areas and response tendencies and to extend the test data base to the most extreme geometries and loadings normally present. The development of deterioration mechanisms can be surmised, considering some of the test results, but predicting the effects of such possibilities requires analytical investigation. The analysis methods used in this study include conventional engineering analysis techniques and finite element (FE) analyses.

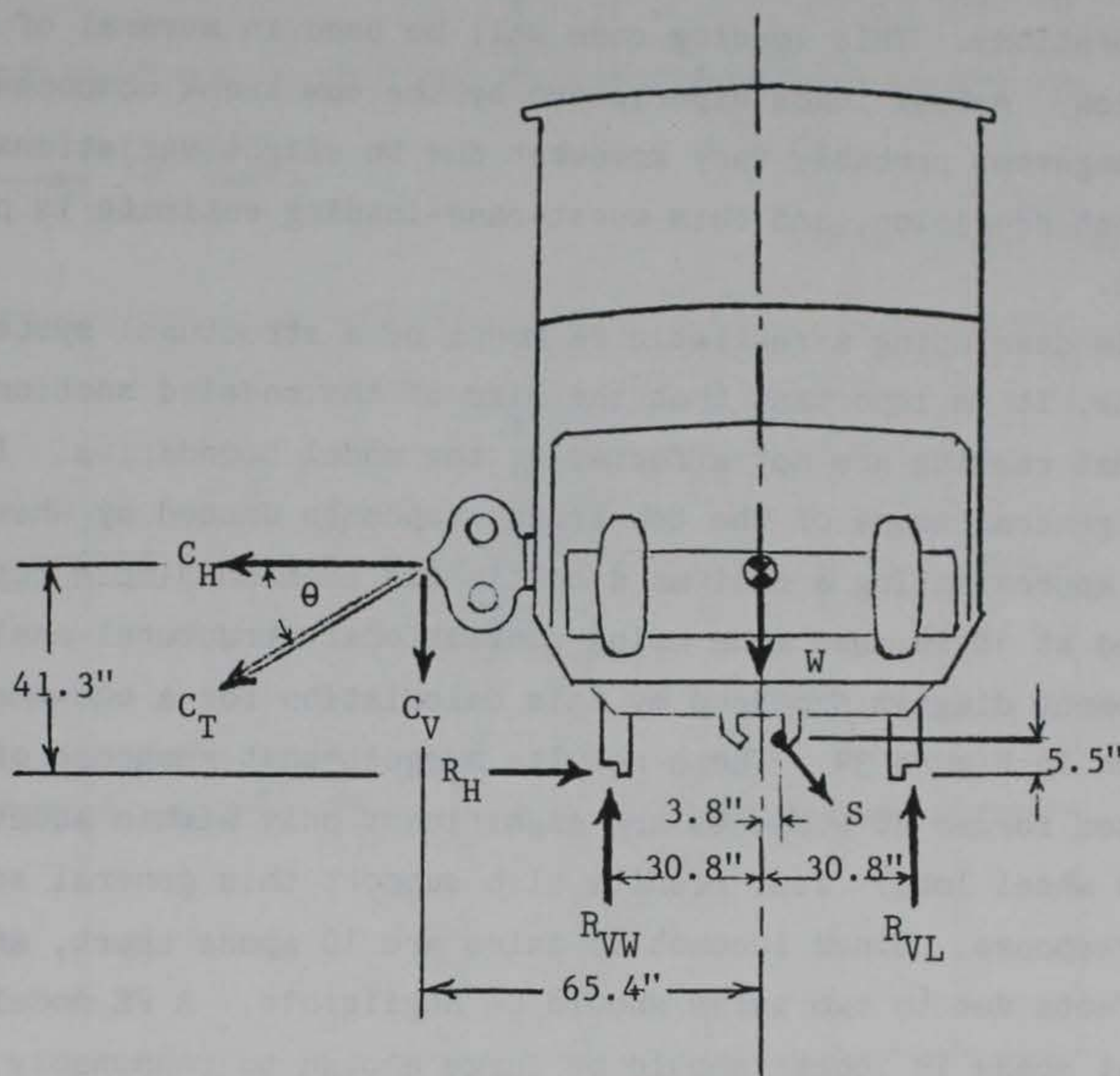
56. FE analysis is an effective tool for large and/or geometrically complex structures, and is most reliable when a structure's material properties are generally homogeneous and isotropic. Accuracy of the results of FE analyses depends significantly on precise definition of structural geometry, external loads, and boundary or support conditions. Composite structures present an additional problem in that interaction between the different materials is not precisely known and therefore further assumptions or approximations must be made in the analysis. Analysis of repaired composite structures presents even more difficulties in that the material properties of the repaired section are not the same as the original structure and the geometric tolerances of the repaired section vary from section to section and in general are expected to be different from those of the original structure. It follows that FE numerical predictions of stresses, strains, and deflections in structural components of the tow track system are of limited reliability, at least in an absolute sense. The greatest value of such FE results is realized when through qualitative interpretation, trends observed in numerical results are consistent with test data trends, and the component response tendencies resulting from situations other than those experienced in testing can be investigated using reasonable variation of FE input parameters.

57. Conventional calculation techniques employing normal stress analysis principles can be used to accurately evaluate isolated structural elements

of relatively simple geometries (such as rails and crossties) once support and loading conditions have been defined. It is impractical to study local stress effects in the concrete surrounding a component using FE techniques because of the difficulty in mathematically modeling the interaction of the different materials, especially considering the consistency variations of concrete cast in small, staggered sections. The general ranges of local concrete stresses can be estimated with simplified calculations by making certain assumptions and approximations. FE analyses and test results are useful in defining the appropriate load representations and boundary conditions for these conventional analysis techniques.

Preliminary Calculations

58. Precise definition of the magnitudes, directions, and points of application of all loads imparted to the tow track system by locomotives is necessary in beginning the analytical investigation. Since locomotive weight and geometry, maximum cable tension, and the general range of cable angles are known, theoretical determinations of loads on the rails and rack can easily be made using the principles of statics, assuming the locomotive acts as a rigid body. Figure 33 is a free-body diagram of a locomotive showing all of the loads associated with one axle. When windlass cables are slack, loads to the tow track system include only the uniform distribution of the locomotive weight (vertical loads of 27.5 kips at each wheel). Since this dead-load-only case is easily defined in testing, it provides a basis for data-versus-analysis comparisons. When cable loads are applied, rail loads can be determined by summing moments about the safety shoe bearing point. Loads on the waterside rail are greatest when the cable angle is below horizontal. As the angle θ (Figure 33) increases, the vertical component of cable tension C_V becomes larger, as does the vertical resultant on the waterside rail R_{VW} . Load on the landside rail R_{VL} decreases. As θ increases with maximum cable tensions, R_{VL} eventually becomes zero. This is the point at which the locomotive safety shoes first engage to resist overturning moment. By summing moments and forces and setting $R_{VL} = 0$, this θ is found to be about 14 deg below horizontal. At this point, $R_{VW} = 63.4$ kips. Cable angles, however, often become more severe than this. By varying θ and solving for the corresponding rail loads, it can be shown that the most severe case for vertical



- W = locomotive weight (55 kips per axle)
- θ = cable angle with respect to horizontal
- C_T = cable tension (35 kips maximum, each)
- C_H = cable tension, horizontal component = $C_T \cos \theta$
- C_V = cable tension, vertical component = $C_T \sin \theta$
- R_H = horizontal rail load (waterside only)
- R_{VW} = vertical rail load, waterside
- R_{VL} = vertical rail load, landside
- S = safety shoe load

Figure 33. Free-body diagram of a locomotive showing all loads associated with one axle

loads on the waterside rail occurs when θ is approximately 60 deg ($R_{VW} = 87.5$ kips, $R_H = 17.5$ kips). Such a cable angle is not uncommon during normal lock operations. This loading case will be used in several of the analyses to follow. Actual loads experienced by the tow track components in a similar arrangement probably vary somewhat due to slight variations in component alignment precision, and this worst-case-loading estimate is probably conservative.

59. In developing a realistic FE model of a structural system such as the tow track, it is important that the size of the modeled section be appropriate so that results are not affected by the model boundaries. In order to predict the general scope of the tow track responses caused by wheel loads, a calculation approximating a rail as a continuous beam on simple supports (ties) spaced at 18 in. was made using conventional structural analysis methods. The moment diagram produced by this calculation for a one-wheel midspan load is shown in Figure 34. These results suggest that response of the rail and associated forces at supports are significant only within about 2-1/2 spans of the wheel load. Test results also support this general scope of the structural response. Since locomotive axles are 10 spans apart, any combined response effects due to two axles should be negligible. A FE model of a track section eight spans in length should be large enough to reasonably investigate the responses of the loads exerted by a single locomotive axle at a variety of specific locations.

60. Bending moment in the rail is a convenient parameter with which FE analyses and test results can be compared. Moment can easily be derived from strain data since the two quantities are directly related. Vertical plane bending in the rail is most accurately documented by the strain gages placed on the lower flange. Since some horizontal-plane bending is also usually present causing the strain measurements on opposite sides to differ, an average value of the lower-flange strains at a given instant is needed to accurately quantify the vertical bending, assuming there are no significant axial forces present in the rail. Moment M can be determined from strain ϵ using the relationships

$$\sigma = \frac{MC}{I}$$

$$\sigma = E\epsilon$$

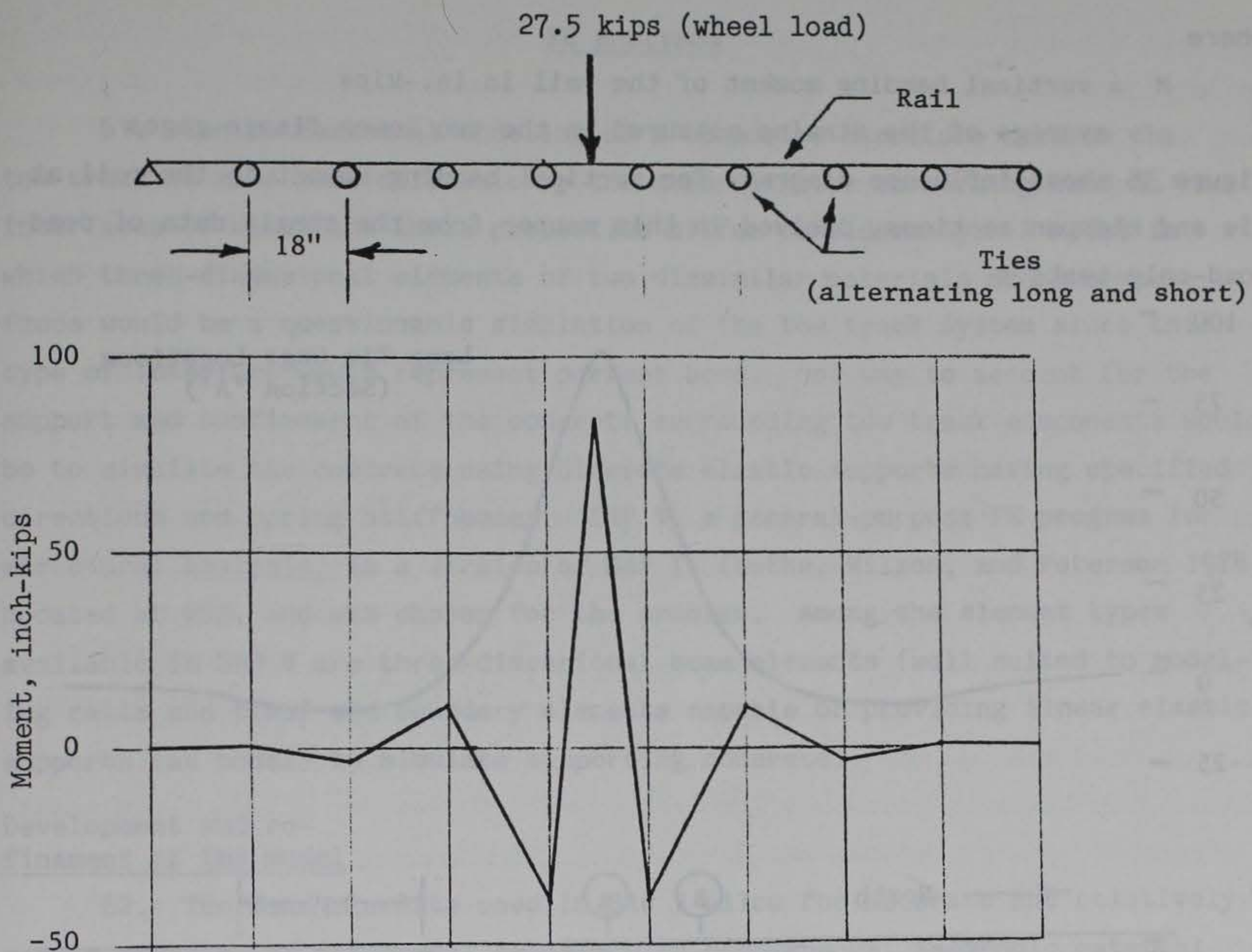


Figure 34. Moment diagram for a beam on multiple simple supports

where

σ = bending stress

C = distance from the neutral axis

I = moment of inertia

E = modulus of elasticity

Since the lower-flange strain gages are found to be 1.7 in. below the horizontal neutral axis ($C = 1.7$ in.), the value for I about the same axis is 32.9 in.^4 , and the value of E for steel is approximately 29,000 ksi, it follows that

$$M \frac{(1.7)}{(32.9)} = 29,000 \epsilon \quad \text{or}$$

$$M = 561,000 \epsilon$$

where

M = vertical bending moment of the rail in in.-kips

ϵ = average of the strains measured in the two lower flange gages

Figure 35 shows influence diagrams for vertical bending moment in the rail at tie and midspan sections, derived in this manner from the strain data of dead-load-only tests.

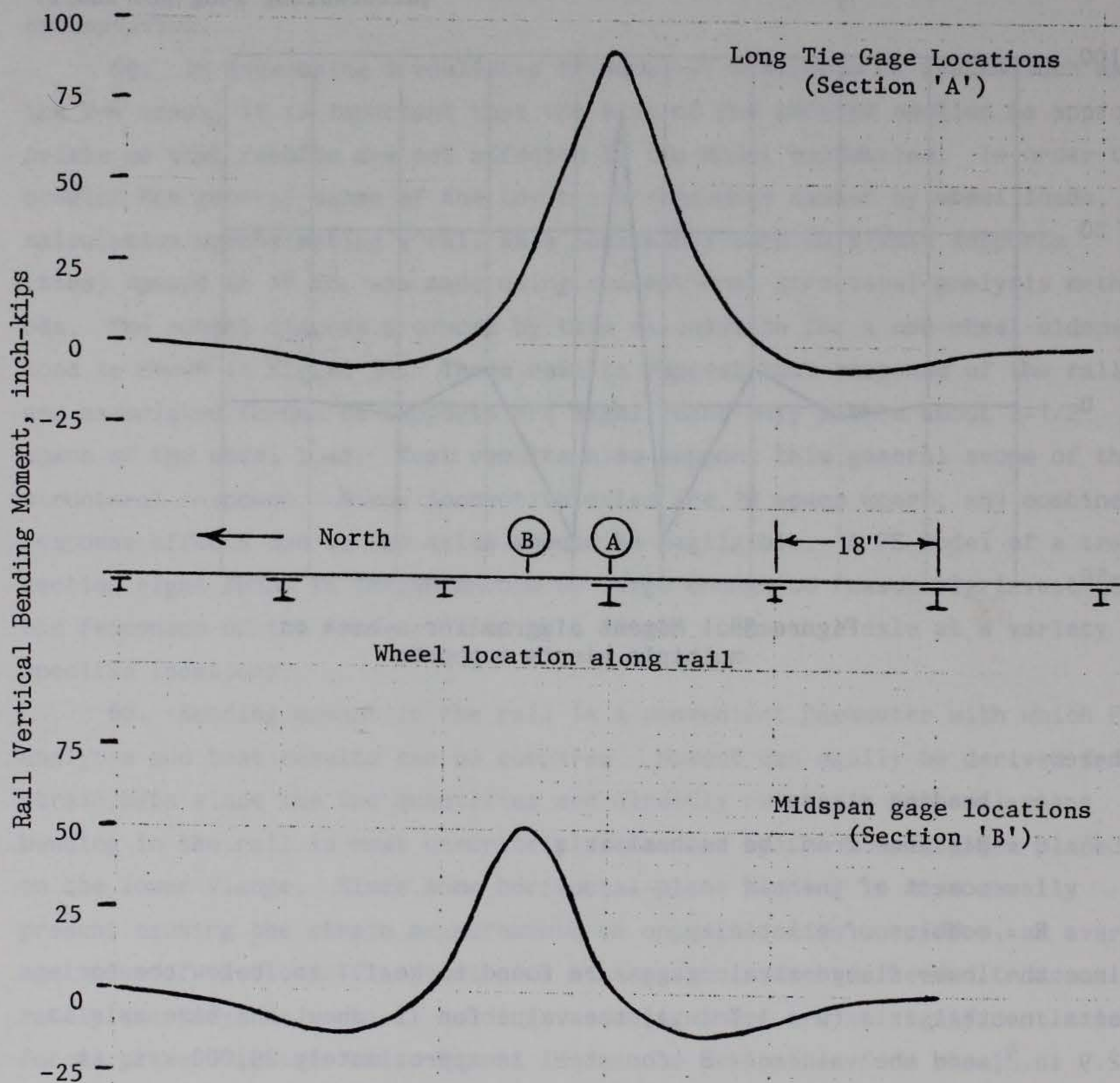


Figure 35. Influence diagrams for rail vertical bending moment induced by a single locomotive wheel (dead load only), as derived from test data

FE Analyses

61. The mathematical modeling of a composite structure such as the tow track is made more difficult by the uncertainties concerning bond at the interfaces of materials whose properties differ considerably. A model in which three-dimensional elements of two dissimilar materials share common faces would be a questionable simulation of the tow track system since this type of interface would represent perfect bond. One way to account for the support and confinement of the concrete surrounding tow track components would be to simulate the concrete using discrete elastic supports having specified directions and spring stiffnesses. SAP V, a general-purpose FE program for structural analysis, is a version of SAP IV (Bathe, Wilson, and Peterson 1974) updated at WES, and was chosen for the problem. Among the element types available in SAP V are three-dimensional beam elements (well suited to modeling rails and ties) and boundary elements capable of providing linear elastic supports (at nodes) to simulate supporting concrete.

Development and re- finement of the model

62. The beam elements used in SAP V allow for accurate and relatively simple modeling of structural members with homogeneous, isotropic material properties whose geometries and structural responses are primarily those of beams. Three different sets of beam properties representing rails, original-style ties (short ties and long ties other than the instrumented one), and the heavier new ties used at the strain-gaged section were defined for use in the model. The size of the modeled section was chosen so as to include eight rail spans (five long ties and four pairs of short ties). This configuration allows at least three spans between the applied wheel loads of interest (near the center of the model) and a model boundary (paragraph 59). A grid consisting of 162 nodes and 286 elements was constructed. Eighty-six of the nodes were used to define the beam elements; many of these were located within a span of a rail or tie to facilitate applying a wheel load or retrieving calculational output at that point. The remaining nodes were used only to define the directions of boundary elements which acted vertically on the structural members. Eighty-nine of the elements were beam elements, one between each consecutive pair of nodes along each member. Crosstie and rail elements share a common node at each intersection which assumes perfect connection hardware.

The 197 boundary elements were arranged so as to simulate all conceivable orientations of concrete confinement and support along the components. The rack was not included in the FE model since test data showed that strains in the rack and the localized responses of ties resulting from rack loadings were insignificant. Figure 36 is a sketch of the finite element grid showing the layout of all nodes and beam elements and the directions of applied boundary elements.

63. The concrete which supports and surrounds tow track components is effectively a medium of continuous, elastic confinement applied along all faces of the components with which contact is maintained. This confinement can be most reasonably approximated in FE analyses with the application of spring forces (boundary elements having specified spring stiffnesses) at nodes in the appropriate directions. Precise properties of repair concrete are not easily defined, however, and typically will vary with the consistency of placement, bond quality, and the strength, age, plastic deformation, and general condition of the concrete itself. The simulation task is further complicated by the substitution of discrete spring forces for a continuous elastic medium. One way to improve accuracy in the modeling of confining concrete is to make preliminary estimates of the spring constants, check FE results against test data generated by identical loading conditions, and refine the array of spring constants through iterative calculations until the FE results compare well with test data. The verified model can then be used in more detailed analyses and in the prediction of component responses to conditions other than those encountered in testing.

64. In the selection of boundary element spring constants, each spring is considered to act on a "tributary" portion of the component element represented by an area extending from the node halfway to each adjacent node. The spring constant K (in kips/in.) can be found by multiplying the length of the tributary portion by the concrete's effective elastic stiffness per unit length K/L (in ksi). The effective K/L for the area of concrete in contact with a component face was estimated using a method presented by Timoshenko and Goodier (1970) for calculating the average deflection over the area of a rectangular, uniform-pressure distribution applied to the surface of a semi-infinite, elastic body. The average deflection Y is found by

$$Y = m \frac{P(1 - \nu^2)}{E\sqrt{A}}$$

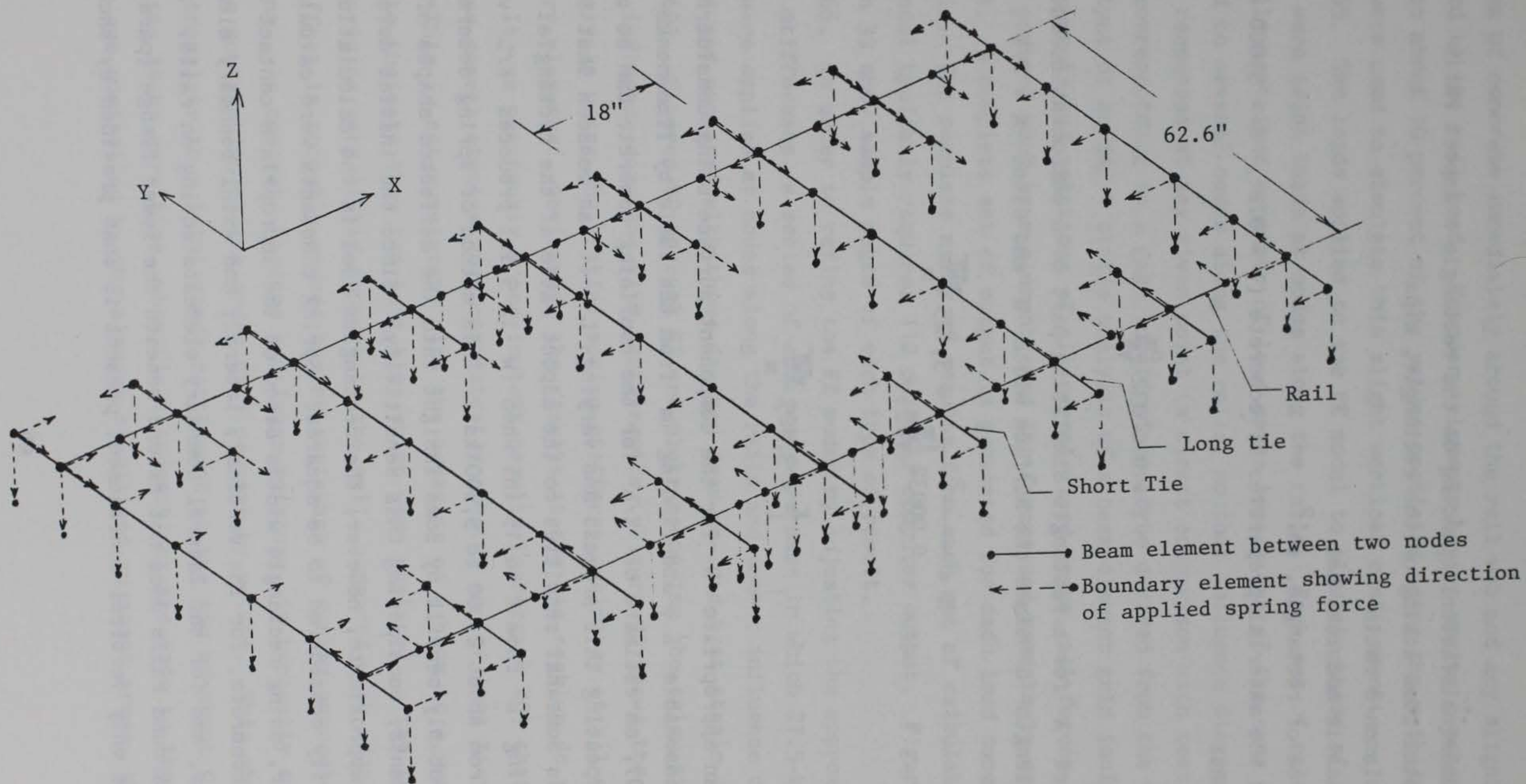


Figure 36. Sketch of the three-dimensional FE grid showing all nodes, beam elements, and boundary elements

where

m = numerical factor depending on the rectangle's aspect ratio

P = total load acting on the rectangle, kips

v = Poisson's ratio

E = elastic modulus, ksi

A = area of rectangle, in.²

Substituting the material properties of concrete (v = 0.2 , E = 3,000 ksi), it follows that

$$Y = 0.00032 \frac{Pm}{\sqrt{A}}$$

Since the area A for a rectangle simulating part of a component surface is the section length L times the surface width W and since K = P/Y , then

$$K = \frac{P}{0.00032 \frac{Pm}{\sqrt{WL}}} = 3,125 \frac{\sqrt{WL}}{m}$$

and

$$\frac{K}{L} = 3,125 \frac{\sqrt{WL}}{m}$$

By choosing an appropriate W for the component surface being considered, choosing a reasonable L , and finding m from the table by Timoshenko and Goodier (1970), an estimate of K/L for the confining concrete can be calculated. By repeating this process and varying L , it can be seen that the calculation is somewhat sensitive to the aspect ratio of the rectangle. For example, varying L from 2 to 15 in. when W is 5 in. produces K/L values which range from about 2,000 to 5,500 ksi. This method of spring determination could probably benefit by some insight into the deflected shapes of loaded components, considering this sensitivity. Since the initial determination is very approximate, however, the rectangles used in the calculations were arbitrarily considered to be squares. Spring constants were calculated in this manner, using rectangle widths based on the appropriate contact areas of confining concrete, for the vertical, lateral, and axial boundary elements acting on ties, and for the lateral boundary elements acting on rails. Since the concrete around rails does not extend beneath the lower flange (paragraph 15), the only vertical confinement present is that provided by shear in

the area of concrete immediately around the rail web and any slight bearing provided to the rail head. Boundary elements having spring constants equivalent to about 10 percent of the values predicted using the methods described above were used to simulate this slight vertical confinement.

65. The loads applied to the FE model to simulate those of locomotive wheels were point loads at nodes along the rails. Each set of calculations typically contained a number of load cases consisting of the same wheel loads applied to several nodes along the rails, so that influence diagrams for component responses at any given point (a direct comparison with test data for a point corresponding to a gage location) could be derived from the results. The output of an SAP V static analysis of a beam-element grid includes the displacements and rotations of all unrestrained nodes, all forces and moments at the ends of each beam element, and the forces and moments in each boundary element. A complete set of output is generated for each load case of an analysis. The complete array of results from each set of calculations for this model typically requires 112 pages of computer output. Figures 37 through 39 show sample pages of each type of result.

66. In order to refine the FE model by adjusting the approximated spring stiffnesses, a series of analyses were made in which 27.5-kip wheel loads were applied at nodes along the rails and moment influence diagrams were plotted and compared with those derived from no-load-test strain data (paragraph 60). Figures 40 through 42 are plots comparing the calculated vertical moment influence diagrams with test results. Figure 40 shows the results of the analysis using the initial spring stiffness estimates at all component boundary elements. Obviously, the results at the tie section do not compare well. It was previously noted in test results (paragraph 40) that measured positive moment strains were consistently greater at the long tie than at mid-span. This is not consistent with the behavior of a beam at a support, but seems to indicate that the long ties which were replaced in the test sections are providing very little support to the rail, compared with adjacent ties. This effect is probably caused by the shrinkage of curing concrete in the test sections. As concrete hardens and loses moisture, it typically experiences plastic contraction on the order of 1 percent by volume. This shrinkage rate would translate to a total grade settlement at the tie of about 0.05 in. After the 24-hr cure time, when final connections are made to the rails whose grades are controlled by the already stabilized adjacent areas, the tie could

possibly be unseated at its foundation while being pulled to the rail grade by connecting hardware. Poor integrity of the tie's foundation could allow rail deflections as though the tie afforded very little or no support. In pursuing this concept, an analysis was made in which all vertical boundary elements supporting the instrumented long tie were removed. As can be seen in Figure 41, the results of this analysis compare more favorably with test results. The SAP V program, as coded at WES, allows for convenient adjustment of all boundary element spring constants with the use of an input factor by which all input spring constants are multiplied. By repeating the analysis and varying this factor, the effects of changing all spring constants by the same percentage were documented. It was found that spring constants with magnitudes of approximately half the original approximations produced the best comparisons of analysis and test results (Figure 42). Notice that the influence diagram shapes and moment values compare very well except at the peaks, when wheel loads are directly over the sections being considered (strain gage locations). At these points of maximum rail deflection, FE analyses predict slightly greater responses than those measured in testing. This effect may be caused by the linear elastic behavior of SAP V boundary elements, when the actual foundation elasticity of tow track components may appear to be nonlinear, if deflections are significant, due in part to imperfect or irregular bond properties along the concrete-steel interface. Having produced calculated component responses to documented test loadings which compare reasonably well with test results, the refined beam-element grid can now be used to predict the qualitative effects of various changes in wheel loadings and component support conditions.

Investigated variables

67. Since the analyses involving the conditions present in test sections included a nonstandard support condition at the instrumented long tie, it is now appropriate to consider the responses in a section of uniformly supported components (presumably more typical of the repaired tow track, at large). For this analysis, all long tie boundary elements were replaced. These results represent the predicted component responses to wheel loads at a typical section of freshly repaired tow track. Plots of the waterside rail's response (vertical bending moment) to dead-load-only and worst-case wheel loads for long tie and midspan sections are shown in Figure 43. The vertical load imparted to a tie by a rail when a locomotive wheel bears directly at

STATIC ANALYSIS

LOAD CASE 1

DISPLACEMENTS/ROTATIONS OF UNRESTRAINED NODES

NODE NUMBER	X- TRANSLATION	Y- TRANSLATION	Z- TRANSLATION	X- ROTATION	Y- ROTATION	Z- ROTATION
1	1.61563D-10	-2.62470D-09	-6.33810D-08	-2.29057D-08	-8.50565D-07	-2.21575D-11
2	1.17750D-11	-2.62470D-09	-5.36366D-07	-2.76045D-09	-8.50565D-07	9.06411D-11
3	-7.68566D-11	-3.30092D-09	-3.14497D-08	1.30828D-08	-8.50578D-07	-2.27288D-11
4	8.01060D-12	-4.06168D-09	3.12057D-09	3.10402D-09	-8.50592D-07	1.12803D-12
5	-2.15986D-11	-4.96734D-09	3.09180D-09	-3.12227D-09	-8.50610D-07	3.98280D-12
6	1.88378D-10	-5.72810D-09	-3.20495D-08	-1.30836D-08	-8.50624D-07	-6.06244D-11
7	1.37234D-10	-3.88694D-09	-5.36369D-07	2.76702D-09	-8.50637D-07	1.94745D-10
8	-3.17650D-10	-2.54926D-09	-6.33735D-08	2.29099D-08	-8.50637D-07	-2.70296D-11
9	1.53925D-11	3.25928D-10	5.96922D-06	2.20340D-08	-1.19511D-06	4.51663D-10
10	2.09521D-10	8.27499D-09	5.96995D-06	-2.23652D-08	-1.19516D-06	2.90889D-09
11	-3.62760D-10	2.49761D-09	2.49235D-06	7.44992D-07	-2.22874D-06	3.33532D-11
12	1.90101D-11	2.49761D-09	1.86766D-05	4.68284D-08	-2.22874D-06	-1.89858D-10
13	2.37728D-10	1.55529D-09	1.69939D-06	-7.84639D-07	-2.22874D-06	6.56365D-11
14	-1.56721D-10	5.81465D-08	1.71429D-06	7.83668D-07	-2.22872D-06	1.69902D-11
15	2.81808D-10	3.11497D-08	1.86776D-05	-4.74974D-08	-2.22872D-06	-1.51444D-10
16	3.51039D-10	2.07237D-08	2.49164D-06	-7.45462D-07	-2.22872D-06	6.45555D-11
17	1.63389D-11	-2.75602D-08	8.60123D-05	-1.94767D-07	8.70474D-06	-8.29409D-09
18	4.96661D-10	-2.88911D-08	8.60137D-05	1.95583D-07	8.70514D-06	-1.41250D-08
19	3.81467D-11	-9.75403D-08	-6.42098D-06	-2.47724D-06	4.42615D-05	-6.35406D-12
20	1.36677D-11	-9.75403D-08	-5.58581D-05	-4.36362D-07	4.42615D-05	2.02790D-11
21	-2.14493D-11	-1.55280D-07	-3.32102D-06	1.32514D-06	4.42618D-05	-2.44753D-12
22	6.95310D-13	-2.20236D-07	3.10815D-07	3.17413D-07	4.42620D-05	-7.10220D-12
23	4.22206D-10	-2.97566D-07	3.08512D-07	-3.18749D-07	4.42624D-05	-5.65508D-11
24	-4.36292D-09	-3.62522D-07	-3.36751D-06	-1.32485D-06	4.42626D-05	1.28258D-09
25	7.11513D-10	-1.54229D-07	-5.58623D-05	4.38663D-07	4.42629D-05	-5.14152D-09
26	9.17236D-09	-1.01151D-07	-6.41874D-06	2.47882D-06	4.42629D-05	1.26238D-09
27	1.67539D-11	-2.56755D-08	-7.57486D-04	-2.49141D-06	6.57934D-05	8.76258D-09
28	1.15192D-09	-7.56442D-07	-7.57510D-04	2.52181D-06	6.57953D-05	-1.87938D-07
29	-4.51022D-10	6.96459D-09	-2.04828D-04	-6.19234D-05	-2.96808D-06	4.18764D-11
30	1.98402D-11	6.96459D-09	-1.54138D-03	-4.54646D-06	-2.96808D-06	-2.35644D-10
31	2.94642D-10	4.33693D-09	-1.40927D-04	6.44055D-05	-2.96808D-06	8.10181D-11
32	2.69020D-08	-4.68594D-06	-1.42152D-04	-6.43221D-05	-2.96805D-06	-7.37773D-09
33	1.59233D-09	-2.36031D-06	-1.54143D-03	4.60497D-06	-2.96805D-06	2.15349D-08
34	-4.12636D-08	-1.57030D-06	-2.04760D-04	6.19629D-05	-2.96805D-06	-3.85519D-09
35	1.33822D-11	-4.84413D-08	-7.37705D-04	-2.39802D-06	-6.48871D-05	-1.42543D-08
36	1.05825D-09	-6.79487D-07	-7.37731D-04	2.42886D-06	-6.48888D-05	1.46834D-07
37	4.15683D-10	-1.87079D-07	-1.02063D-05	-2.75720D-06	-4.17526D-05	-3.27270D-11
38	6.92421D-12	-1.87079D-07	-5.03674D-05	-2.49572D-07	-4.17526D-05	1.91874D-10
39	-1.88997D-10	-2.59935D-07	-5.64345D-06	1.73596D-06	-4.17528D-05	-5.05809D-11
40	-1.32560D-11	-3.41898D-07	6.68156D-07	3.53765D-07	-4.17531D-05	1.63059D-11
41	-3.04878D-10	-4.39474D-07	6.61776D-07	-3.56274D-07	-4.17534D-05	-2.70907D-12
42	3.77784D-09	-5.21437D-07	-5.71067D-06	-1.73572D-06	-4.17537D-05	-9.26810D-10
43	5.24164D-10	-2.85890D-07	-5.03759D-05	2.52757D-07	-4.17539D-05	3.51114D-09
44	-7.46183D-09	-2.10486D-07	-1.02015D-05	2.75921D-06	-4.17539D-05	-5.20624D-10
45	-1.83609D-12	-4.37419D-08	6.79697D-05	-1.04136D-07	-8.19723D-06	1.39456D-08
46	3.71687D-10	-5.59032D-08	6.79687D-05	1.05457D-07	-8.19779D-06	2.24670D-08
47	4.05034D-10	4.66187D-09	2.07917D-06	6.23724D-07	1.55705D-06	-3.83829D-11
48	-1.05964D-11	4.66187D-09	1.56012D-05	4.13014D-08	1.55705D-06	2.10840D-10
49	-2.62835D-10	2.90300D-09	1.42172D-06	-6.54312D-07	1.55705D-06	-7.16381D-11
50	2.65261D-10	5.03672D-08	1.43429D-06	6.53496D-07	1.55690D-06	-9.09168D-11
51	2.19209D-10	2.88817D-08	1.56019D-05	-4.18441D-08	1.55690D-06	1.94169D-10

Figure 37. Sample page of SAP V output for node displacements and rotations in a beam-element grid analysis

BEAM ELEMENT FORCES AND MOMENTS

BEAM NO.	LOAD NO.	AXIAL R1	SHEAR R2	SHEAR R3	TORSION M1	BENDING M2	BENDING M3	P/A+M2/S2	P/A-M2/S2	P/A+M3/S3	P/A-M3/S3
1	1	4.740E-22	5.462E-04	-8.758E-06	1.108E-21	-2.280E-23	-6.810E-20	7.242E-23	-2.947E-24	-6.732E-21	6.520E-21
		-5.817E-22	-5.462E-04	8.758E-06	-1.535E-21	8.495E-05	5.298E-03	2.321E-05	-2.321E-05	5.235E-04	-5.235E-04
1	2	4.423E-21	9.459E-03	-6.131E-05	3.329E-21	-6.659E-22	-2.531E-19	4.992E-22	1.888E-22	-2.747E-20	2.366E-20
		-6.124E-21	-9.459E-03	6.131E-05	-4.179E-21	5.947E-04	9.176E-02	1.625E-04	-1.625E-04	9.067E-03	-9.067E-03
1	3	8.020E-21	2.313E-02	-1.378E-04	4.315E-21	-1.218E-21	-4.987E-19	7.395E-22	2.126E-22	-4.955E-20	3.853E-20
		-1.143E-20	-2.313E-02	1.378E-04	-5.168E-21	1.337E-03	2.244E-01	3.652E-04	-3.652E-04	2.217E-02	-2.217E-02
1	4	1.753E-20	1.612E-04	-1.410E-04	4.599E-22	-8.126E-21	-3.524E-20	7.739E-22	4.963E-22	-4.503E-21	3.576E-21
		-2.441E-20	-1.612E-04	1.410E-04	-5.666E-22	1.368E-03	1.564E-03	3.738E-04	-3.738E-04	1.545E-04	-1.545E-04
1	5	5.220E-20	6.506E-03	7.226E-05	1.075E-21	-1.721E-21	-1.608E-19	6.892E-21	6.234E-21	-9.724E-21	1.629E-20
		-6.586E-20	-6.506E-03	-7.226E-05	-1.289E-21	-7.009E-04	6.310E-02	-1.915E-04	1.915E-04	6.236E-03	-6.236E-03
2	1	-9.042E-05	-3.811E-04	3.881E-06	5.441E-07	-8.438E-06	-2.151E-03	-1.748E-05	-1.287E-05	-2.277E-04	1.974E-04
		9.042E-05	3.811E-04	-3.881E-06	-5.441E-07	-3.503E-05	-2.118E-03	5.600E-06	2.474E-05	-1.941E-04	2.244E-04
2	2	-3.427E-04	-1.032E-02	-6.830E-05	5.643E-07	9.113E-04	-8.766E-02	1.915E-04	-3.065E-04	-8.720E-03	8.604E-03
		3.427E-04	1.032E-02	6.830E-05	-5.643E-07	-1.464E-04	-2.788E-02	1.750E-05	9.751E-05	-2.698E-03	2.813E-03
2	3	-6.936E-04	-2.569E-02	-1.736E-04	4.481E-07	2.250E-03	-2.206E-01	4.984E-04	-7.312E-04	-2.191E-02	2.168E-02
		6.936E-04	2.569E-02	1.736E-04	-4.481E-07	-3.057E-04	-6.710E-02	3.284E-05	1.999E-04	-6.514E-03	6.746E-03
2	4	6.456E-04	-1.263E-04	-1.365E-03	6.274E-04	1.482E-02	-6.744E-04	4.158E-03	-3.942E-03	4.168E-05	1.750E-04
		-6.456E-04	1.263E-04	1.365E-03	-6.274E-04	4.679E-04	-7.405E-04	1.952E-05	-2.362E-04	-1.815E-04	-3.516E-05
2	5	-2.326E-03	-7.686E-03	-1.598E-03	1.246E-03	1.902E-02	-6.212E-02	4.533E-03	-5.314E-03	-6.529E-03	5.748E-03
		2.326E-03	7.686E-03	1.598E-03	-1.246E-03	-1.215E-04	-2.396E-02	3.570E-04	4.234E-04	-1.977E-03	2.758E-03
3	1	-9.042E-05	3.435E-05	-4.718E-06	5.441E-07	3.503E-05	2.118E-03	-5.600E-06	-2.474E-05	1.941E-04	-2.244E-04
		9.042E-05	-3.435E-05	4.718E-06	-5.441E-07	2.442E-05	-1.685E-03	2.184E-05	8.500E-06	-1.513E-04	1.817E-04
3	2	-3.427E-04	-3.530E-04	-2.066E-05	5.643E-07	1.464E-04	2.788E-02	-1.750E-05	-9.751E-05	2.698E-03	-2.813E-03
		3.427E-04	3.530E-04	2.066E-05	-5.643E-07	1.138E-04	-3.233E-02	8.861E-05	2.640E-05	-3.137E-03	3.252E-03
3	3	-6.936E-04	-9.803E-04	-4.223E-05	4.481E-07	3.057E-04	6.710E-02	-3.284E-05	-1.999E-04	6.514E-03	-6.746E-03
		6.936E-04	9.803E-04	4.223E-05	-4.481E-07	2.263E-04	-7.945E-02	1.782E-04	5.455E-05	-7.734E-03	7.967E-03
3	4	6.456E-04	-3.284E-05	-1.145E-04	6.274E-04	-4.679E-04	7.405E-04	-1.952E-05	2.362E-04	1.815E-04	3.516E-05
		-6.456E-04	3.284E-05	1.145E-04	-6.274E-04	1.911E-03	-1.154E-03	4.138E-04	-6.304E-04	-2.224E-04	5.733E-06
3	5	-2.326E-03	-2.010E-03	-1.407E-04	1.246E-03	1.215E-04	2.396E-02	-3.570E-04	-4.234E-04	1.977E-03	-2.758E-03
		2.326E-03	2.010E-03	1.407E-04	-1.246E-03	1.652E-03	-4.915E-02	8.415E-04	-6.104E-05	-4.467E-03	5.247E-03
4	1	-9.042E-05	-8.723E-07	-1.095E-05	5.441E-07	-2.442E-05	1.685E-03	-2.184E-05	-8.500E-06	1.513E-04	-1.817E-04
		9.042E-05	8.723E-07	1.095E-05	-5.441E-07	1.887E-04	-1.698E-03	6.673E-05	-3.639E-05	-1.526E-04	1.830E-04
4	2	-3.427E-04	-2.517E-06	-9.810E-06	5.643E-07	-1.138E-04	3.233E-02	-8.861E-05	-2.640E-05	3.137E-03	-3.252E-03
		3.427E-04	2.517E-06	9.810E-06	-5.643E-07	2.610E-04	-3.237E-02	1.288E-04	-1.380E-05	-3.141E-03	3.256E-03
4	3	-6.936E-04	-4.558E-06	-3.725E-06	4.481E-07	-2.263E-04	7.945E-02	-1.782E-04	-5.455E-05	7.734E-03	-7.967E-03
		6.936E-04	4.558E-06	3.725E-06	-4.481E-07	2.822E-04	-7.952E-02	1.935E-04	3.928E-05	-7.741E-03	7.974E-03
4	4	6.456E-04	-1.083E-04	1.554E-04	6.274E-04	-1.911E-03	1.154E-03	-4.138E-04	6.304E-04	2.224E-04	-5.733E-06
		-6.456E-04	1.083E-04	-1.554E-04	-6.274E-04	4.200E-04	-2.779E-03	-2.231E-04	6.434E-06	-3.829E-04	1.663E-04
4	5	-2.326E-03	-4.349E-03	-9.350E-04	1.246E-03	-1.652E-03	4.915E-02	-8.415E-04	6.104E-05	4.467E-03	-5.247E-03
		2.326E-03	4.349E-03	9.350E-04	-1.246E-03	1.568E-02	-1.144E-01	4.674E-03	-3.893E-03	-1.091E-02	1.169E-02
5	1	-9.042E-05	-3.126E-05	2.671E-05	5.441E-07	-1.887E-04	1.698E-03	-6.673E-05	3.639E-05	1.526E-04	-1.830E-04
		9.042E-05	3.126E-05	-2.671E-05	-5.441E-07	-1.479E-04	-2.092E-03	-2.523E-05	5.557E-05	-1.915E-04	2.219E-04
5	2	-3.427E-04	3.784E-04	3.637E-05	5.643E-07	-2.610E-04	3.237E-02	-1.288E-04	1.380E-05	3.141E-03	-3.256E-03
		3.427E-04	-3.784E-04	-3.637E-05	-5.643E-07	-1.973E-04	-2.760E-02	3.602E-06	1.114E-04	-2.670E-03	2.785E-03
5	3	-6.936E-04	1.038E-03	3.510E-05	4.481E-07	-2.822E-04	7.952E-02	-1.935E-04	-3.928E-05	7.741E-03	-7.974E-03
		6.936E-04	-1.038E-03	-3.510E-05	-4.481E-07	1.601E-04	-6.643E-02	7.263E-05	1.601E-04	-6.448E-03	6.681E-03
5	4	6.456E-04	-1.679E-05	1.292E-04	6.274E-04	4.200E-04	-2.779E-03	2.231E-04	-6.434E-06	3.829E-04	-1.663E-04
		-6.456E-04	1.679E-05	-1.292E-04	-6.274E-04	-2.048E-03	-2.990E-03	-6.678E-04	4.512E-04	-4.038E-04	1.872E-04
5	5	-2.326E-03	2.364E-04	-1.258E-03	1.246E-03	-1.568E-02	1.144E-01	-4.674E-03	3.893E-03	1.091E-02	-1.169E-02

Figure 38. Sample page of SAP V output for beam element forces and moments

BOUNDARY ELEMENT FORCES / MOMENTS

ELEMENT NUMBER	LOAD CASE	FORCE	MOMENT
1	1	-0.54622E-03	0.
1	2	-0.94594E-02	0.
1	3	-0.23130E-01	0.
1	4	-0.16120E-03	0.
1	5	-0.65055E-02	0.
2	1	-0.87580E-05	0.
2	2	-0.61310E-04	0.
2	3	-0.13779E-03	0.
2	4	-0.14105E-03	0.
2	5	0.72260E-04	0.
3	1	-0.14942E-02	0.
3	2	-0.30693E-01	0.
3	3	-0.75644E-01	0.
3	4	-0.43657E-03	0.
3	5	-0.20958E-01	0.
4	1	-0.17619E-04	0.
4	2	-0.22241E-04	0.
4	3	-0.28255E-04	0.
4	4	0.11787E-02	0.
4	5	0.18370E-02	0.
5	1	0.16661E-04	0.
5	2	0.15571E-03	0.
5	3	0.35676E-03	0.
5	4	0.10779E-02	0.
5	5	0.14376E-02	0.
6	1	-0.85992E-05	0.
6	2	0.47640E-04	0.
6	3	0.13139E-03	0.
6	4	0.12508E-02	0.
6	5	0.14573E-02	0.
7	1	-0.41548E-03	0.
7	2	-0.99635E-02	0.
7	3	-0.24705E-01	0.
7	4	-0.93486E-04	0.
7	5	-0.56865E-02	0.
8	1	-0.62350E-05	0.
8	2	0.10846E-04	0.
8	3	0.38500E-04	0.
8	4	0.26992E-03	0.
8	5	-0.79429E-03	0.
9	1	0.35222E-04	0.
9	2	-0.35048E-03	0.
9	3	-0.97576E-03	0.
9	4	0.75461E-04	0.

Figure 39. Sample page of SAP V output
boundary element forces and moments

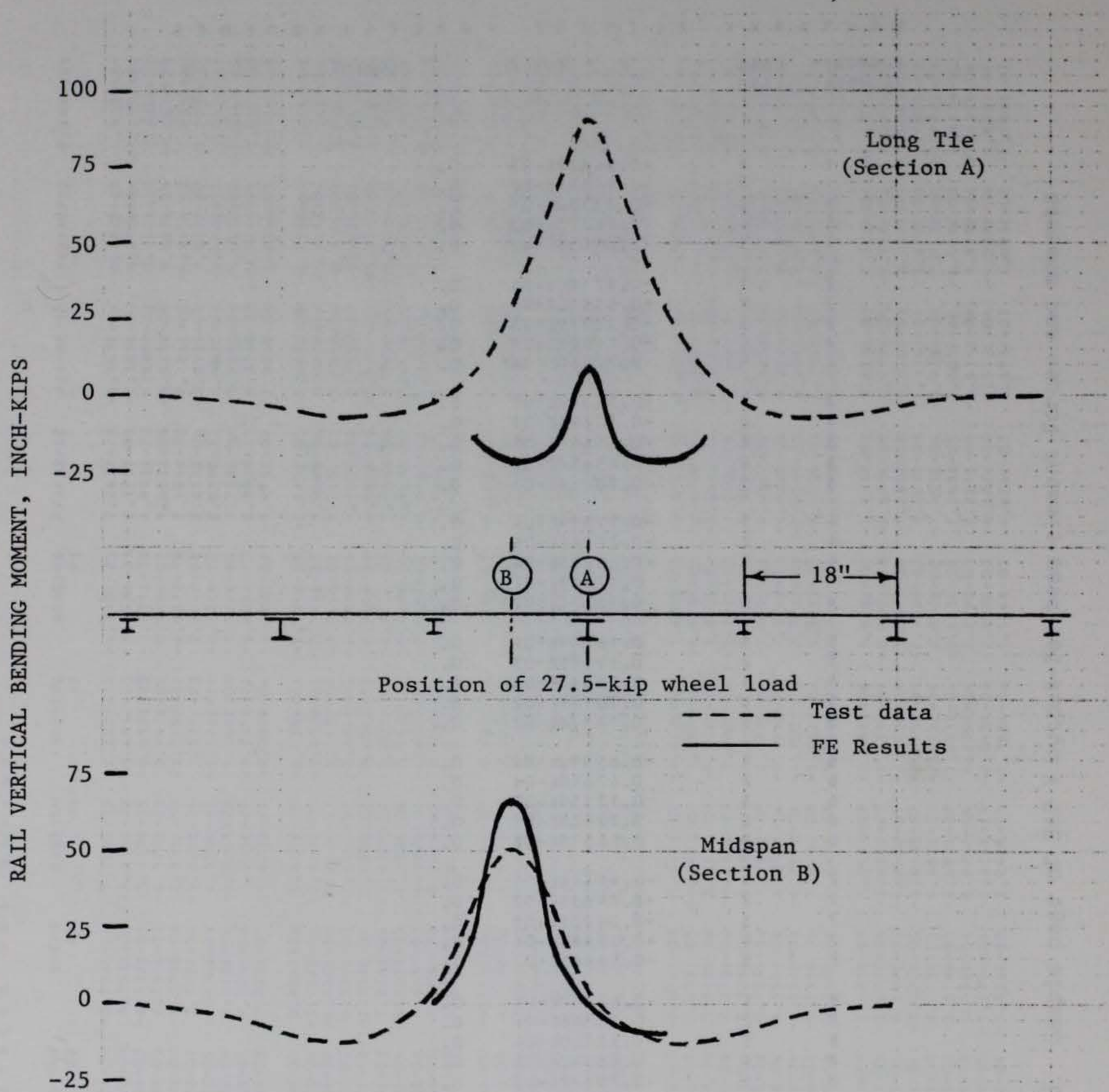


Figure 40. Influence diagram comparisons of test results and FE analyses using calculated boundary element spring constants and uniform support conditions

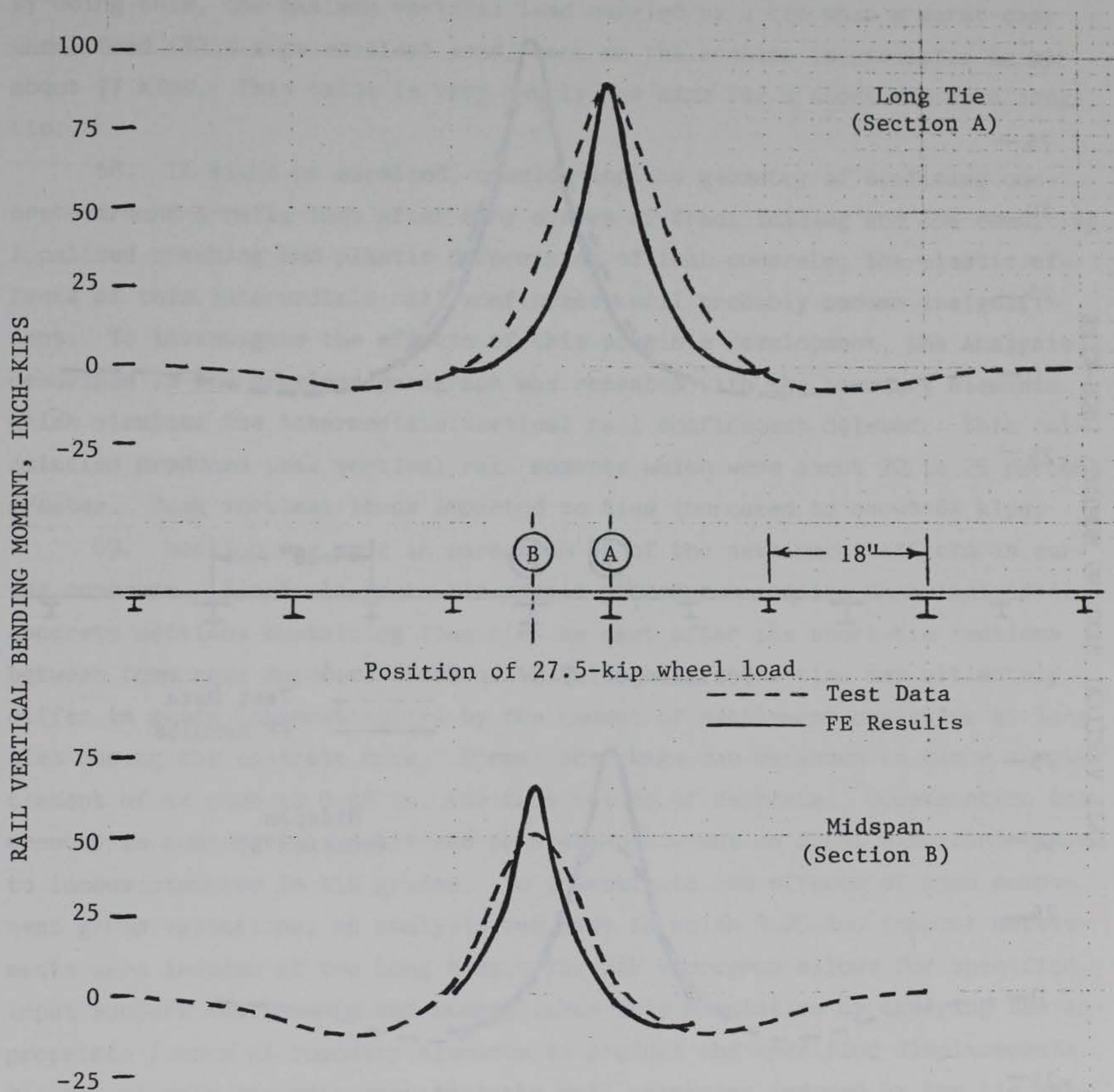


Figure 41. Influence diagram comparisons of test results and FE analyses after removal of long tie (Section A) vertical supports

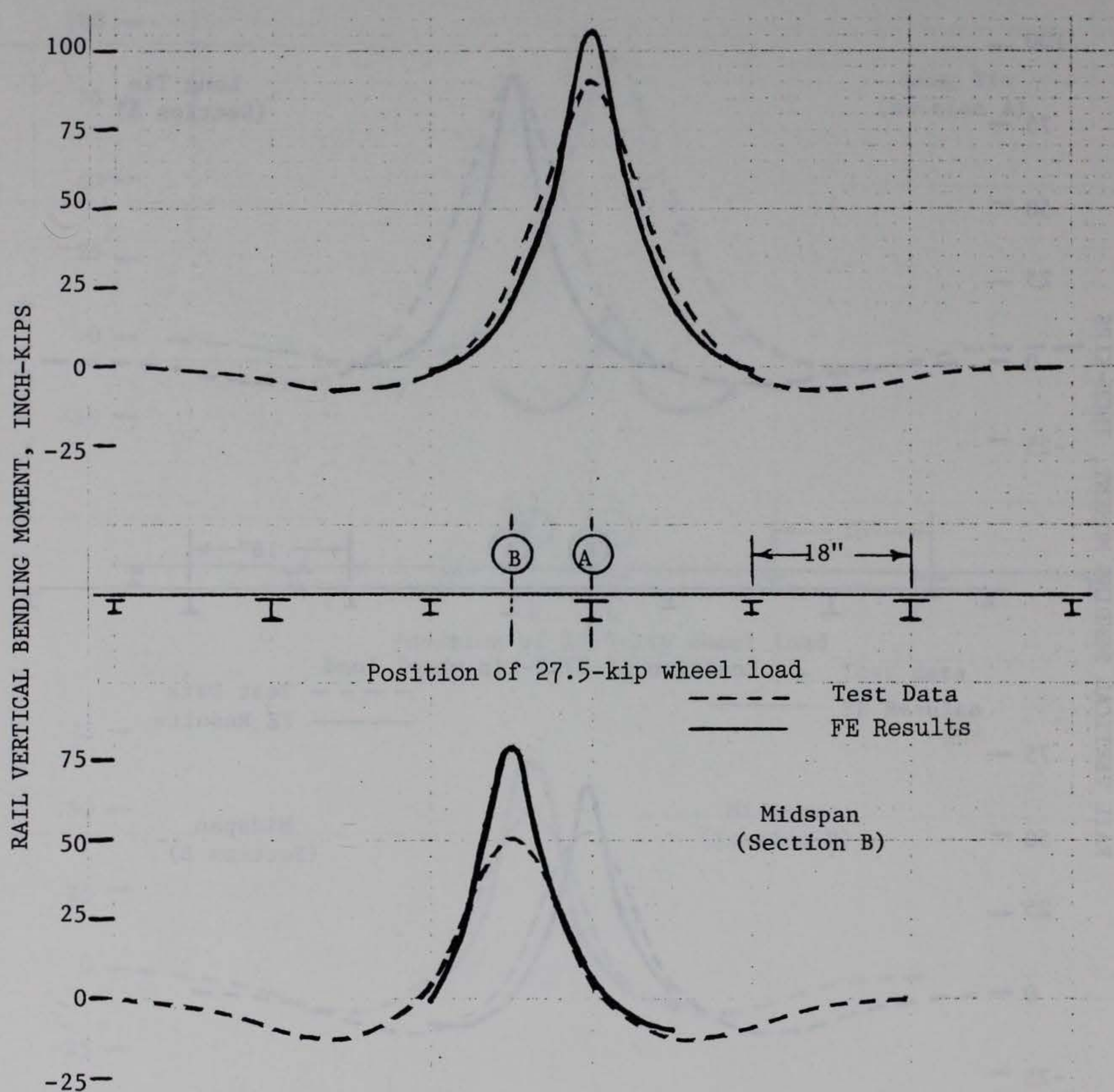


Figure 42. Influence diagram comparisons of test results and FE analyses after iterative refinement of boundary element spring constants

that section can be predicted by summing the spring forces in the vertical boundary elements (found in the SAP V analysis output) which act on that tie. By doing this, the maximum vertical load carried by a tie when a worst-case wheel load (87.5 kips vertical load) acts on the section is predicted to be about 77 kips. This value is very nearly the same for a short tie as a long tie.

68. It might be surmised, considering the geometry of confining concrete around a rail, that after many cycles of track loading and the resulting localized cracking and plastic deformation of that concrete, the elastic effects of this intermediate rail confinement will probably become insignificant. To investigate the effects of this possible development, the analysis described in the previous paragraph was repeated with the boundary elements which simulate the intermediate vertical rail confinement deleted. This calculation produced peak vertical rail moments which were about 20 to 25 percent greater. Peak vertical loads imparted to ties increased to about 82 kips.

69. Mention was made in paragraph 66 of the settlement effects in curing concrete. Since alternate tie repair procedures require that individual concrete sections containing long ties be cast after the short-tie sections between them have cured, it follows that long and short ties may ultimately differ in grade (theoretically) by the amount of settlement occurring at long ties during the concrete cure. Normal shrinkage can be shown to cause a settlement of as much as 0.05 in. for this volume of concrete. Construction tolerances in component assembly and concrete placement no doubt also contribute to inconsistencies in tie grades. To investigate the effects of such component grade variations, an analysis was made in which 0.05-in. support settlements were induced at two long ties. The SAP V program allows for specified input support settlements and accomplishes this simulation by applying the appropriate forces at boundary elements to produce the specified displacements. Results of this analysis show that the rail responses induced by the tie settlements (ranging from about 400 in.-kips of positive moment at the long ties to about 200 in.-kips of negative moment at the short tie) are superimposed with rail responses caused by wheel loads. The maximum loads carried by the short tie between the two settled long ties increased by about 65 percent.

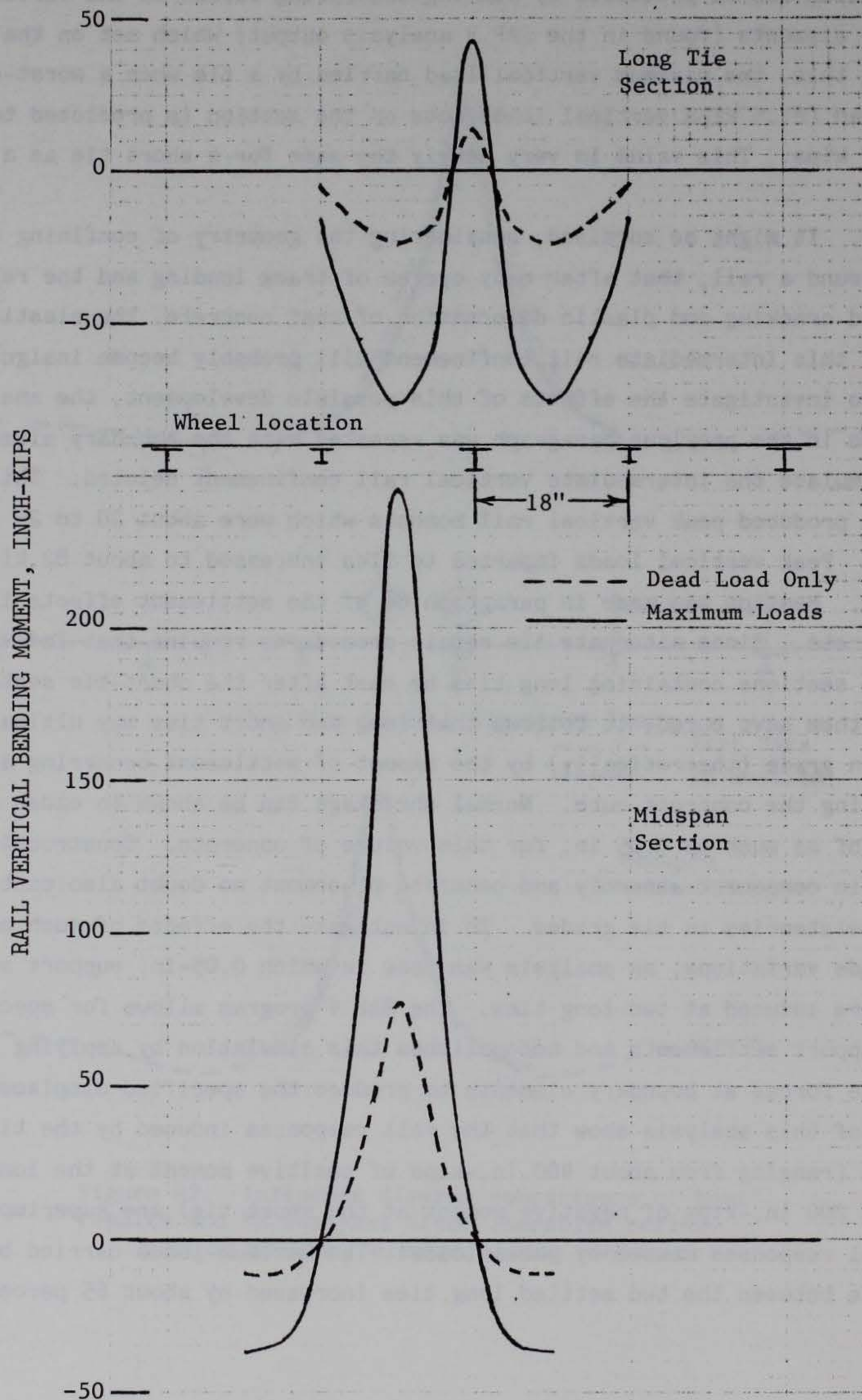


Figure 43. Influence diagrams for FE predictions of waterside rail response to dead-load-only and worst-case wheel loads at tie and midspan sections

Supporting Conventional Analyses

70. An important factor in considering the long-term stability of a composite structure such as the tow track is the difference in response behaviors of concrete and steel when each is subjected to repeated or sustained loadings. Steel will continue to respond elastically through multiple load-unload cycles, unless its yield point or fatigue endurance limit has been exceeded. Concrete, however, actually experiences small plastic deformations as a result of repeated or sustained loadings which are well below the ultimate strength. The ultimate grade inconsistencies of ties along a repaired tow track section due to the differential settlement effects discussed in the previous section are probably less severe than the calculations suggest, since all of the concrete in the section was still relatively green when final hardware connections were made, and the reaction forces in the deformed rail likely caused some plastic creep in the fresh concrete and subsequent redistribution of the residual forces. While these considerations made precise quantifying of component stresses more difficult, the related inconsistencies in bonding conditions and component foundation qualities may contribute to the accelerated deterioration of concrete in certain areas.

71. Within the scope of these tests and analyses, none of the measured or predicted worst-case rail responses have resulted in critical stresses in the rail section. Although the total states of stress in a rail are relatively complex due to the combinations of all types of beam responses and certain localized effects, the general response shapes and magnitudes bear many similarities to those which might be observed in a typical railroad rail (Ahlbeck et al. 1976, Johns and Davies 1976). Local stresses in ties and concrete are somewhat more difficult to quantify, however, and few documented structural analogies are available to provide insight into long-term problems associated with such a repaired, composite structural system. Some results of these tests and analyses have suggested that certain conditions which may be present or may develop could cause excessive stresses in localized areas of tie sections. There likely exists a continuing process of load redistributions in the tow track, caused by plastic deformations and possible local yielding of supporting concrete, which could result in the premature deterioration of certain components.

72. Rails in a freshly repaired tow track section appear to be slightly

confined by the concrete in contact with rail webs (paragraph 64). The tendency of the rail to deflect vertically between ties is initially resisted by this slight confinement. This resistance was simulated in a simple calculation by a series of elastic supports between two crossties, and the rail was analyzed as a beam on an elastic foundation (Timoshenko 1958). In response to an average vertical wheel load (50 kips), the shear stress predicted in this confining concrete was approximately five times the allowable value. After the shear capacity of this concrete has been exceeded and localized cracking has occurred, the confinement effects are no longer present, and any initial resistance provided is redistributed to the adjacent ties and their foundations.

73. The consistency of concrete on the undersides of the upper flanges probably varies considerably. Pockets of air which become trapped in this area during concrete placement have no route for escape, and visual inspection of the placement quality here is not possible. Observed bending of a tie web in test results (paragraph 46) suggests that uniformity of this concrete was less than ideal. Since the extreme edges of the tie upper flanges are loaded heavily when rails assume deflected shapes, localized stresses in this concrete area are probably significant. Considering the volumetric changes of the concrete during curing, plastic creep resulting from repeated loadings, and the possibilities of voids and localized overstressing, it is not unreasonable to assume that the entire rail loading imparted to a tie might eventually be borne by a section whose upper flanges no longer benefit from substantial support of concrete. Upon the development of this condition, and assuming that integrity of the concrete around the tie lower flanges is acceptable, the entire load exerted by the rail will be carried in the web of the tie, directly beneath that rail. Stresses in the web will be greatest near the top, where the load is carried almost entirely by an area the width of the rail. When the tie section being considered is an original-style tie which has a web thickness of $1/4$ in., the theoretical localized stress resulting from an 82-kip rail loading would be about 63 ksi. Of course, certain construction tolerance irregularities and support settlement effects have been shown analytically to cause even greater tie loadings. Stresses of this magnitude are beyond the yield of most mild steels. Plastic deformation of steel is experienced when yield is exceeded. As deformations occur, additional load redistributions may eventually cause adjacent local areas to experience

overstressing; connection hardware becomes more severely stressed and component alignment suffers. This type of mechanism is thought to be responsible for the damages first observed in tie webs like those seen in Figure 9.

Although ties found to be damaged are repaired or replaced in the alternate tie repair procedure, many of the original long ties are found to be undamaged and are reused, as are virtually all short ties. Both these original sections and the W6 x 20 I-beam sections typically used as replacements have 1/4-in.-thick webs which would be prone to overstressing under the conditions described above.

74. The progressive deterioration process is quite difficult to conclusively document since it involves many uncertain tolerances and a continuously variable array of support conditions and loading distributions. It also follows that the time period required for such a process to take place cannot be reasonably predicted within the scope of these tests and analyses.

PART VI: CONCLUSIONS

75. Measurable strains in tow track components are highly localized with respect to locomotive wheel position. Strain magnitudes almost always decayed to less than 10 percent of peak values when locomotive wheels moved 2 ft away from gage locations.

76. None of the measured or predicted responses of the waterside rail implied critical stress levels in the rail itself. Predictions assumed proper alignment and attachment hardware conditions.

77. No critical responses were observed in gate recess area components. Lateral stability of the waterside rail and its supporting girder appears to have been improved by repair modifications.

78. Damage to the rack, which has necessitated the replacement of many sections, appears to have been caused by normal mechanical wear and/or excessive wear resulting from component misalignment. Strains measured in the rack did not exceed about 65 $\mu\text{in./in.}$, and calculations agree that rack loadings should not be excessive.

79. Relative precision of component assembly and concrete placement during the alternate tie repair process appears to affect the severity of stresses experienced by some components. Different responses were observed in identical tests at two sites which were alike in structural geometry. Analyses confirm the sensitivity of component responses to construction tolerances.

80. The concrete which partially surrounds the rail in a repaired track section initially carries a portion of the rail loads and influences that rail's response. Test data compare more favorably with analytical predictions which simulate this concrete with intermediate elastic supports than those which include only the tie supports.

81. Localized excessive shear stresses in the concrete around rail webs between ties will probably cause cracking and deterioration in the immediate vicinity. The portions of rail loads initially supported by this confinement will be redistributed to ties.

82. Plastic deformations and localized deteriorations of concrete will probably cause long-term progressive redistribution of loads and eventual localized overstressing and alignment degradation in components of the crosstie-supported tow track.

83. Reused original tie sections and W6 x 20 I-beam replacement sections would appear to be particularly susceptible to overstressing in the webs under waterside rails after certain support and loading conditions have developed during the process of progressive load redistribution.

84. Within the scope of these tests and analyses, it appears unlikely that crosstie components and the concrete which supports and confines them will be substantially more resistant to progressive structural damage as a result of alternate tie repair procedures. Although the integrity of rails and racks does not seem threatened by present stress levels, accelerated wear conditions may eventually develop when deterioration of the foundation and supporting crossties begins to affect component alignment.

REFERENCES

- Ahlbeck, D. R., et. al. 1976 (Nov). "Evaluation of Analytical and Experimental Methodologies for the Characterization of Wheel/Rail Loads," Battelle-Columbus Laboratories, Columbus, Ohio.
- Bathe, K. J., Wilson, E. L., and Peterson, F. E. 1974 (Apr). "SAP IV--A Structural Analysis Program for Static and Dynamic Response of Linear Systems," Earthquake Engineering Research Center, Berkeley, Calif.
- Johns, T. G., and Davies, K. B. 1976 (Nov). "A Preliminary Description of Stresses in Railroad Rail," Battelle-Columbus Laboratories, Columbus, Ohio.
- Timoshenko, S. P. 1958. Strength of Materials, Part II, Van Nostrand Reinhold Co., New York.
- Timoshenko, S. P. and Goodier, J. N. 1970. Theory of Elasticity, 3rd ed., McGraw-Hill, New York.

Table 1
Maximum Measured Strains, μ in./in.

<u>Component</u>	<u>Gage Location</u>	<u>Gage No.</u>	<u>Site 1</u>	<u>Site 2</u>	<u>Site 3</u>
Rail	Head	ERL1A	-450	600	280
		ERL2A	380	-480	-220
	Web	ERL3A	-460	-630	-650
		ERL4A	-520	-670	-280
	Lower flange	ERL5A	--	310	450
		ERL6A	180	-95	110
Tie	Web	ET1C	-320		-420
		ET4C	-45		-220
Girder (gate recess)	Web	EG5A		-380	
		EG8A		120	
	Support straps	ESP1		315	
		ESP2		340	

Note: Positive strains are tension.